Strengthening conservation and management of Lumbini, the birthplace of Lord Buddha, World Heritage Property

UNESCO project FIT/536NEP4001 funded by the Japanese Funds-in-Trust for the Preservation of the World Cultural Heritage

Conservation of archaeological remains Final report







FIT/536NEP4001 Final report N° KAT/2013/PI/H/7 CLT/KAT/2013 © UNESCO, 2013 Printed in Nepal The present technical papers are made exactly from the draft the authors prepared. The designations employed and the presentation of material throughout this publication do not imply the expression of any opinion whatsoever on the part of UNESCO concerning the legal status of any country, territory, city or area of its authorities, or concerning its frontiers or boundaries.

Table of Content

Introduction	4
1. Purposes	5
2. Agenda of the conservation activities	6
3. Training activity	9
3.1. Ordinary maintenance	11
4. Characterization of the original materials and their degradation	12
4.1. Marker Stone	13
4.2. Nativity Sculpture	14
4.3. Ashoka Pillar and Capital	15
4.3.1. The pillar	15
4.3.2. The Capital	16
4.3.3. The restoration materials	17
4.3.3.1. Metallic belts	17
4.3.3.2. Mortar	18
4.3.3.3. Epoxy plaster	18
4.4. Conclusions	19
4.4.1. The original materials	19
4.4.2. The old restoration materials	19
4.4.3. The degradation mechanisms	20
4.5. Masonry	21
4.5.1. In situ XRF analysis	22
4.5.2. Colour analysis	25
4.5.3. Sampling and analytical planning	26
4.5.4. Analytical results	26
4.5.4.1. Mortars	26
4.5.4.2. Bricks	28
4.5.5. Degradation processes	31

4.5.5.1. Biological degradation	31
4.5.5.2. Salt distribution inside the masonry	32
4.5.5.3. Interactions with the environment	33
4.6. Aquifer	33
4.7. Indoor microclimate	37
4.7.1. Thermo-hygrometric modeling	39
4.7.2. Evaluation of the impacting light on degradation	40
4.7.3. Pilgrims attendance impact	41
4.8. Remarks on the degradation mechanisms of the Mayadevi Temple	41
4.9. Stability of the Ashoka Pillar	42
5. Restoration activity	43
5.1. Nativity Sculpture	44
5.2. Marker Stone	45
5.2.1. Building the new protective bow	46
5.3. Ashoka Pillar	46
5.3.1. Restoration of the Capital	48
5.3.2. Casting of the inscription	49
5.4. Pottery	49
5.5. Masonry	50
5.5.1. Describing the degradation of the masonry	50
5.5.2. Restoration of the masonry	50
5.6. Criteria for the long-term conservation	51
6. Future activities	52
6.1. Minimizing the negative impact of the aquifer	52
6.2. Restoration of the Mayadevi Temple masonry	52
6.3. Proposal for the optimization of the shelter	53
6.4. Monitoring of the Ashoka Pillar	53
Bibliography	54

Introduction

The inscription of Lumbini in the World Heritage List in the year 1997 was based on criteria (iii) and (vi), which refer respectively to:

(Criterion iii) As the birthplace of the Lord Buddha, testified by the inscription on the Ashoka pillar, the sacred area in Lumbini is one of the most holy and significant places for one of the world's great religions.

(Criterion vi) The archaeological remains of the Buddhist viharas (monasteries) and stupas (memorial shrines) from the 3rd century BC to the 15th century AD, provide important evidence about the nature of Buddhist pilgrimage centres from a very early period. Ashoka

Taking into account the universal value of the religious and archaeological significance of the monuments contained within the Sacred Garden Area, as defined by the Kenzo Tange Master Plan (Tange and Urtec, 1978), and in particular the Ashoka Pillar, the Nativity Sculpture and the Marker Stone. However, since the Outstanding Universal Value (OUV) of the monument also depends on the conservation of the archaeological remains, which is affected by the high frequency of touristic visit and pilgrimage, the incorrect use of the monuments may negatively influence the OUV. In particular, referring to the Boccardi and Gupta report (Boccardi and Gupta, 2005), "The issue of the Mayadevi Temple is an example, or symptom, of this problem and of the possible resulting conflicts. The new Temple, built to respond to the demands of the worshippers, was indeed criticized by the World Heritage Committee for having a negative impact on the archaeological remains; for affecting the visual experience and understanding of the site (both with respect to its historic significance and spiritual meaning); and for not entirely conforming to the religious needs of the pilgrims. It is important to stress that the use of the site, including by pilgrims, could have a negative impact on both values if it involves alteration of the tangible features that represent them."

However, the actual state of conservation of the archaeological remains of the Mayadevi Temple is also due to its recent history and to the effects that both the archaeological excavations and the building of the new shelter produced on the decay mechanisms.

In November 2005, Boccardi and Gupta emphasized that: "One of the issues raised by the construction of the new Mayadevi Temple was the preservation of the archaeological remains contained inside, as a result of the special microclimate created by the building. In this respect, the Mission observed that the ancient structures under the Temple are being heavily affected by moss and efflorescence, most likely due to water damp from the ground, incorrect temperature and relative humidity, combined with a lack of adequate ventilation. The level of the water in the ground, as the temperature, are apparently subjected to extensive fluctuations throughout the year, thus increasing the intensity of the physical, chemical and biological processes affecting the materials within the Temple."

This statement confirms that all archaeological remains are in need of conservation intervention to stop and control the degradation processes. Similar observations were arrived by Atzori (Atzori, 2006) as a result of the survey carried out in August 2005, when "... it is clear that, despite the above-mentioned interventions," regarding the activities to be undertaken to decrease the aquifer influence, "the ground water level of the area is still too high. Most of the lowest brick rows of the archaeological remains at the Mayadevi Temple are soaked with

water". As a consequence, most of the sun-exposed remains suffer biological attack due to the moss and green algae growth, which is also influenced by the microclimate inside the shelter.

Based on the conclusion and recommendation of these technical reports, in the month of June 2009, the UNESCO/Japanese Funds-in-Trust planned a mission that aimed to prepare the project with the objective of defining all activities to be undertaken to implement the archaeological research, the development of an integrated management plan and any necessary conservation works (UNESCO, 2009).

In particular, the conference pointed out that: "The very slow implementation of the Master Plan and the uncertain approach to the management of the World Heritage Site have generated a number of problems over the years, one of them being the construction of a visually problematic shelter - building (the "Mayadevi Temple") in 2002 to protect the archaeological vestiges surrounding the "marker stone", which indicates the place where Buddha appeared. This shelter building has also added to the hydrological risks to the ruins" (as written at point 2 of the said project), and consequently suggested" to attain the following objectives:

- a) Resolution of urgent conservation problems affecting the Ashoka Pillar, the Marker Stone, and the Nativity Sculpture as well as putting rapidly into place a monitoring system for the Mayadevi Temple in order to be able to ascertain corrective measures to the Temple itself, as well as to determine the future of the structure (shelter) on the basis of its impact on the archaeological vestiges that it contains;
- e) Improvement of the knowledge and skills of materials conservation personnel and archaeological staff of the LDT and the DOA", as in point 9 of the same project proposal.

1. Purposes

The general purposes of the conservation activity were defined in the 2009 meeting, and explained in the Mission Report (Meucci, 2009), when: "according to the specific issue of the Group 3 (Evaluation of the possibilities and methodologies for the Mayadevi Temple and Archaeological Remains Conservation in the Sacred Garden area), the field activity was carried out to obtain direct information on the state of conservation of the archaeological remains. The conservation necessities of the existing and potential archaeological sites in the area individuated by the Master Plan of Lumbini were evaluated as well".

The analysis of the state of conservation of the most relevant archaeological remains in the Sacred Garden area, although carried out without any instrument and based on the visual recording only, allowed individuating that: "The degradation of the archeological structures is mainly related to the environmental conditions such as air temperature and relative humidity, as well as the abundance of the rains in the monsoon period. The active deterioration processes involve in fact the water content of the archaeological remains and of the subjacent soil, whose value is directly connected to the level of the underlying aquifer. The most diffused degradation pattern is ascribed to the biological attack made by algae and cyan bacteria growths, which produce green compact patinas on the surfaces wetted by the water capillary action; furthermore the biological growing increases when incident light impacts the surfaces."

The other prevalent degradation patterns affecting the masonry and all porous materials were the disaggregation of the bricks of the external and upper rows that are the most exposed to the environment and the presence of efflorescence in the dry areas. On the base of these observations, the mission report concluded that: "The degradation is due both to the presence of liquid water into the pore structures and to the water evaporation rate, which is affected by the sun radiations impacting the surfaces, by the wind speed and by the texture of the material. The frequency of the wet/dry cycles will also change the rate of the degradation, as well as the presence of soluble salts in the water absorbed by capillary. As a consequence we observe that the brick structures inside the Mayadevi temple suffer mechanical damages more than the remains outdoor."

Owing to a lack of analytical data, which are the only objective values that allow the precise application of the proper conservation methodologies, general criteria regarding the conservation of the archaeological remains were suggested. However, since the conservation process requires the physical materials to achieve a new stable equilibrium within the exhibition environment after the restoration has been completed, the objective may be achieved by applying both direct and indirect restoration methodologies. Direct restoration concerns all activities carried out on the exposed surfaces, both to eliminate the effects of degradation and to remove the factors that cause decay.

Indirect restoration involves all activities that allow a decrease in the degradation rate through modification of environmental parameters such as the indoor microclimate of the shelter.

The capability to apply the outlined conservation criteria needs two fundamental things: a precise knowledge of the materials to be restored; and the availability of specialized personnel. As a consequence, the conservation activity was planned to reach these peculiar goals.

2. Agenda of the conservation activities

The conservation activities have been carried out according to the following agenda with reference to the UNESCO contracts.

1) 16-24 June 2009 Contract N°: IC/09/CLT/06

The contract envisaged the following activities:

- (a) Participate in the working meetings organized by UNESCO with the Japanese and Nepalese authorities (in particular in a tripartite final meeting of the Lumbini Development Trust, Department of Archaeology and UNESCO, which is scheduled on the last day of the mission in Lumbini);
- (b) Lead the Mayadevi Temple and Archaeological Conservation Working Group to address issues pertaining to the Mayadevi Temple and archaeological sites (both existing and potential) in the Sacred Garden of the Lumbini World Heritage Site;
- (c) Participate in field and site visits in company with representatives of UNESCO. the Japanese and Nepalese authorities, related international consultants and local experts, and conduct a technical examination of the Mayadevi Temple and archaeological sites (excavated or unexcavated) to collect necessary information and data that needs to be taken into account during discussion and later in the project document writing and reporting;

(d) Advise to UNESCO and the Nepalese authorities, on technical matters during and after the mission in formulating a full project proposal to be submitted to the Japanese Funds-in-Trust. This would include a work plan, time schedule, implementation and cost estimates and identify the responsibilities of all the parties involved, including those of UNESCO, the Japanese and Nepalese authorities regarding the project's implementation.

2) 1-8 August 2010 Contract N°: KAT/10/CLT/05

The activities to be carried out were:

- (a) Participate in the launching of the UNESCO/Japanese Funds-in-Trust project for the Preservation of the World Cultural Heritage "Strengthening the Conservation and Management of Lumbini, the Birthplace of Lord Buddha" on 3 August 2010 in Lumbini;
- (b) Participate in field visits in company with representatives of the Japanese and Nepalese authorities, related international and local experts and UNESCO as scheduled in the programme;
- (c) Contribute to initial and expert group review meetings on main project activities and outputs from 2-5 August 2010 in Lumbini;
- (d) Lead the expert group review meeting concerning the project activity 1 "Conservation of archaeological remains and architectural optimization of the shelter including mitigation of micro-climate and hydrological effects inside the Mayadevi Temple";
- (e) Contribute towards the drafting of the Implementation Plan and Project Coordination Arrangement for August 2010 July 2011 for activity 1, in cooperation with Nepali experts, authority and institutions, notably the Department of Archaeology and the Lumbini Development Trust, as well as international experts for archaeological investigation and conservation;
- (f) Participate as a panelist during the meeting of Lumbini stakeholders on emerging issues facilitated by the Lumbini Development Trust on 5 August 2010 in Lumbini;
- (g) Participate in the first meeting of the International Scientific Steering Committee (ISSC) on 5 August 2010 in Lumbini;
- (h) Contribute to the preparation of a summary report on the preliminary findings of group discussions and decision of the ISSC during its first meeting for debriefing to the Nepali and Japanese authorities;
- (i) Participate in the press conference on the above project to be held on 6 August 2010 in Kathmandu:
- (j) Prepare the final mission report on the above-activities.

3) 2-20 February 2011 Contract N°: KAT/11/CLT/04

During the mission the activity were:

- 1) Carry out a mission to Kathmandu and Lumbini, Nepal, from 2 to 20 February 2011 (including travel time) in order to:
- a. Undertake practical training of national staff on restoration activities;
- b. Organize laboratory and restoration yard;
- c. Carry out first conservation interventions on archaeological sections;
- 2) Carry out analytical investigations of stone materials in co-operation with the University of Rome and other laboratories in Italy.

- 3) Carry out a mission to Kathmandu and Lumbini, Nepal, from 2 April 2011 to 8 May 2011 (including travel time) in order to:
- a. Undertake restoration of the Marker Stone, Ashoka Pillar and Nativity Sculpture;
- 4) Participate in the second meeting of the International Scientific Steering Committee (ISSC) in July 2011 in Lumbini;
- 5) Purchase unit to study micro-climate and hydrological effects in the Mayadevi Temple.
- 6) Submit to UNESCO for approval:
- a) by 10 February 2011:
- i) A detailed work plan of the first field mission;
- ii) Estimate of microclimate equipment.
- b) by 28 February 2011:
- i) Final mission report on the first field mission, in both hard and electronic copies;
- ii) An original invoice for the purchase of travel tickets including boarding cards and hotel bills at respective places of stay.
- c) by 25 March 2011:
- i) A detailed work plan of the second field mission (April/May 2011).
- d) by 16 May 2011:
- i) Final mission report on the second field mission, in both hard and electronic copies;
- ii) An original invoice for the purchase of travel tickets including boarding cards and hotel bills at respective places of stay.
- e) by 4 July 2011:
- i) A provisional travel itinerary of the mission.
- f) by 22 July 2011:
- i) Final mission report on the July mission, in both hard and electronic copies;
- ii) An original invoice far the purchase of travel tickets including boarding cards and hotel bills at respective places of stay.

4) 4-26 February 2012 Contract N°: KAT/12/CLT/02

The planned activities were:

- a. Review and monitor the restoration of the Ashoka Pillar, the Nativity Sculpture and the Marker Stone, carried out in the first year (2011);
- b. Review and elaboration of micro-climate data from February2011;
- c. Sampling of the masonry inside the Mayadevi Temple according to their dating and location for the Study of the masonry inside the Mayadevi Temple in Lumbini, as proposed by the University of Rome "La Sapienza";
- d. Study of the underground water inside the Mayadevi Temple;
- e. Installation of the protective box for the Marker Stone.

5) 4-26 February 2012 Contract N°: KAT/12/CLT/03

The mission aimed to achieve:

- a. Installation of the additional three microclimate monitoring units inside the Mayadevi Temple during the mission in Lumbini from 4-26 February 2012.
- b. Analytical investigation of the samples taken in 2012.

6) 5-21 January 2013 Contract N°: KAT/12/CLT/30

The planned activities were:

- a. Restoration of a limited area of the masonry inside the Mayadevi Temple in order to verify the restoration methodologies as well as the cost and duration of the intervention for the entire masonry;
- b. Assess in situ the impact of the environment on the degradation of the masonry of the Maya Devi Temple;
- c. Measure the impact of the pilgrims on the environment dose to the Marker Stone and the Nativity Sculpture;
- d. Clean reference sections of the trenches excavated by the archaeological team inside the Mayadevi Temple;
- e. New sampling of the masonry inside the Mayadevi Temple recording dating and degradation;
- f. Review of the micro-climate inside the Mayadevi Temple to assess the microclimate variations in order to verify the test conservation conditions;
- g. Study of the aquifer under the brick structures of the Mayadevi Temple;
- h. Assess the deepness and volume of the external wells and measure the difference in height between the South West Well and the Sacred Pond to verify the possibility of using the pond as a water transfer reservoir;
- i. Preliminary monitoring of the stability of the Ashoka Pillar;
- j. Review and monitoring the restoration of the Ashoka Pillar, Nativity Sculpture and Marker Stone carried out in the first two years of the project.

3. Training activity

The first phase of training was carried out in the mission accomplished in February 1st – 21th, 2011 and involved six people coming from the Department of Archaeology and the Lumbini Development Trust. These were:

Responsible for LDT: Basanta Bidari.

Students:

Himal Kumar Uperti – LDT;

Parsu ram Rai – LDT;

Kamalesh Prasad Verma – LDT;

Sunil Dahal - LDT;

Hari Dhoj Rai – LDT;

Devendra Bhattarai - DoA.

The trainers were Mr Costantino Meucci, chemist-conservator; and the restorer Ms. Domizia Colonnello.

The training sessions focused on the nature and the degradation mechanisms of the stone materials; and on conservation materials and methodologies. At the end this part of the training, documentary materials were given to the students in order to provide them with the minimal bibliography necessary to increase their knowledge (Annex 1, 2, 3). At the same time, practical training was also performed to equip the students with basic skills in the practice of restoration. During the practical training the following activities were carried out:

- Collecting information regarding the state of conservation of the Marker Stone, Nativity Sculpture, Ashoka Pillar and the Capital;
- Recording the level of damage affecting stone surfaces;
- Sampling the aforementioned monuments and definition of an analytical plan;
- Performing cleaning tests, both biological and chemical;
- Monitoring the microclimate within the Mayadevi Temple;
- Monitoring of water content of the walls in the trenches excavated by the archaeological team.

Most of these activities were performed using special tools and equipment that became part of the technological assets of the LDT Conservation Team, such as the microclimate probes; the hygrometer; and the CO₂ automatic probe. The recorded data is part of the documentation produced by the first year activity.

During the practical training, students analyzed the monuments and recorded in different ways their state of conservation. All historical information has been recorded in conservation forms and all data regarding the distribution of the degradation patterns and the activities to be carried on to achieve the conservation was logged appropriately (Annex 4).

As for the restoration planning, several cleaning tests were performed both on the Nativity Sculpture and on the Ashoka Pillar in order to assess the best solution to remove the organic layers intentionally applied. The efficacy of several cleaning solutions was then tested which obtained very good results on both the Ashoka Pillar and the Nativity Sculpture. Cleaning tests allowed the conservationists to determine the best materials and methodologies in order to remove the organic material multilayered on the Ashoka Pillar surface and on the Nativity Sculpture. Aiming to verify the suitability of the shelter for the good conservation of the contained monuments and the masonry, a microclimate monitoring campaign was started on 11 February 2011 by using three automatic probes in order to detect:

- the outdoor reference values of temperature and relative humidity;
- the indoor values of temperature, relative humidity, and intensity of light close to the Marker Stone and Nativity Sculpture;
- the values of the surface temperature of the Marker Stone inside the protective box.

The state of degradation of the masonry within the Mayadevi Temple was preliminarily tested by using the manual water-meter. Measuring the water content of the bricks in the three trenches recently excavated allowed analysis of the location and size of the aquifer that extended beneath the Mauryan temple. All bricks revealed the saturation levels, thereby revealing that the water capillary is still active. Finally, while waiting for permission to sample the DoA, only small superficial, yet detached patinas, were taken from the Ashoka Pillar in order to collect information about the chemical composition of the superimposed layers object

of the cleaning tests. During the practical training all frontal classes were performed regarding the most important aspects of the deterioration and restoration and all classes were supported by technical presentations (Annex 5).

The second phase of training was based on the restoration of the said three monuments, according to the planning of activities as for the contract and developed from 2 April 2011 to 8 May 2011.

The restoration involved the Nativity Sculpture, Marker Stone and Ashoka Pillar and its capital and have been carried out in the form of a practical training workshop to train the LDT Conservation Team in restoration activities. All restoration interventions are amply discussed in chapter 5. At the end of the training, technical documentations regarding the restoration procedures (Annex 6) and the restoration materials (Annex 7) were given to the team. In order to complete the supporting documentation for the training exercises, the ordinary maintenance rule was given as well. This is useful to preserve the state of conservation of the restored documents (Meucci, 2011).

3.1. Ordinary maintenance

Maintenance allows the preservation of the historical monuments from further degradation caused by the environment and human activities. Ordinary maintenance generally consists of simple actions that do not affect the state of the surface and these are easy to do. The choice of procedures is directly related to several factors, such as:

- the state of conservation of the goods (monuments, physical structures and components);
- the nature of the objects;
- the conditions of exhibition:
- the impact of the environment on the conservation.

The monuments recently restored in the Sacred Garden area differ in several of the above items and consequently need different maintenance procedures.

Ashoka Pillar and the Capital

The risk of degradation of this monument is high because of the continuous flux of pilgrims and the offerings they place upon it. The lower section of the Pillar and the inscription suffer the highest risk of damage because of both the proximity to the external protective fence and the nature of the offerings. These generally consist of organic materials that adhere to the stone surfaces. Furthermore, since the bottom of the pillar is wet because of the water capillary from the ground, the risk of degradation increases. The maintenance takes into account the necessity to remove all organic materials applied to the surfaces and the remedial action consists of:

- Removing the not surface powder with a dry soft brush;
- Washing the dirty surfaces with neutral soap solution and water using a soft sponge;
- Softly drying the surfaces with non-abrasive cotton.

The conversation team were reminded to avoid inadvertently damaging any of the structures with the following message:

BE CAREFUL: AVOID ANY USE OF ORGANIC SOLVENTS LIKE ACETONE AND ALCOHOL THAT WILL REMOVE THE PROTECTIVE LAYERS.

Nativity Sculpture

Due to its location, the lower part of the sculpture suffers the main risk of degradation both because of the impact of the visitor's activities and of the microclimate. Nevertheless, the light impacting the surface of the top of the sculpture might be harmful as well.

The routine maintenance procedures consist of:

- Periodically removing the powder that does not adhere to the surface area by wiping with a dry soft brush;
- If necessary, washing the dirty surfaces with a vegetable green soap solution and water using a soft sponge;
- Softly drying the surfaces with cotton.

Marker Stone

The peculiar location of the Marker Stone increases the risk of damage owing to the microclimatic conditions and the necessity to be protected against the impact of the pilgrims. The temporary protection with the existing box do not works properly because of the increase of the relative humidity due to the reduced exchange of the air, but it is necessary to avoid the offerings that directly impact the monument.

The routine maintenance consists of:

- Avoiding offerings being deposited in the area surrounding the Marker Stone;
- Reducing the level of artificial light to the minimum;
- Regularly cleaning the surroundings of organic materials and dust;
- Switching on the UV lamp every two days during the night;
- If necessary, spraying biocide solution on the Marker Stone and its surroundings and waiting two weeks to assess the efficacy of this treatment.

BE CAREFUL: AVOID CLEANING THE MARKER STONE WITH WATER AND MECHANICAL TOOLS:

AVOID ANY USE OF ORGANIC SOLVENTS AND CHEMICALS TO CLEAN THE STONE'S SURFACE.

4. Characterization of the original materials and their degradation

Analytical investigation are necessary to correctly individuate the most proper and suitable methodologies and materials to carry out the restoration with conservative intent. Owing to the religious significance of the monuments, only a very limited number of samples were taken from the Marker Stone, Nativity Sculpture and Ashoka Pillar; on the contrary, a very large number of samples have been extracted from the masonry within the Mayadevi Temple aiming to assess the degradation mechanisms and to individuate the best restoration solutions. The

analytical activity started In 2011 and was concluded In 2013, being developed in several steps both in the laboratory and on site.

The scientific restoration process needs precise knowledge of the original materials and of the degradation processes before the restoration can commence. The same philosophy was applied to the restoration of the archaeological monuments in the Sacred Garden of Lumbini, namely: the Marker Stone, Nativity Sculpture and Ashoka Pillar. The investigation activity was accomplished in two different phases directly connected with the practical training carried out in February and in March-April 2011. The knowledge process took into account both the distribution of the typical damages; directly recorded observing the monuments; and the analytical investigations carried out on the samples taken during the field activities. In the year 2011, only 15 samples were taken from the three monuments during the restoration process (Table 1) in order to assess the composition both of the original materials and of those used for the restoration, as well as the degradation products. The results of the analysis carried out on each sample are summarized in the analytical cards collected in the Annexes 8, 9, 10, 11 and 12.

4.1. Marker Stone

The samples taken from Marker Stone (MS) pertain to the powder that is in contact with the monument and that was collected without affecting the integrity of the stone. This philosophy of sampling was necessary to avoid detaching even small stone chips from the sacred relic. As in the sample cards (Annex 8), the samples were collected by using a soft brush from the top and from bottom of the MS respectively, aiming to individuate the presence of dangerous chemical compounds, which potentially affect the conservation of the monument.

The mineralogical composition of both samples (Table 2) confirms that the powder that deposits around and on the Marker Stone probably comes from the soil; quartz is the most abundant component, while micas-illites and calcite are secondary. The two samples differ because of the presence of chlorites in MS2, which pertain to the ground, and of the gypsum in MS1. This compounds pertain nor to the stone composition, neither to the soil; thus, gypsum may be considered an environmental pollutant, or the result of the primary degradation of the Marker Stone by gaseous aggressive pollutants.

Determining the concentration of the soluble salts in both samples (Table 3) allowed the conservationists to verify that no soluble components came from the soil; on the contrary, both sulfates and nitrates concentrate on the exposed surface (fig. 1), confirming their provenance from the environment. In particular, gypsum seems to be a pollutant component, which may originate both from the fine powders dispersed in the air and from the gaseous atmospheric pollution rich of Sulfur dioxide (produced both by diesel engines of the power generators and from the brick firing kilns and other industrial activities).

The presence of nitrates, on the contrary, is generally related to biological pollution, due both to the green algae developing on the surface of MS and to the presence on the site of mice and other small animals. Nitrates are, indeed, the degradation products of organic compounds, which in the present case, derive from both the proteins of the cellule walls and animal droppings, as well as the offerings of the pilgrims. However, the presence of mice and

other animals increases the external contribution to the organic pollution in contact with Marker Stone.

4.2. Nativity Sculpture

Sampling aimed to characterize all products pertaining to the original substratum, as well as the materials applied in the restoration and the extraneous materials coming from the interactions with the environment and eventually deposited on the surface. Looking at the cross section of a small scale of stone (see Annex 11) allowed the conservationists to determine that the texture is clastic and that the micritic cement is composed of silicate compounds, mixed with clay minerals. Angularly-shaped quartz prevails in the skeleton, but feldspars are also present. Hydrated iron oxides and hematite crystals are homogeneously distributed in the cement justifying the red colour of the stone. The mineralogical composition of the stone substratum (Table 4) confirmed that quartz and feldspars are the basic components of the stone, to which micas-illites also pertain. On the contrary, calcite, dolomite and gypsum are components extraneous to the stone composition and might come from the polluted environment.

The salt concentration of samples NS1 and NS2 (Table 5) indicated that atmospheric pollution plays a double role in the degradation process; the air-dispersed powder contains some sulfates and chlorides, while nitrites and nitrates derived from the biological degradation of the organic materials (probably the same that affect the Marker Stone). The degradation of the stone indicates that gaseous sulfur oxides also act on the stone matrix, generating a relevant quantity of gypsum, which causes powdering and scaling of the stone. The small quantity of oxalates may be related to the degradation of organic materials like proteins and oils that are applied to the surface through the pilgrim's offerings. This degradation mechanism is preferably activated by humidity and bacteria, but all micro-organisms are effective as well.

As for the protective layers applied during the last restoration, the micro-FTIR analysis carried out on sample NS3, allowed individuating three different layers (fig. 2). Table 7 summarizes the information obtained by micro-FTIR analyses performed using a spectrometer connected with a microscope. The inner layer N3-1a shows the presence of natural ochre, which may be assigned to the hydrated iron oxides contained in the soil. That means that a thin layer of dust, made of soil powder, deposits on the exposed surface of the sculpture contributing to create a brown adhering patina. The subsequent application of a vinyl resin, which in Europe is commonly called Vinavyl or Vinapas, contributed to consolidate the layer, creating the hard patina covering the sculpture.

The medium layer that contains inorganic silicate compounds, pertaining both to the component of the soil and the substratum, might be identified as a concretionary layer probably produced by the deposition of air-dispersed powders. This seems to be confirmed by the presence of carbonate compounds, which are absent in the stone composition. The last layer NS3-1c represents the external surface of the Nativity Sculpture and shows the remains of the organic compounds used for the protection of the stone, that is an Acrylic resin, which may be identified as poly-methyl-meta-acrylate Paraloid B72.

4.3. Ashoka Pillar and Capital

The samples taken from the Ashoka Pillar may be divided in two series: the samples pertaining to the pillar (namely AS1, 2, 3-1, 3-2, 7,8 and 9) and that from the capital (AS4, 5 and 6), as described in Annex 8. As for the Sample Description Cards, specimens pertain both to the stone materials and to the possible degradation products or intentionally applied materials. Since the state of degradation of the two stone artifacts differ, the results of the analytical investigations will be discussed separately.

4.3.1. The pillar

The column was originally carved in a sandstone quarry in the North of India (Bidari, 2007). The stone is characterized by the abundance of silicon oxide (quartz) and other silicon compounds, identifiable as feldspars. As reported in Annex 9 - Petrography Analytical Cards, the rock shows a clastic texture (fig. 3) with crystals of quartz dispersed in a microcrystalline matrix mainly composed of quartz and clays; hydrated iron oxides are mixed to the cement as well. Some elements of the skeleton are rounded denouncing an aerial corrosion process (generally produced in desert environment). The presence in the matrix of small quantities of clay materials (Table 7) indicates that the deposition occurred in a water basin, where silicates degraded producing clay.

However, the structure is compact with a small porosity, generally inter-granular, and round shaped.

The matrix of the stone do not shows signs of degradation, but, on the external surface, some crystals of gypsum growth perpendicularly to the surface. This confirms that the industrial pollution directly affects the area surrounding the Sacred Garden. The results of the micro-FTIR analysis (see Annex 10) confirmed that the external layer of the Pillar surface contains gypsum mixed with acrylic resin, identified as Paraloid B72 (Table 8). The sample analyzed shows a very interesting stratigraphy owing to the presence on the stone surface of three different layers (fig. 4).

Looking at Table 8 makes it possible to verify that the surface of the stone is affected by the presence of proteins, mainly due to the pilgrim's offerings. The second layer is composed of natural ochre that may be attributed to the soil powder deposited on the surface by the wind and glued on the surface by the subsequent application of the acrylic resin (Paraloid B72). Finally, the most external layer contains crystals of gypsum, probably due to the influence of industrial pollution.

The presence of several over imposed protective and degradation layers on the stone surface of the Pillar is also proved by the SEM/EDS analysis carried out on a small chip of stone. Table 9 summarizes the most important data offered by the analytical technique, while the detailed analytical data for each sample are reported in Annex 11 - SEM-EDS Analytical Cards. The data of Table 9 represent the complete stratigraphy of the Pillar obtained by comparing the composition of the different analyzed areas. The presence of the organic protective layer (fig. 5) corresponds to the highest concentration of carbon (C). At the same time, the concentration of silicon, which is the main component of the stone, decreases, while that of the iron slightly increases. This is caused by the natural degradation of the sandstone, whose external surface changes in composition because of the impact of the air pollution and of the sun rays. Furthermore, the air pollution changes the composition of the external layer

owing to the deposition of dust and mineral particles produced by the industrial activity in the surroundings. Figure 6 shows how the composition of the external layers changes owing to the pollution.

The highest values of the iron concentration correspond to the stone surface, whose colour is justified by the presence of hydrated iron oxides in the texture. The iron concentration decreases in the organic protective layer but increases on the exposed surface because of the deposition of the soil powder. Calcium shows the same trend, though the concentration values are smaller as well as that of magnesium. The presence of these elements confirms the deposition on the surface of the Pillar of the air-dispersed powder containing calcite and magnesite - both connected to cement production. Finally, the presence of small quantities of sulfur, whose concentration increases at the external layer, demonstrates that the air pollution directly impacts the monument, affecting its conservation. The damage produced by the gaseous acidic pollution (mainly due to sulfur oxides) consist in the chemical degradation of some components of the stone (preferably feldspars) and in the increasing of the external porosity, which causes the chemical corrosion of the stone.

Indeed, observing the surface of the Pillar, a peculiar degradation pattern was individuated; the micro-scaling and powdering starting from the black spots. Since the black spots are homogeneously distributed inside the matrix of the sandstone, this degradation risks affecting large parts of the Pillar. In order to define the mechanism and the causes of this peculiar decay, two small samples were taken from the degraded areas of the monument.

The first (sample AS7) represents the scaling pattern, while the second (sample AS8) is constituted by the powder inside the black spot that are part of the stone texture. During the sampling, we noted that the powdered spots were more soft than the areas that were not decayed and that the micro-fissuring directly started from the inside of the degraded black spots. Thus, the original material must have suffered some chemical transformation changing the mineralogical composition of the black spots.

Figure 7 shows how the chemical elemental composition of the stone changes according to the degradation. Sample AS7 clearly indicates that the degraded areas differ from the average composition of the matrix mainly in the potassium (K) and alum (AI) content; this means that the black spots, which contains chlorites and feldspars, transform in clays when acidic solutions are deposited on the stone surface. The effects of this chemical reaction are more evident in the sample AS8, where the concentration of alum and potassium increases because of the high degradation of the stone. Furthermore, when the black spot degrades, the iron content increases owing to the destruction of the matrix, caused by the acidic attack. This is proved by the presence in the spectra of small quantities of sulfur, which is related to the industrial pollution produced by the boundary industries.

4.3.2. The Capital

The X-Ray diffraction analysis of sample AS6 (fig. 8) shows the presence of amorphous materials and traces of gypsum that are the only compounds extraneous to the stone composition (see Annex 12). This, in fact, pertains to a sandstone, whose main components are the feldspar, while chlorites and micas are secondary. The peculiar degradation observed on the vertical surface of the Capital and the micro-scaling affecting the stone may be due to the influence of the climate and also to the chemical aggressiveness of the air pollution.

However, the degradation mechanism should be peculiarly investigated in order to really understand the impact of the pollution on the degradation of the stone. On the contrary, the impact of the anthropoid presence on the degradation mechanism of the monument clearly appears: FTIR analysis carried out on the patina samples collected from the top of the Capital (see Annex 10 - FTIR Analytical Cards) confirm the presence of several organic compounds that pertain to different organic materials (Table 10).

Polysaccharides and proteins are the main components of the organic materials applied as offerings (fig. 9) directly on the top of the Capital. Also the grease compounds (often containing ester groups, generally referable to oils) pertain to the worship practice, as confirmed by the presence of abundant calcium stearate, which is the main component of common candles. Thus, the human presence and associated religious activities caused the dark-grey and black patinas that cover the surface of the Capital and hide the natural original pink color of the stone. However, all these materials do not act chemically on the stone, but induce the growth of micro-organisms that might directly affect the stability of the stone matrix. The same could happen when pigeon droppings impact on the stone surface, owing to the high content of phosphoric acid of the excrement. In all cases, since the organic compounds deeply penetrate the stone, all chemical reactions connected with their presence will develop inside the stone porosity, changing the equilibrium of the stone's material.

4.3.3. The restoration materials

The restoration materials were applied to the monument in order to increase the stability and to protect it from mechanical stresses. According to this approach, metallic belts and epoxy plaster respectively were applied on the Pillar. Studying these materials allows an appreciation of their impact either on the degradation and the conservation of the monument.

4.3.3.1. Metallic belts

The metallic belts were not analyzed since their composition is known and they pertain to an alloy of different metals with copper as the predominant metal. The damage potentially induced by the belts are both mechanical and chemical. In the first case, increasing the pressure on the contact surface between the stone and belt may generate micro-fissuring of the stone. In the second case, corrosive products may act directly on the surface of the stone. Figure 10 clearly shows how the presence of the belt increases the deposition of dust and the rate of the corrosion process. The light brown dust deposit (left side of the picture) formed inside the small space between the stone surface and the belt and its thickness increased because of the percolation of the rain water. The water absorbed by the dust deposit activates the corrosion processes of iron and copper and the chemical compounds produced by the chemical reactions accumulates in this space. The shape of the hydrated iron oxides (the rust) and of the black iron compounds on the right side of the figure confirms that the corrosion process is cyclic. Finally, since the corrosive products diffuse inside the porosity, the stone will be affected by reddish spots that are very difficult to remove.

The analytical results (see Annex 11, Cards $4-1 \div 4-4$) confirm that the corrosion process involves the metallic components of the belt. Indeed, the main components of the layer between the stone and the belt contain iron and copper, plus the prescence of molybdenum (fig. 11) due to the use of some kind of special alloy. Comparing the distribution of sulfur and calcium (fig. 12) allowed the investigators to deduce that gypsum forms a crystal felt inside the silicon, characterized by the ground powder (fig. 13). However, sulfur is homogenously

distributed in the dust layer, as well as calcium. This implies that the direct impact of the environment on the exposed materials. On the contrary, iron, which is one of the common components of the ground powder, increases in concentration in small areas only where the corrosion processes prominently occur. No peculiar distribution of copper was identified - probably due to its low concentration in the sample.

4.3.3.2. Mortar

The materials used in the restoration of the Ashoka Pillar consist in the mortar applied to fill the joint between the Pillar and the cap and the epoxy plaster applied to fill the vertical fissure affecting the stability of the Pillar. The mortar applied to fix the stone cap of the Pillar was achieved in two separated layers that slightly differ in colour and texture (fig. 14). In spite of the appearance, both layers contain neither cement, nor gypsum, as confirmed by data reported in Annex 13 – HPLC Analytical Cards. On the contrary, both plasters were made by mixing lime with sand. The mineralogical composition of samples is resumed in Table 11. Comparing the data emphasizes the similarity in the composition: both mixtures contain quartz and micas as an aggregate fraction (see Annex 12 - XRD Analytical Cards), while dolomite may relate both to the added fraction and to the binding lime fraction as an impurity of the original limestone.

Simlarly, the presence of vaterite and portlandite in the mixtures is due to the differences in the chemical reactions involved by the hardening process. Portlandite is in fact the calcium hydroxide [Ca(OH)2] that did not react with the carbon dioxide to form a solid calcium carbonate which hardens the mortar. The presence of portlandite in the inner layer of mortar demonstrates that the lime did not complete the hardening process because of two different factors: the lack of carbon dioxide due to the application of the external mortar layer; and the use as a binder of calcium oxide instead of the hydrated calcium oxide.

When the binder is calcium oxide, the water added to the mixture is insufficient to guarantee the complexion of the carbonation because water is also necessary to evolve the calcium oxide hydration process - which is energetically preferred. The drying of the mortar and the reduced capability to absorb carbon dioxide from the environment caused the hardening process to slow down. Furthermore, the use of calcium oxide as a binder seemed to be confirmed by the presence of vaterite in both layers. Vaterite is a meta-stable phase of calcium carbonate which may form in mineral springs and also in saturated portlandite solutions at a low temperature and with a lack of water (Albright, 1971). Since the presence of water, vaterite converts into calcite, which is the most stable phase in room conditions, the presence of the mineral in both layers confirms the use of quick lime as binder in a mixture with an insufficient content of water. Furthermore, the high temperature reached through insulation increased the water evaporation rate, thereby reducing the capability of portlandite to react and conver into calcite.

4.3.3.3. Epoxy plaster

The plaster used to fill the vertical fissure – which affects the stability of the Pillar – results from a mixture of epoxy resin and a sand rich with natural yellow earth (see Annex 10 – FTIR Analytical Cards, Card N° 2). The mixture is compact and relatively hard – confirming that the resin used to produce the plaster did not relate to the class of the hardening epoxy resin, but to that of the epoxy glues. However, FTIR did not show the presence of any degradation products, which degrades the mechanical resistance of the plaster.

4.4. Conclusions

The laboratory investigations carried out on the 15 samples taken from the three monuments (Ashoka Pillar; Nativity Sculpture; and Marker Stone) allowed the collection of most of the available information, both on the original materials and their degradation mechanisms, and also on the nature of the materials used in the old restorations.

4.4.1. The original materials

Owing to the immense religious value of the Marker Stone, the sampling of original materials was possible only from the Nativity Sculpture and the Ashoka Pillar. The small chips of stone pertaining to the substratum of both monuments analyzed were strictly connected to the degraded material. Thus, the information collected was limited to stone identification and it was impossible investigate their provenance.

The sandstone of the Ashoka Pillar is well known to archaeologists because of historical information about the quarry from which the column was excavated. The petrography confirms that the texture of the stone is mainly due to the aggregation of feldspars and quartz crystals, homogeneously dispersed in a matrix that also contains clay minerals and iron oxides. The shape of the skeleton indicates that the sandstone originated from an origin in a water basin of two mineral fractions: the oldest is round; while the most recent is angularly shaped. However, the stone is compact and the porosity is low and homogeneously diffused in the matrix. The black spots present in the matrix are mainly composed of chlorites and feldspars. These play a fundamental role in the degradation processes, owing to the chemical reactions with the acidic pollutants.

The Nativity Sculpture texture shows the presence of different facies of sandstone; the matrix is made of micro-crystals of silicate compounds and quartz, and hydrated iron oxides and hematite crystals as well. The skeleton is represented by pheno-crystals of quartz and feldspars. The presence of abundant hematite justify the reddish color of the stone, due to the casual distribution of the oxide in the matrix, which was generated by the alternative deposition in a dry environment of sand particles and clay minerals which are rich in iron oxides.

The Capital may have a similar composition but since the only information we have about the material is derived from the SEM/EDS analysis, it is impossible to determine the texture and the structure of the stone. However, the pink colour of the cleaned surfaces indicates that the matrix of the sandstone probably includes red hematite crystals.

4.4.2. The old restoration materials

The analysis carried out on the samples taken from the Nativity Sculpture and Ashoka Pillar confirmed the use of synthetic materials in the restoration of both monuments. The Nativity Sculpture was treated with two different products, whose action differs owing to the different chemical composition. Since the vinyl resin is the main component of some common industrial glues (Vinavyl or Vinapas), the treatment of the stone surface with this compound allowed a hardening of the eventually degraded areas, but the water adsorption was reduced as well. The subsequent application of an acrylic resin, which was identified as Paraloid B72, increased the waterproofing of the exposed surfaces, but also the capability of the dust adhesion because of the increase of the dielectric power of the treated surfaces. At the same time, both treatments contributed to a change in the colour of the stone from a reddish hue to

deep brown. Furthermore, the presence of these synthetic layers induced the activation of some peculiar degradation processes, ranging from the darkening of the surface to the chemical aggressiveness of the pollutants. In the case of the Ashoka Pillar, the restoration materials varied in a wide range, from the mortars applied on the top of the column, to the metals of the belts rimming the pillar.

Though the belts do not affect directly the conservation of the stone, their composition seems to be affected by the environmental pollution detected in the area. The corrosive products, indeed, contributed to a change in the colour of the stone in the areas that are in contact with the belts. However, the role played by the metallic rings is fundamental in guaranteeing the stability of the pillar. The same function was played by the epoxy plaster applied to fill the vertical fissure, affecting the pillar from bottom to top. The analysis confirm that the plaster was obtained by mixing a commercial epoxy resin with sand. During the last restoration, we ascertained that the plaster did not fill completely the fissure and that it was a little elastic and soft, probably due to the use of an adhesive epoxy resin.

As for the traditional mortar applied to fill the connection between the top of the pillar and the cap, the analytical results confirmed the use of traditional materials such as lime and sand, but the practice to use quicklime instead of hydrated lime for the mixture ensured that the hardening process was not completed. Indeed, the inner layer of the mortar contains calcium hydroxide (portlandite) that forms by the hydration of the calcium oxide, and vaterite, which is a calcium carbonate that forms by the portlandite carbonation in a deficiency of water. The detection of an acrylic resin on the external surface of the pillar confirms the use of Paraloid B72 (or a similar compound) as a waterproofing agent.

4.4.3. The degradation mechanisms

Comparing the results of the analysis carried out on the three monuments allowed us to verify that the Sacred Garden area is polluted by air dispersed gaseous and solid compounds, as recently confirmed by the EIA report. The Marker Stone shows the presence of several soluble salts in the dust deposited both on the surface and on the pavement. Figure 15 clearly displays that all anionic species are abundant on the surface, except for the nitrites, which are the first step of the degradation of the organic substances (mainly proteins) induced by microorganisms of the nitrogen cycle (both fungi and bacteria).

Sulfates are related to the presence of crystalline gypsum that may be considered a pollutant of the dust, while nitrates are due to the same demolition cycle that originates nitrites. The source of chlorides is difficult to individuate because of the lack in the surroundings of heavy industries (metallurgical and similar) that use hydrochloric acid. However, it is possible to hypothesize that chlorides are derived from the soil or from underground water, but this hypothesis needs further analysis for it to be confirmed.

The chemical and mineralogical composition of the dust collected on the top of the Nativity Sculpture confirms that the air dispersed fine powder is polluted by the presence of compounds, namely calcite, dolomite and gypsum, whose composition differs from that of the soil.

The location of the samples taken from the Nativity Sculpture allowed us to verfify that the soluble salts (fig. 16) originate from different sources. Indeed, while nitrites and nitrates may be due to biological degradation mechanism, which involves the organic materials layered on

the surface by the pilgrims, oxalates are produced by the chemical degradation of proteins and oils by peculiar species of fungi and bacteria in a humid environment. All these compounds are present in the dust, thereby confirming that the inside environment of the Mayadevi Temple is heavily polluted owing to the diffusion in the air of all degradation compounds produced at the ground level.

The distribution of these solid pollutants in the air is probably due both to the natural circulation of the air and to the presence of pilgrims and their activities. On the contrary, gypsum could be produced by two different mechanisms, both related to air pollution. In the first case, gypsum is one of the solid components of the dust, while in the second case, gypsum may be derived from the direct chemical interaction of sulfuric acidic solutions within the stone matrix. The SEM/EDS analysis carried out on sample NS2 (fig. 17) confirms that the degradation of the stone matrix is also due to the chemical reaction of some components (mainly feldspars) with sulfur dioxide. Indeed, the three layers identified in the sample (inner, middle degraded and external surface) are represented by the fingerprint curves of figure 18: both in the inner layer and in the middle degraded layer of the stone. The chemical degradation caused the matrix to be partially destroyed; producing an increase in the concentration of gypsum (fig 19). On the contrary, the external layer shows the increase of carbon and oxygen concentrations owing to the presence of organic restoration compounds.

The investigations carried out on the samples taken from the Ashoka Pillar allowed us to precisely individuate the origin of some pollutants and the degradation mechanism involved. Gypsum, calcite, dolomite and magnesite are present in the form of the fine powder that deposits on the surface: all compounds are part of the cement production cycle, both as primary components of the clinker (calcite, dolomite and magnesite) and as a secondary component, adding to the clinker to regulate the hardening process (gypsum). Crystalline gypsum and sulfates are present in the degraded organic patinas on the Capital and also in the dust deposit beneath the belts justifying their possible double origin. Furthermore, the gypsum crystals that form inside the black spots are due to the direct chemical reaction of the mineral components of the spots (chlorites and feldspars) with the acidic solutions produced by the atmosphere polluted by sulfur dioxide. Owing to the chemical degradation, the spot matrix softens, while the growth of the gypsum crystals causes the fissuring of the stone matrix close to the degraded black spots. The same mechanism happens inside the dust deposit between the belts and the pillar: here, the water retained by the dust increases the rate of the chemical reactions inducing the generation of a felt of gypsum crystals that act mechanically on the stone surface producing micro-fissuring and micro-scaling. The effects of the chemical corrosion of the stone may be also observed on the southern side of the Pillar where a large part of the surface is deeply corroded according to the water flowing lines. In conclusion, the analytical investigation converged to identify in the atmospheric pollution (most probably induced by industrial activity) one of the main causes of degradation - but all human activities near the monuments contribute to their degradation according to the numerous and very complex biological and chemical mechanisms involved.

4.5. Masonry

The present chapter summarizes the results achieved both during the field activity, and by the lab researches and analysis in the period dating from January 2011 to January 2013. The activities were carried out by the following team:

Coordinator: Costantino Meucci

Researchers: Daniela Ferro (CNR – Rome)

Maria Pia Sammartino (University of Rome "La Sapienza")

Giovanni Visco (University of Rome "La Sapienza")

Anna Candida Felici: (University of Rome "La Sapienza")
Loredana Carratoni: (University of Rome "La Sapienza")

Restorers: Domizia Colonnello, Serena Finocchio

Students: Ilaria Marzocchini

Gaia Quattrociocchi

Ilaria Serafini

Two months after the 2011 mission, on March 2011, Ms. A.C. Felici left the project.

4.5.1. In situ XRF analysis

The analysis was performed by using a portable instrument supplied by the Ars Mensurae Company of Rome and managed by Ms A.C Felici and Ms G. Quattrociocchi; the characteristics of the instrument and operative conditions were:

Tube mini-X with anode Au, working at : V = 30 kV I=15 μ A t=180 s.

The analysis aimed to verify the possibility of determining the elemental composition of reference bricks pertaining to several building phases of the temple. They were selected according to the assessed archaeological chronology of the structures. The following sectors were tested within the Mayadevi Temple:

- Trenches C5, C7, C13;
- · Walls South and West;
- Central Core;
- Bricks recovered by the archaeological team from Trench C5 and dated to the pre-Ashoka period;
- · Bricks from C8 damaged by efflorescence.

The other goal was also assess the reliability of the technique in determining the chemical composition of the fired bricks in order to characterize each chronological phases on the base of the brick composition and technology. The obtained results confirmed the relative usefulness of the technique because of the great variability of the recorded data and their casual dependence from the brick texture. Nevertheless, all recorded data will be discussed and aim to individuate a common fingerprint useful to discriminate the chronological sequence.

Pre-Ashoka bricks from Trench C5

The tall bricks recovered from the platform of the pre-Ashoka phase of the Temple (Coningham and Acharya, 2011) found in Trench C5, were subjected to XRF analysis (figure 20) owing to their peculiar size and apparent texture; indeed, they appear very porous and fragile because of the great abundance of straw mixed with the clay and the apparent low-firing temperature. Before performing the analysis, small areas of the brick surfaces were mechanically cleaned by scalpel to prevent the mud layer adhering to the surface which alters the compositional values.

A comparison of the elemental content percentage deduced by the single spectra allowed the team to verify that the peculiar texture of the bricks may greatly influence the chemical composition of the sample (figure 21) for the secondary and traces elements since the very high content of iron strongly reduced the significance of the analysis.

The left chart clearly shows that the only element affected by the brick texture is calcium, whose abundance varies from 0.53 per cent to 14.21 per cent probably due to the composition both of the clay and of the temperature. The right chart, on the contrary, confirms that all the metallic elements have a little change in concentration probably depending on the nature and provenance of clay and temper. The most significant variations regard zinc, zirconium, barium and lead that may be related to the nature of brick components.

In particular, referring the zirconium content to that of the manganese allowed us to verify that most of the samples were concentrated in a restricted cluster as shown by figure 22, even if the elemental composition may differ slightly according to the peculiar production technology (presence of straw, abundance and composition of temper, etc.). Nevertheless, the presence of zirconium seems to be directly related to the nature of the sandy temper, since this element is a common accessory mineral of igneous rocks, such as syenite, granite and diorite that arer concentrated in beach sand and it is generally found in association with ilmenite, rutile etc. as it occurs in the sand on beaches in Australia, South and West Africa and India (Duggan, 1988).

The same origin of these bricks is also confirmed by the concentration of the samples in the restricted cluster individuated by the Zn versus Pb chart of figure 23: the two elements are, in fact, generally associated in the same deposits and their presence is reported in 49 localities in different parts of Nepal. On this basis, it seems possible to distriguish bricks according to their chemical composition and the provenance of the temper.

Trench C5

Owing to the discovery of the aforementioned bricks, the C5 trench made it possible to link the chemical composition of the bricks with the archaeological stratigraphy, as shown in figure 24. Represented in the chart is the manganese content versus the zirconium percentage. This do not help in identifying the chronological sequence because of the variability of the chemical composition of the C5 brick samples (figure 25): contrary to the sequence of figure 5, samples C5R2, C5R3 and C5R5 only better fit with the reference MD samples, while C5R0 and C5R1 greatly differ, as well as the C5R4 sample. This is probably due to the use of recycled materials in the rebuilding of the temple and also possible differences in technology, the origin of the clay and the temper. Comparing the composition of the C5 samples confirms that the calcium content varies in a wide range (from about 2 per cent to about 16 per cent) owing to the different composition of the clay and the temper.

Trench C7

Trench C7 shows the complete sequence of the Ashoka building phases that are differentiated in the southern and northern walls by an offset at about 87 cm high from the pebbles on the ground. This probably corresponds to a new building phase, which developed in the second Ashoka or Muryan phase of the use of the temple. Furthermore, the sequence is congruent with that of trench C5 where the building phase has been more precisely individuated owing to the presence of the pre-Ashoka platform. Nevertheless, the comparison of the XRF data did

not allow individuating significant differences in the elemental composition of the bricks, probably due to the inefficacy of the analytical technique.

Trench C13

The element content values are widely dispersed in the series, confirming that the indetermination of the analyzed area and the geometry of the detector may affect the recorded spectrum and then the significance and reliability of the measure (figure 27). Nevertheless, the presence of significant quantities of copper in sample C13R4, which was taken from the highest raw brick, indicates that this level probably hosted metallic elements made of copper alloys, with reference to the decoration of the temple.

Wall South & Wall West

The comparison of the analytical data recorded on both walls shows that the brick rows may be ascribed to different building phases (figures 28&29). The lowest level of the walls pertain to the first phase that is commonly identified as Ashoka. A second phase may be ascribed to the ten rows above the ground floor since their compositions are very similar as for the Zr and Mn content.

This second phase may also contain sample WS6A owing to its location in the cluster defined by all the phase II samples. The upper rows of the West Wall, on the contrary, defines a fourth phase, which might correspond to a different building phase. However, the ascertained rebuilding phases using original ancient materials and techniques make it very difficult to identify the restoration intervention and consequently define the best compositional fingerprint that may allow an identification of the bricks of several archaeological phases as described by the reference literature on the basis of shape and size (Mishra, 1996). Since the brick composition may vary in both clay origin and tempera quality, a more complex analysis is needed to characterize the masonry of each building phase.

Central Core

Nevertheless, the central core of the Mayadevi Temple is the most complex masonry to be investigated from a chronological point of view. The XRF in situ analysis confirmed that they are similar except of samples C7, which were taken from the decorated bricks of the Gupta period at the top of the structure. Comparing the distribution of the central core samples with those of the external walls and of the reference pre-Ashoka MD-C5 bricks (figure 30) allowed the investigators to verify that all the CC samples are aligned in a very restricted range of Mn per cent values, while the Zr per cent range is wider, as well as for the Md-C5 samples. On the contrary, as for the Mn content, both WS and WW samples greatly vary while the Zr per cent range is very little, probably due to the fact they belong to different building phases.

Figure 31 shows how the two groups of samples, taken from the trenches and from the external walls respectively, distribute with respect to the MD-C5 pre-Ashoka bricks that we consider as reference samples. The cluster grouping the bricks of the trenches quite perfectly overlaps with that of the reference samples, while the wall samples distribute in a wider cluster all around the MD-C5 samples, thereby confirming the possible different origin of clay and temper. Contrary to these peculiar distribution patterns, the comparison of the iron and calcium content of all samples gives the possibility to ascertain the influence and significance of the main components of the bricks on their distribution in the binary chart Fe versus Ca (figure 32). As the chart shows, all samples align very close to the trend line, but they

distribute in a different way probably according to the different chemical composition of the body. Although this result encourages the use of the XRF analytical technique that aims to identify the fabric composition without sampling the brick, the large variability of the experimental values and problems induced by the necessity to use the instrument in a difficult environment as in the Mayadevi shelter (the technique needs electricity to work properly and the X-Ray emission may be dangerous for the investigators) make the method unreliable and not responsive to analytical needs. Nevertheless, the preliminary results helped in the selection of samples to submit to the laboratory analytical protocol.

4.5.2. Colour analysis

The instrumental measure of colour is the analytical technique that may allow the investigators to identify differences in the brick masonries that exist within the Mayadevi Temple. The colour of the superficial layer of the bricks depends on several factors, such as: firing technology, clay composition, degradation and restoration, as well as water content. During the field activity, several on site investigations were carried out on the same measuring points in order to compare the recorded values and to merge the information they contain.

The first problem posed by the technique is the reliability of the data since both the state of conservation and the cleanness of the exposed surfaces may affect the measure. However, increasing the number of determinations makes it possible to do the statistical evaluation of the data and verify the significance of the calculated colour values. Thus, mathematically processing the experimental data allows drawing the graphs of the following figure 33, where the probability that the true value is similar to the average value is graphed versus the differences of the average of the experimental values with the average value of the color ΔE , which is calculated with reference to the white instrumental colour values.

A similar trend is shown in the charts of figure 34 where the maximum variation was detected in the North Wall of the Central Core where several phases and collapses are present. Most of the values concentrate in the restricted range that varies about ± 5 from the average. Comparing all the experimental data allowed the ivestogators to verify that the absolute colour decreases from the bricks of the trenches to the wall masonry, probably due to the water absorbed by capillary by the deepest brick rows inside the trenches (figure 35). Owing to the complexity of the problem, in this section only the colour values are discussed; conclusions about the interpretation of the analytical data is discussed later. Nevertheless, analyzing the trend of the brightness and colour values in the opposite walls of Trench C, located in the north-west corner of the temple (figure 36), we notice that the brightness varies with the height, increasing in the most exposed rows.

However, the differences in the colour values may indicate that the two walls were built using bricks of different origin, even if the water content unquestionably influences the colour value. The lowest row probably contains bricks of a different nature, as well as the upper rows that change in colour; furthermore, in both walls the evaporation affecting the highest analyzed rows allows the colour value to decrease owing to the whitening of the surface.

On the contrary, the trend of the other analyzed trenches (figure 37) is homogeneous and differs from that of the C-East and C-West walls: the brightness constantly decreases from the lowest to the upper rows, while the colour slightly increases. The differences in the colour average values of each row and trench may be due to all parameters characterizing the brick

body, such as the nature of the clay, production technology and firing conditions. Also the walls show variations both in brightness and in colour according to the height of the analyzed point. Generally speaking, the brightness tends to increase with the height in the Central Core because of the dryness of the upper rows, while in the west and south walls the brightness values vary in a very restricted range. As a consequence the colour changes in different ways according to the composition and production technology of the bricks, but also with their content of water.

4.5.3. Sampling and analytical planning

Aiming to characterize the building materials and their degradation mechanisms, several samples were taken from the onsite analyzed masonries and from the aquifer beneath the temple as well. Many samples were also obtained by the onsite analytical investigations, such as those coming from the salt extractions made by Japanese paper. The following table 11 resumes the complete list of samples, with reference to their location and significance, while Annex 14 contains the description cards of all samples. The listed samples have been subjected to several analysis in order to assess not only the composition and degradation mechanisms, but also ascertain both the possible provenance of the materials and the production technology of the bricks. The best compounds suitable for the masonry conservation were studied as well, in order to define the possibility to carry out the restoration of the Mayadevi archaeological remains in the unfavourable environmental conditions produced by the presence of the aquifer beneath the shelter.

4.5.4. Analytical results

This chapter summarizes all analytical results obtained both on site and in the laboratory in order to characterize the building materials and their degradation products. This allows individuating both the degradation mechanisms and the best solution for restoration. The building technique observed on site shows that the walls were built using fired bricks and a very soft mud mortar as bedding mortar that needs to be characterized as for the mineralogical composition and the firing technique in order to individuate the degradation mechanisms and the external causes of decay. This will help determine the best possible conservation solutions.

4.5.4.1. Mortars

The composition of the mud mortars used to assemble the masonry is one of the elements that we have to take into account in order to ascertain their factor in the degradation processes of the bricks and to determine the role they had in the compactness of the walls. The latter represents an approach to determine the possible contribution of the original mud mortar to the increase of the mechanical resistance of the masonry - that is the effectiveness of the restoration. Furthermore, assessing the chemical and mineralogical composition of the different mud mortars will help in individuating the best chemical compounds to apply in the restoration and also the behaviour of the restored structure in the actual conservation conditions.

According to these aims, during the mission held in February 2011, a limited number of samples were taken from the open trenches in order to preliminary investigate the composition of the mud mortars and the attachment they have with the brick in the vertical sequence which probably represents a chronological series. Table 12 lists all the samples taken from the masonry in 2011, while detailed descriptions of the mortars are reported in the Annex 15.

From the petrographic point of view, all samples are composed by an illite matrix that generally contains small quartz crystals and opaque minerals. Muscovite, hematite, hydrated iron oxides and spinel were all present as well. Table 13, which summarizes the data obtained by petrographic analyses, shows that the mortars are similar, except for the presence of rock fragments and chamotte; the latter is in fact a marker that allows the investigators to distinguish the different kinds of materials and mixtures used to assembly the masonry.

The mortar samples adhering to the bricks were analyzed by petrography, postponing to a second phase the study of the building technology. Like the previously discussed samples, the mud mortar adhering to the bricks is mainly composed of illite-montmorillonite silt that encloses the most abundant fraction of quartz and secondary feldspars (figure 38) that may be referred both to the natural mineral fraction of the soil and to the aggregate fraction, intentionally added to the mortar to regulate the shrinkage during the drying process.

The porosity of the mortar is generally high, ranging from about 10 to 20 per cent and it is due both to the evaporation of the mixing water and to the degradation of the masonry during the burial and after the excavation. This second life phase seems to be the most dangerous owing to the capillary processes and to the salt crystallization within the mortar. Indeed, the soluble salt content detected in some samples taken from Trench C7 (labeled as MD3-1 to MD8) compared with that of the clay taken from the lowest level in Trench C5 (figure 39). This indicated that some of the soluble chemicals are also present in the soil beneath the masonry, confirming that probably they come from the aquifer.

Observing the thin cross section of the brick samples taken on 2010 from trench C7 and connected with the mud mortars makes it possible to ascertain the presence of remains of a white layer mortar made by lime adhering to the brick surface (samples MD4, MD5 and MD6). As described in the petrography cards of Annex 3, this mortar is covered by the mud incrustation produced by the burial, but is generally layered on a surface different from that were the mud mortar is present. It is interesting to note that the composition of this mortar consists of a mixture of lime and quartz sand, mainly composed of white quartz, to which an aggregate fraction of spatic calcite is added (figure 40). It was noticed that in most cases the lime plaster is layered on a thin yellow patina made of silt which adheres directly to the brick's surface.

As reported in the petrography cards, the composition of this mortar strongly differs from that of the mud mortar and of the yellow patina, confirming that the wall was originally plastered and probably painted, owing to the presence of traces of black and red pigments on the external surface of the plaster. This presence, indeed, is in accordance with the yellow patina observed on the external surface of some brick samples taken from the trenches. XRD analysis performed on all the samples (see table 14) indicated that all the samples have a similar composition owing to the predominant presence of quartz, which is the mineral fraction of the aggregate – both natural and added to the mortar. Feldspars and plagioclases are also present, but in a different concentration, as well as calcite that is more abundant in the clay and soil samples. As for the clay minerals, both illite-micas and chlorites are commonly present, although in small quantities.

The same finely powdered samples were submitted to SEM-EDS analysis in order to quantitatively determine their chemical composition. As for the data resumed in table 15, the content of the prevailing components allowed individuating that all the samples have a similar

fingerprint, with small differences in the calcium content, due to the presence of calcite in the sample. On the contrary, trace elements vary significantly according to their provenance and origin. Comparing the content data (figure 41) gives a possible indication that the clay beneath the masonry in trench C5 (sample MD7) did not contains any elements except for a very low quantity of chromium, which is also present in the majority of the samples. On the other hand, most of the mortar samples have chemical composition similar to that of the external soil (sample SG1), confirming that they were obtained through mixing natural clay with the minimal fraction of soil able to reduce the shrinkage during the drying period. As for the presence of phosphorus, the maximum content was found in the soil, probably due to phosphate pollution, as well as sulfur that is a typical product of the polluted atmosphere.

According to the potassium and iron content, the samples may be grouped in two different clusters that refer to the clay and soil composition respectively (figure 42): as previously reported, sample MD3-1 is similar to the soil sample, as well as the so called pavement MD8, which fills the external walkway all around the Mayadevi Temple. The presence of the yellow patina on a part of the analyzed samples needs to be better investigated in order to determine its chemical and mineralogical composition; nevertheless, all petrographic observation carried out on the thin sections allowed individuating some interesting information about the characteristics of these patinas. Figure 43 shows the stratigraphy of the samples according to their possible chronological sequence.

It appears evident that in the majority of the sequences, the lime mortar covers the yellow patina being generally present in all samples pertaining to the Ashoka phases I and II of the temple chronology. Thus, in this period the external surfaces of the masonry were finished with a white lime plaster this was probably painted. The presence in all samples of the silt yellow patina may be due to different causes. The mineralogical composition of the patina confirms that its main component is a silt, that is a granular material whose quartz particles range between 0.0039 to 0.0625 mm, and that may be generally mixed with clay in all sedimentary rocks and soils. Thus, the presence of the thin yellow layer made of silt may be due to the casual flooding of the area and the consequent deposition of the siliceous minerals suspended in the water of the river.

The second hypothesis is that the layer has been intentionally applied to the wall as a primer to prepare the surface for painting since the layer of clay reduces the absorption of the binder and the colour retains its proper brightness and tone. In both cases, covering the walls with the lime plaster must be related to a second living phase of the monument: in case of flooding, the plastering resulted from the intentional restoration of the building. In the second case the presence of the lime plaster indicates the intentional rehabilitation of the temple.

4.5.4.2. Bricks

The limited sampling carried out in February 2011 aimed to identify the composition and texture of the bricks in order to plan the analytical investigations. Petrography (see Annex 16) confirmed that the four samples taken from the East wall of trench C7 have a porphyric texture with a matrix containing illite minerals as the main component, while sparitic calcite is present in sample MD6 only. All samples, except MD4, contain straw remains, while temper differentiate because of the presence of limestone fragments in sample MD6 only. Quartz is the prevailing mineral of temper, while spatic calcite is present in samples MD4 and MD6. Chamotte in round particles is a common component of the body. The sampling held in the

year 2012 took into account the several building phases of the brick structures aiming to differentiate them according to their location and chronology. In particular, the open trenches allowed the collection of brick samples in the vertical sequence representing the most probable chronological series.

Composition and texture

The petrographic analysis carried out on the masonry samples confirmed that the bricks pertain to different groups according to their composition as the following table shows.

Group 1 is characterized by the presence of straw mixed with the clay (figure 44) to regulate the shrinkage during the drying and the firing. The texture is generally porphyric and the porosity varies in the range 10 ÷ 40 per cent, mainly due to the straw marks created by the firing (figure 45). The matrix is characterized by the prevalent presence of acicular crystals of feldspars and muscovite, often as illite minerals and by the secondary presence of hematite and spinel, while the sparitic calcite is sporadic and in the minority. The skeleton is composed of both stone fragments and crystals and chamotte particles are generally present. The only stone fragments detected pertain to mudstone and rarely to sandstone; their shape is generally sub-round owing to the soil degradation processes both in water and the open air. The crystalline fraction of the skeleton ranges between 10 and 40 per cent, while the shape is from angular to sub-round according to the origin of the crystals; the sub-round particles are generally minor in size and pertain to the clay, while the bigger angularly shaped particles pertain to a fresh quartz sand added to function as temper (figure 46).

Group 2 is the most abundant and is characterized by the absence of straw and in general by the absence of stone fragments in the skeleton, except for a few samples from trenches C7, C5 and CW where mudstone was detected. The matrix structure is mainly amorphous, but a micritic fraction pertaining to illite-muscovite is present as well (figure 47); also acicular feldspars and hematite are present, while sparitic calcite is mainly present in the mudstone added samples.

The porosity generally ranges between 10 and 30 per cent; the skeleton abundance is also in the same range $10 \div 30$ Per cent. The crystalline aggregate is mainly composed of quartz, which originiates both from the clay and from the temper: the last is bigger in size and generally sub-round and probably pertains to a quartz sand partly made smooth by water (figure 48). Hematite crystals are present, as well as hydrated iron oxides that mainly pertain to the matrix.

Group 3 (Subgroup 1) is composed by the samples that contain mudstone fragments (figure 49) added to the clay in order to reduce the shrinkage and is composed of samples pertaining to group 1 and 2. The petrography and composition are consequently to be referred to the previously discussed groups. However, the majority of the samples contain both straw and sparitic calcite. This sub-group indicates that in the preparation of the compound of clay the artisan used both organic and mineral fraction in order to reduce the shrinkage of the bricks. Also chamotte is generally part of the mixture, while sandstone fragments are sporadic and probably related to the chamotte, since sandstone is outcropping in the area and the main component of the powdered soil as well.

Group 4 may also be called Sub-group 2 because it is composed by elements pertaining to both Groups 1 and 2, and also to the Group 3 (or Sub-group 1); this group is characterized by the presence in the matrix of sparitic calcite (figure 50), as well as illite-muscovite minerals.

Although in some of the samples mudstone is found, the presence of calcite in the matrix indicates that it was a natural component of the clay, as well as the traces of pyroxenes. This allows individuating in the chemical composition of the bricks the possible marker to identify the nature of the clay materials used in the brick making. The distribution of figure 51 indicates that lower is the value of the SiO₂/CaO ratio higher is the calcium content, that is the calcium carbonate content in the brick. The graph also shows that the majority of the samples refer to clay compounds very rich in calcite (mainly due to the mudstone), while sample C5-E4 only might pertain to a mainly silicatic clay, owing the high value of the SiO₂/CaO ratio and the absence of mudstone in the temper.

Taking into account the quantitative composition obtained by SEM/EDS analyses, it is possible individuate five different groups according to the SiO₂/CaO ratio value (figure 52):

```
Group 1 - the ratio varies in the range 0 \div 10,
Group 2 - the ratio varies in the range 10 \div 20,
Group 3 - the ratio varies in the range 20 \div 40,
Group 4 - the ratio varies in the range 40 \div 80,
Group 5 - the ratio varies in the range 80 \div 160.
```

The first and second groups contain the samples with a presence of calcite both in matrix and in aggregate, while in the other groups the calcite content progressively decreases and the clay became quartzitic (that is generated from the degradation of silica rocks). Referring to the silicate composition, in fact, all the samples distribute in a very close cluster (figure 53) where only two samples stand separately, owing to their high calcite content. The same distribution is obtained (figure 54) taking into account the composition of the crystalline skeleton; the increase of the calcium oxide content allows the samples to distribute in a very thin cluster where the aluminum oxide content is constant, as well as in the sodium and potassium oxides content.

Comparing the distributions of figure 55 allows the investigators to verify that the presence of mudstone selects all samples preferably made with a marl clay, while the sub-group that contains mudstone is clearly grouping bricks obtained with different materials and technology: the clay materials are in fact different, and the variation of the MnO/K₂O content implies that also the temper differs.

Technology

Studying the texture and composition of the bricks allowed individuating that several technologies were applied to produce the bricks. As previously discussed, two main groups were individuated; with and without straw in the mixture. The presence of straw identifies a cluster to which pertain very porous bricks with marks or remains of unfired straw, generally iso-oriented within the body. The addition of an organic fraction to the clay aimed at improving the workability of the bricks, both increasing the drying time and reducing the shrinkage. Sometimes the bodies of the bricks pertaining to this group showed the presence of mudstone and sandstone fragments that might be referred both to the intentional addition (mudstone is part of the temper) and to a casual impurity. It is the case of the sandstone fragments, which may be related to the presence of chamotte, since sandstone outcrops are present in the area around Lumbini.

Observing the results of thermal analysis (Table 17), also allowed the investgators to hypothesize that the firing temperature varied between about 520°C and about 550°C according to the residual composition of all analyzed bricks and the kiln technology. Furthermore, the comparison with table 18 allows better interpretation of the analytical data resumed in table 17. When the straw is absent, in fact, the thermal effects of the organic fraction are absent and the loss of the swelling water of the clays may be recorded. Similarly, the absence of calcite in the brick samples makes it possible individuating the loss of lattice water of the illite minerals and/or montmorillonite (if present).

Materials provenance

According to the analytical data, three different clays seem to be used to produce the bricks. The elements that may help in distinguish the clays are respectively the presence of sparitic calcite in the matrix, the size and shape of the quartz crystals in the matrix and the abundance and quality of the temper. The presence into the matrix of sparitic calcite indicates that the clay pertains to a marl clay due to the deposition of the silt in a water basin, close to limestone outcroppings. The round and sub-round shape of the smallest quartz crystals found in the matrix also indicates the deposition in a water basin, where the skeleton was leached. As for the temper, both shape and size of the crystals indicates the addition to the natural clay of quartz sand to control and reduce the shrinkage during the firing; the angular and sub-angular shape of the crystals confirm that the sand is fresh, as well as their relatively high size. Unfortunately, the lack of clay reference samples taken from the quarries inhibits the possibility to individuate the provenance area of the clay and of the sand.

4.5.5. Degradation processes

Observing the masonry shows how the bricks are seriously damaged by salt efflorescence, scaling and fissuring, and that these peculiar degradation patterns mainly concentrate at the top of the walls and where the capillary stops. Thus, the evaporation processes (in every cases connected with the microclimate variations within the Mayadevi Temple) regulate both the rising damp and the salt crystallization (figure 56).

As previously noted, discussing the mud mortars, the origin of the soluble chemicals is directly connected with both the soil composition and the quality of the aquifer beneath the temple. As highlighted before, the degradation mechanisms of the masonry correlate with both the underground waters and the indoor microclimate; indeed, water capillary affects the masonry until the floor level so that the water content detected in several locations of the masonries varies from the minimum value of 0.53 per cent in the West wall to about 140 cm height, to the maximum value of 1.49 per cent at the floor level close to the Marker Stone. Obviously, where the masonry is wet, biological degradation appears, while in the areas where evaporation occurs efflorescence, scaling and powdering may happen.

4.5.5.1. Biological degradation

No specific analysis was performed to individuate the biological species that grow on the walls of the Mayadevi Temple because the appearance of the biological patinas is typical of mosses and green algae. The biological patinas are well adhered to the surfaces and they develop more extensively on the light exposed walls according to the sun's orientation. This explains

why the South exposed surfaces present very compact and deeply coloured green patinas that perfectly define the portion of the wall affected by the capillary. The damages induced by algae and mosses are double and depend on the peculiar metabolism they develop, but in all cases the contemporary presence of water and salts is needed to favour their growth (Ricci, 2000).

As per the observation of some authors (Caneva, Nugari and Salvadori, 1991), the appearance of the green patinas may change according to the biologic species that colonizes the substratum; both algae and cyan-bacteria produce in fact green patinas that generally differ in the gelatinous consistence of the bacterial patinas and also in the chemical action on the substratum. The algae cling to the surface the production of acidic substances which react with the sensitive components of the substrate causing the vacuolization of the external surface. On the contrary, the bacterial colonies develop chemical reactions that are able to synthesize the cell components and the enlargement of the colony. The degradation mechanism of mosses consists in two different activities; the action of the rhizoids that chemically corrodes the substratum and the mechanical stress due to their penetration inside the pore structure of the material. In all cases, water, light and warm temperatures are necessary to activate the mechanisms.

4.5.5.2. Salt distribution inside the masonry

Two different methodologies were applied to assess the salt concentration within the masonry; the extraction from the surface through the use of wet Japanese paper and the stratigraphic sampling of the bricks. Both sampling procedures were carried out with reference to the height of the sample location in order to define the trend of the salt concentration in both directions. Samples of the aguifer were also taken to compare their salt content with that of the masonry.

Figure 57 shows the trend of the salt concentration in the West wall of Trench C with reference to the water saline composition, which is impossible to represent in the same chart owing to the different measure unit. Observing the chart allows individuating that sulphates are the most abundant compounds both in water and in masonry; indeed, the concentration is high in water and increases at floor level (-7 cm point) where evaporation induces that gypsum forms. Also, the nitrates content increases at the floor level, probably due to organic pollution caused by animals and pilgrims. The opposite East wall shows a completely different trend because the only chemical detected refers to nitrates, that is the salt produced by or the demolition of organic matter, either by nitro-bacteria metabolic activity; anyway, the trend is similar because the nitrate concentration varies from 0.04 to 0.09 ppm starting from the lowest level to the floor, confirming the presence of the organic pollution of the ground level.

Assessing the salt content of the samples taken from the body of the bricks at different deepnesses gives the possibility to follow the salt distribution inside the masonry. Figure 58 represents this trend as per the West wall of Trench C13: three different locations were established as a reference, respectively at -115 cm, -73 cm and - 32 cm high from the bottom (labels C13-W1, C13-W2 and C13-W3). Comparing the distributions of each ion confirms that the concentration decreases from the outside to the inside according to the salt solubility: chlorides and fluorides tends to concentrate in the inner layers because of their high solubility, while sulphates concentrate at the external layer owing to their trend to precipitate in saturated solutions. The vertical distribution of ion concentrations confirms that aguifer may be

considered the preferential source of salts, as table 19 shows, mainly as regard fluorides and chlorides.

4.5.5.3. Interactions with the environment

The water evaporation rate directly depends on the microclimate conditions of the volume isolated within the shelter, as well as on the frequency of visits and the number of pilgrims. Delaying the discussion to the paragraph presenting the results of the microclimate monitoring, in this present section we observe that all evidence of decay induced by salts appear during the dry season, while the degradation induced by capillary increases during the rainy season. The peculiar distribution of the temperature gradient both in horizontal and vertical sections cause the capillary to potentially increase because of the air exchanges due to the opening of the opposite doors to the wind and the strong sunlight on the terrace which causes the salt crystallization processes to occur. As previous analysis proves, the human activity also affects the conservation of the monuments in different ways.

Indeed, the industrial activity produces aggressive substances, while the everyday human waste causes the pollution of underground water.

4.6. Aquifer

Soil beneath the Mayadevi Temple is a compact layer of clay which saturates with water when the aquifer rises and also contributes to a rentation of water in contact with the masonry, causing capillary. As figure 59 shows, the level of the aquifer seasonally changes affecting the masonry in different ways.

During the dry season, the level decreases till its minimum value and the salts crystallize inside and on the brick surface. The speed of the evaporation process determines the degradation mechanism; in the case of a slow rate efflorescence form, whilst cryptoefflorescence are produced when the evaporation rate is high. This causes scaling and fissuring of the bricks that consequently tends to powdering in a short time. Furthermore, all pollutants affecting ground waters and river water transferred to the masonry changes the chemical equilibrium of the materials. Indeed, the chemical analysis carried out on the water and brick samples confirmed the presence of small quantities of acetate, formiate and bromate ions. These may be linked to the industrial activity (paper and food production) north of Lumbini. These ions change the pH values (all measures confirm basic values) and the chemical reactions of the materials in contact with the aquifer.

Aiming to assess the influence that the aquifer fluctuations have on the degradation processes of the masonry, during the mission of January 2013 all masonry inside the shelter was investigated by the portable equipment Aqua-Boy checking the water content of the bricks. The measurements were done at different height and distance in order to obtain a grid with vertical and horizontal distribution of the water content values. Using an IR camera made it possible to record the distribution of water inside the masonry and the direct dependence of the water content by the level of the aquifer.

South Wall

The masonry exposed to South was investigated in three different location; verticals A and B corresponded to the right side of the wall respect to the entrance, while location H is on the left side; figure 60 shows the location of all measurement points at the under-ground level, while

the values in the labels refer to the water content percentage. The figures 61, 62 and 63 show the trend of the water content values in the several verticals checked, while table 20 summarizes all detected values.

Observing the table allows individuating that the water content decreases with the height, reaching the minimum value in the sun lighted bricks and in the most exposed ones because of their angular location. On the contrary, the rows located at ground level reach the water saturation value of about 6.36 per cent, owing to the capillary induced by the aguifer. This trend was perfectly confirmed by the investigation made by using an IR camera, which allows recording by digital photos the surface temperature of the area checked.. The temperature of the material is due both to its nature (texture and composition), and to the energy impacting on it; however, the evaporation of the water contained into the structure also contributes to vary the temperature values. Thus, measuring the surface temperature aims to individuate the presence of water inside the structure. According to this concept, figure 60 clearly shows how water distributes inside the South Wall that was investigated; the cold areas (blue and green) corresponding to the wet masonry concentrate at ground floor and on the core of the wall, where mud filled during the burial and after the collapse of the external wall. A similar distribution was observed in the left side of the wall where (figure 64) the lowest values of temperature are recorded at the bottom of the wall, close to the external trench, refilled by pebble after the excavation. This indicates that the trench is a sort of reservoir of water and that the water rises up the wall by capillary, starting from the bottom of the exposed part of the wall. Furthermore, the direct sun lighting on the top of the wall increases the water evaporation rate and also the effects of the capillary, causing brick damage.

East Wall

As figure 60 shows, six different locations were checked at the left and right respectively to the so called East Entrance of the last phase of the temple. According to the data resumed in table 21, the water content varied between 2.98 per cent at the top of C1 location and the saturation point of 6.36 per cent at the lowest levels in all locations. Comparing the images of figure 65 confirms that the presence of compact and unexcavated soil from C1 location to D1 location induces that the water content of the walls increases with the level of the aquifer that extends beneath the temple. As for the information obtained by IR investigations, water concentrates at the bottom of the exposed wall in contact with the soil, confirming that the whole masonry is heavily saturated.

The three locations D show a similar trend even if the refilling of trench C exposes part of the wall below the soil level. The data reported in table 21 (figure 66) indicates that only in the central area (location D2) the highest two points recorded a lower water content, while the entire masonry reaches the saturation value of 6.36 per cent, except for some points of the external C3 location. Comparing these data with those collected by the IR camera (figure 67), allowed the investigators to verify that the false brick wall adhering to the unexcavated soil is warmer than the original wall. On the contrary, the ancient masonry revealed extended cold areas where water concentrates and evaporates. Thus, capillary from the aquifer affects the water saturation rate, but transversal diffusion of water from the central area of the temple occurs as well. The investigations of trench C12, where an old well preserved pavement was found (figure 68), confirmed this hypothesis since the walls of the trench appeared warmer than the bottom and the top, corresponding to the ground floor and to the elevated part of East Wall.

North Wall

Three locations corresponding to different conservation situations were investigated: D4 is the rebuilt extremity of the restored East Wall, location E is the central part of the wall in front of the entrance door, while location F is at the North-West corner of the perimetral wall (figure 69). Comparing the recorded values of water content (table 22) indicated that each location behaves in a different way owing to their peculiar shape. Sector D4 shows the minimum value (figure 70) in the intermediate location, which corresponds to the inner oldest wall reach of water, as measurements on North Wall confirmed. In location E, the high level of the pebble refilling the trench indices that water rises to the top wetting the whole masonry. Indeed, looking at the IR image (figure 71) confirms that, regarding the entrance door, only the temperature of the upper brick row has an influence, thereby increasing the effects of the capillary. The last location F has some differences due to the peculiar geometry of the wall: indeed, the North-West corner shows that the water content decreases with the height being minimum at the top, which is directly exposed to sunlight, while the bottom is water saturated.

West Wall

Along the West Wall six different locations were checked (figure 72) in order to individuate eventual anomalies in the masonry, owing to the high values of water content detected in the inside surface of the same wall. As figure 73 reveals, the wall is water saturated till the top level confirming what was observed by IR inspection. The FLIR image of figure 72 shows that the bottom of the wall is colder than the top both because of the capillary and this is attributed to the air circulation inside the Mayadevi Temple.

The comparison of all the data recorded allowed us to obtain the charts of figures 74, 75 and 76 where the horizontal distribution of water absorbed by the masonry is depicted in the top, intermediate and ground level respectively. This kind of graphic representation helps in understanding how water distributes into the masonry in the whole protected area of the Mayadevi Temple. As figure 76 shows, the pavement and the walls at ground level are water saturated, owing to the presence and influence of the aquifer, which preferably extends in the North-East – South-West direction. This representation matches very well with the data of the level of liquid water in all external wells and also in the trenches inside the shelter. Comparing figure 76 with figure 77, confirms that the aquifer is deepest in the South-West corner of the temple, while the opposite South-East corner is higher, and consequently the masonry in this location is dyer than in the other sides.

The drying mechanism of the masonry is well explained by figure 78 where the superficial temperature of trench C6 is displayed; after the excavation, the clay at the bottom of the trench is dry, while the lower temperature of the walls indicates that the masonry is still water saturated (the recorded value was indeed 6.36 per cent) because of the reduced capability of the bricks to release the absorbed water.

On the contrary, the green-yellow areas on the walls indicate that the evaporation preferably occurs from the mud mortar, which is more porous and compact than the bricks. Another important question is how the presence of the aquifer affects the degradation processes. Analyzing the water samples taken in 2011 from all excavated trenches and external wells allowed ascertaining that both specific conductivity and salt concentration vary in the several locations; as figure 79 shows, the water sampled in trench C (at the south-east corner of the temple) has the maximum conductivity, that is the highest salt content, since the conductivity is an indirect way to measure the concentration of the total chemical compounds solubilized.

Conductivity decreases in the south-west well, where the water level is highest and the dilution maximal. Thus, the water conductivity values in the reference locations allow hypothesizing some differences in the soluble salt concentration inside the Mayadevi Temple area. Analyzing the water from the same locations confirms that the quantity of salts varies, as well as the ions concentration (figure 79). Indeed, fluorides and chlorides are low, while nitrates increase from the SW well to trench C13. Sulfate abundance does not vary very much, but slowly increases from the Marker Stone to Trench C.

This represents an apparent anomaly because the soluble chemical compounds naturally tend to distribute homogeneously in the whole water volume. In the present case, on the contrary, the maximal concentration was found in trench C, while it is minimal in the aquifer from SW-Well. However, the most precise evaluation of the influence of the aquifer and the salts contained on the masonry may be done by comparing the distribution in the whole Mayadevi Temple area of the salt content, both of the aquifer and of the masonry at the ground level.

Figures 80 and 81 directly compare the distribution of fluorides and chlorides in the aquifer and in the ground level of the masonry respectively. Aquifer reveals the highest fluorides concentration in the pipe located in trench C13, that is close to Marker Stone and represents the top quote of the aquifer; on the contrary, at the ground level of the masonry, the highest concentration of fluorides were detected in the area from trench C7, the South Wall and the South-West corner, that is close to the external well where the fluoride content is 1.86 ppm. (table 23). Comparing these values with those of the lowest level of the masonry inside the trenches, confirms that fluorides come from the aquifer and distribute inside the masonry according to their solubility.

As for the chlorides, figure 81n shows how the highest concentration were detected in the trenches C13 and C, while at the ground level the maximal values were recorded in trench C and in the West Wall, both close to the source. This distribution confirms that in trench C chlorides come directly from aquifer by capillary, while in the West Wall it is possible to hypothesize a horizontal transfer from trench C13.

Nitrates show a different distribution (figure 82) because the concentration is very low in the aquifer and in the whole area of the temple, but highly increases in trench C13, where the lowest brick row contains 0.12 ppm only. Comparing this plan with the distribution of nitrates in the ground level of the masonry confirms that the West Wall and Trench C-west side are the location with the maximal values. Since the aquifer collected in the external South-West well contains a very low quantity of nitrates, we can hypothesize that the source of this salt is contained or in the masonry, either in one unexcavated trench and that the high concentration measured in the water of trench C13 is caused by the extraction activity of the aquifer.

Observing the charts of figure 83 indicates that sulfates mainly concentrate in the water retained in trench C, distributing along the diagonal line joining the N-E corner to the S-W well. Contrary to this trend is the distribution of this salt in the ground level masonry, where the maximal concentration were detected in South and West walls. However, since the area corresponding to the trenches C5, C8 and C9 is that where efflorescence occur, it is possible to hypothesize that in this same area is located a source of sulfates, as confirmed by the previously discussed analyses. In conclusion, fluorides and chlorides were directly absorbed by capillary from the aquifer, while nitrates and sulfates have a source within the Mayadevi area and are diffused into the masonry by the capillary according to the fluctuations of the aquifer level.

4.7. Indoor microclimate

Microclimate monitoring inside the Mayadevi Temple started on 2010 aiming to record the variation of the critical parameters able to affect the conservation of all archaeological remains within the shelter. Aiming to characterize the behaviour of the indoor volume, several probes have been placed in peculiar locations to obtain both vertical and horizontal trend (figure 84). In particular:

Probe N° 1: Marker stone

Probe N° 2: Nativity Sculpture (bottom)

Probe N° 3: Nativity Sculpture (top)

Probe N° 4: South door

Probe N° 5: Walk way

Probe N° 6: North door

Probe N° 7: Stupa, North window, external

Probe N° 8: North door external reference.

The microclimate data have been monitored by using separate HOBO data loggers that allow recording each 30 minutes the punctual values of RH, temperature, dew point and impacting light.

Unfortunately, the external north door reference probe do not provide data because of the failure of the battery, and the data recorded by the remaining probes refer to the following periods:

Probe N° 2: Nativity bottom - From 12th February 2011 to 20th April 2011 and 26th April 2011 to 12th February 2011

Probe N° 3: Nativity top - From 15th April 2011 to 11th February 2012

Probe N° 5: Walk way - From 28th April 2011 to 12th February 2012

Probe N° 1: Marker Stone - From 29th April 2011 to 8th November 2011

Probe N° 4: South door -From 28th April 2011 to 12th February 2012

The data has been processed starting from 2:00 PM evaluating the average value of the parameters each eight hours, aiming to obtain simplified charts that properly represent the daily and long-term trend of the parameters. Indeed, the information about RH percentage and temperature fluctuations are necessary to evaluate the influence of the microclimate on the degradation processes of the masonry. Analyzing the data of the probes located along the horizontal section confirms that temperature varies according to the daily fluctuations regularly decreasing with the seasonal climate. Furthermore, decreasing the outdoor temperature induces that the variation range of the indoor values also reduces, as figure 85 shows.

In this monitoring period, the Marker Stone shows the lowest values of temperature and the Nativity Sculpture (at the bottom location) and South Door show the highest and comparable values, while the walkway location has an intermediate trend, similar to that of the Marker Stone in the lowest values. This peculiar trend is probably due to the morphology of the archaeological structures within the shelter. Indeed, both the Marker Stone and walkway are partially protected against the air circulation from the north to south doors that, on the contrary, directly impacts the bottom of the Nativity Sculpture.

Observing the curves of figure 85 evidently appears an anomaly in the period from June 24th and July12th when a sensible decrease of temperature, which corresponds to an important increasing of RH percentage (with a few day of delay) appears. Comparing the data with the meteorological archive of Nepal confirms that the monsoon season caused very strong rain (from 61.8 mm on June 30th to 106.6 mm on July 2nd) to which corresponds a great variation of the indoor microclimate parameters.

However, the average values of the whole period (figure 86) show that the Marker Stone is the most stable location (with reduced fluctuations between minimum and maximum values) and that the South door location really represents the external climate weather.

It is very interesting to observe that in the Marker Stone location (outside the protective box) the fluctuation of the microclimate parameters are strictly related to the external values, but that Dew point never reaches the average temperature, so that no water condensation may append on the archaeological remains. Nevertheless, after the rains the temperature of the walkway location, which represents the average value of the soil, decreases more than that of the Marker Stone (figure 88), because of the increasing of water evaporation from the ground level caused by the saturation of the soil beneath the masonry. This is confirmed by the trend of the relative humidity values in the vertical section recorded in the same period (figure 89). Indeed, in that period the Marker Stone location constantly records temperature values higher than those of the Nativity locations, except for the rain period between June 29th and July 2nd. The abundance of rains, indeed, caused that indoor temperature generally decreased (figure 90) causing the increasing of relative humidity to the maximum values recorded in the whole period.

As figure 90 shows, the average temperature value of the Marker Stone location suffers the lowest fluctuation because of the peculiar geometry of the site, which is protected from the draft by the walkway and the central core of the Mauryan Temple. The variation range increases in the Nativity top location owing to the influence of the terrace warming and cooling. Analyzing the data recorded from the starting of the monitoring till the last date in January 2013 gives the possibility to verify the annual trend of the microclimate parameters. Figure 91 and figure 92 respectively summarize the temperature and relative humidity fluctuations in the long period.

The temperature strongly varies in the north external locations, where the daily cycle is characterized by great thermal excursion between day and night. The south door location is on the contrary more stable but reaches the same values of the north door, as well as the walkway location. Compared to the other locations, the Marker Stone probe recorded the lowest values, with the greatest differences in the warm and dry season from April to September, while in winter the temperature values tend to equilibrate reducing the variation range.

Looking at the relative humidity curves of figure 92 confirms the regular trend of all probes except for the Marker Stone location. Indeed, staring from mid January 2012 the RH values remain nearly constant and higher than 93 per cent, although the external reference values highly decrease. This is probably due to the increasing of the level of the aquifer developing beneath the temple which directly affects the water content of the masonry, but the encasing of the Marker Stone with the new protective box certainly contributes to increase the RH value in the volume protecting the Marker Stone. This peculiar trend is confirmed by the data recorded in the vertical section (figure 93), where the external terrace probe shows the highest

daily variation, to which adapt both bottom and top Nativity locations, contrary to the Marker Stone that reaches values close to the saturation point.

In order to assess the efficacy of the new protective box in the conservation of the Marker Stone, a short monitoring was carried out in the period 9-16 January 2013 locating one probe measuring temperature and relative humidity inside the box and a temperature detector in contact with the glass of the box. The chart of figure 94 clearly shows that in the first monitoring time, the glass temperature was lower than that of the inside volume and constantly lesser than the Dew point value, thus able to cause vapour condensation on the inner surface of the glass. On the contrary, when the glass temperature increases reaching the same value of the air inside the box, the Dew point value is lesser than glass temperature except for the coldest hours in the night, when vapour condensation may happen. In the same period relative humidity varies between 94 and 96 per cent, so that the Dew point may be reached very easily. Nevertheless, to avoid vapour condensation it would be sufficient to increase the air circulation inside the box opening a small window in the south side.

4.7.1. Thermo-hygrometric modeling

Aiming to individuate the presence of anomalous distribution of the microclimate parameters in the plan of the temple, 16 probes were placed in peculiar locations that cover the whole archaeological area (figure 95). All the probes were planned to record temperature, relative humidity and light intensity each 30 minutes except probe W1, which was dedicated to the contact temperature of the external surface of the glass covering the Marker Stone and the MS probe that was located inside the protective box to record simultaneously average temperature and relative humidity, impacting light and the contact temperature of the inner glass surface of the box. Recording started on January 8th at 12:00 AM and ended on January 16th at 12:00 AM. All probes were readout on 10th, 15th and 16th January in order to check the efficacy of the monitoring and to verify the impact of the outdoor climate fluctuations on the indoor parameter values. The statistic data are summarized in the following table 24, where only Marker Stone and W1 probe values are highlighted because of their peculiar location, which was functional to verify the behaviour of the protective box and the reason of the water condensation inside the box itself.

Comparing the data and the locations of all probes allows individuating three cross section north-south oriented, which cover the whole area within the Mayadevi Shelter. Representing the recorded data on charts confirms that the temperature slightly increases from North to south, while at the Marker Stone location the maximum relative value is recorded. The highest differences in the temperature values refer to the minimum recorded that show how the external climate influences the indoor microclimate: both entrances contribute to the periodic oscillations of the temperature values, but the temperature gradient tends to reduce to the minimum value at Marker Stone location, as figures 96 and 97 show.

Different trends show both eastern and western cross sections (figure 98), where the temperature values slightly increase from north to south. In particular, the eastern cross section shows that the north location H1T1 was a little colder than the middle and south locations, as well as in the western cross section. However, the reference D1-N north probe, located on the north door, recorded the lowest value, while the D2-S probe, which is located on the south door, showed the highest average temperature among all probes, except for the

Marker Stone probe. The last, indeed, was located inside the protective box and suffers the influence of the lamps that light the Marker Stone.

Looking at the relative humidity values recorded in the same period (figure 99) evidently appears how the minimum and the maximum values differ according to the peculiar location of the probes. The eastern cross section relative humidity had a constant difference between the maximum and minimum values although it decreases from north to south, according to the corresponding increase of temperature. The western cross section, on the contrary, showed that relative humidity tends to equalize reducing the differences between maximum and minimum values from north to south. The greatest fluctuations have been recorded in the central cross section that shows how the external reference probe EXT-N, which is the North reference probe, recorded the highest values in both maximum and minimum fluctuations, but presents a gradient lower than that recorded in the south D2-S probe. However, the distribution of relative humidity along the section decreases from north to south according to the corresponding increasing of temperature.

Figure 100 displays the distribution of the average values of temperature and relative humidity within the area of the Mayadevi Temple in the short period of the monitoring, held between 8 and 16 January 2013. Comparing the figures with the previous charts allowed the investigators to confirm that the indoor microclimate strictly depends on the external fluctuations of the climate parameters: the two doors directly affect the values in the immediate vicinity, but the preferential pilgrims pathway from the north door entrance to the south door exit also contributes to reduce both the temperature and the relative humidity. On the contrary, the western side of the temple seems to be relatively colder and humid than the eastern section, although the average values of both parameters are similar.

4.7.2. Evaluation of the impacting light on degradation

The short monitoring carried out in the whole area covered by the shelter, locating the probes in peculiar areas, also allowed recording the intensity of the light impacting the masonry in the different hours from the early morning to the night. Delaying the discussion of the daily fluctuations of light intensity to a second phase, it is possible verify how the sun exposure determines the intensity of the light impacting the walls structures within the Temple. Figure 101 clearly shows how the south-east corner of the Mayadevi Temple is strongly lighted, while the north-east corner receives about one tenth of the previous value. Obviously, the south and west sides are the most influenced by the sun radiation because of the direct impacting of the sun rays that enter the windows of the protective shelter. The impacting light changes its intensity according to the hour and the season, directly influencing the superficial temperature of the masonry and the evaporation rate. Consequently, all degradation processes related to the salt and water diffusion inside the masonry may be accelerated by the light. Comparing the light fluctuation of the several locations evidently appears that the maximum intensity is reached in the H3 South-East corner at 2:30 PM, while the H1T1 location reaches the maximum intensity about at 11:30 AM. The following location in the south side H7 records the maximum values between 11:30 Am and 1:30 PM, according to the inclination of the sun rays. However, the intensity of the impacting light regularly varies during the day according to the general climate conditions.

4.7.3. Pilgrims attendance impact

In order to verify the influence of pilgrim visitors on the conservation processes, in the short period between 9th and 16th January 2013 the carbon dioxide content was detected close to the Marker Stone location, by using the manual probe, which was part of the equipment used by the LDT's conservation team. The measurements were made at fixed hours in order to compare the recorded values. The general trend indicated that the average value of the CO2 concentrations increases with the average temperature detected inside the protective box (figure 102), but also showed that the inside values are higher than the external reference values recorded early in the morning, when the monitoring started.

Nevertheless, the daily fluctuations of the CO2 content must be referred both to the number of visitors and the frequency of the visits, as the data of figure 102 demonstrates. The more precise characterization of the negative impact of carbon dioxide on the degradation processes within the Mayadevi Temple could be carried on by continuously monitoring both the CO2 content and the number and frequency of visitors in the Marker Stone vicinity. Indeed, since this relic is made of calcareous conglomerate, this might be affected by the high concentrations of carbon dioxide.

4.8. Remarks on the degradation mechanisms of the Mayadevi Temple

The analytical campaign carried out both on-site and in the laboratory gave the possibility to ascertain most of the parameters that affect the conservation of the site and of the archaeological remains.

The original masonry suffers a double interaction with the environment; the presence of the aquifer beneath the structures and its level fluctuations, which causes the water saturation of the bricks and mortar and the production of efflorescence, plus the daily modification of the indoor microclimate that causes water condensation on the materials during the rainy period, and scaling, efflorescence and powdering of the masonry in the dry season.

However, also the composition of the building materials may influence the degradation rate because of the chemical composition and production technology. Indeed, the mortars adhering to the brick surfaces pertain to two categories since they were obtained both by using silt mud, and lime. In the first case, which is preferably found in the upper levels of the masonry, the mud mortar is characterized by the presence of natural soil mixed with quartz sand, while the silt and the clay minerals are the only responsible for the hardening of the mortar. The lime mortar, which is made by lime and quartz sand, was found in the pre-Ashoka structures and needs to be further investigated in comparison with the fragments found during the excavation of the chambers in order to assess both their precise composition and the technology.

The presence of thin layer of artificial yellow patinas on the exposed surfaces of the bricks opens the door to new conjectures about the external appearance of the temple and the technology of the historic period. Indeed, the same brick composition and firing conditions indicate that the production technology has changed little over the centuries, although the clay materials and their sources were the same.

As for the degradation, according to Norma UNI –11182:2006, "Cultural heritage. Natural and artificial stone. Description of the alteration - Terminology and definition", the visible forms of deterioration can be individuated as:

- biological attack (macroscopic presence of micro and/or macro-organisms such as algae, fungi, lichens, mosses, higher plants);
- efflorescence (superficial appearance of crystalline or powdery or stringy, usually whitish);
- crumbling (de-cohesion with fall of the material in the form of dust or tiny fragments);
- fissuring (solution of continuity in the material that implies the displacement of the parts);
- scaling (presence of flakes of irregular shape, and non-uniform thickness, generally related to fissuring).

Figure 103 shows the distribution of the degradation patterns on the masonry within the Mayadevi Temple, as was individuated in the first phase of the on-site work. The most diffuse degradation pattern is crumbling, to which fissuring is constantly related; both are due to the combined action of water evaporation and microclimate fluctuation, but the peculiar location of the damaged bricks also influences the degree and speed of the alteration. Indeed, both the top of the walls and the edges of the masonry are the most affected by the degradation.

On the contrary, scaling and efflorescence concentrate in limited areas generally overlap. In particular, the floor edges of the chambers C8, C10 and C11 show evidence of both degradation patterns during the dry season: indeed, water evaporation causes efflorescence, to which fissuring, scaling and crumbling are generally correlated. As for biological degradation, it evidently appears that the growth of algae and moss is related to the light entering the shelter from the most lighted southern side. However, the water distribution inside the masonry also contributes to the growth of the biological patinas, as well as the presence of salts in the masonry (sulphates, in fact, take part in the process).

Comparing the mosses distribution with that of the water absorbed into the masonry (figures 103 and 104) confirms that both phenomena are strictly correlated, also depending on the aquifer fluctuations according to the weather. Microclimate fluctuations play a fundamental role in the degradation processes because of the influence that the indoor temperature has on the water evaporation rate from the ground floor and masonry. Furthermore, since the indoor area is always open and in connection with the external environment, all weather changes discharge on the indoor microclimate, influencing both the superficial and the environment temperature, as well as the relative humidity values. Also pilgrims and visitors influence the indoor microclimate, mainly in all areas around Marker Stone and Nativity Sculpture causing an increase of the carbon dioxide content, which chemically may affect the stone degradation rate. Both the laboratory and on-site conservation tests confirm that the products and solution chosen to perform the restoration tests work properly so that it is possible to plan the restoration activity of all archaeological remains within the Mayadevi Temple. The same data allowed the team to plan the new and more effective rehabilitation of the shelter, with the aim to guarantee the best conservation of the site.

4.9. Stability of the Ashoka Pillar

One of the problems posed by the Ashoka Pillar concerns its stability, owing to both the inclination that the pillar suffers and the vertical crack affecting the entire height from top to bottom. Since during the restoration we observed that the vertical crack is open and probably crosses the pillar, at the end of the restoration activity a strain gauge was located cross the fissure in the eastern side (figure 105) in order to record its elongation for a relatively long

time. As figure 106 shows, the monitoring started on February 14th at 6:00 AM and stopped after 24 hours. The trend of the dynamic solicitation indicates that in the night the stress reaches its minimum value, while it increases when sunlight starts to impact the eastern surface of the Pillar.

Calculating the values of the elongation allowed the investigators to ascertain that the decrease of temperature in the night causes the fissure to reduce by about 0.0122 mm and this widens in the morning when the sun light impacts the surface of the Pillar. Thus, the fissure is probably open and the epoxy plaster applied to fill it do not stop the effects of the thermal solicitations. Aiming to verify this peculiar phenomenon, during the mission 2013, two strain gauges were placed on the crack at the opposite sides of the Pillar corresponding to the widest part of the vertical fissure. However, due to the unfavourable weather, the monitoring was carried out for a short time only. Anyway, the recorded data was significant. Figures 108 and 109 show the trend of the detected parameters (temperature, relative humidity and elongation) in the time range 11:00 AM - 4:00 PM on January 18th. Both figures show that the elongation is strictly related to the fluctuation of the temperature, which changes according to the insulation of the pillar. In particular, when the temperature reaches its maximum value of about 28°C, the width of the western fissure reduces, while at the opposite eastern side the crack width increases (figure 110). Recording the distribution of temperature of the central area of the pillar in the eastern and western side respectively (figure 111) indicates that the difference of temperature between the southern exposed surface and the north side ranges from 8 to 10°C, and this value is sufficient to cause the opposite movement of the crack. Furthermore, the plaster filling the crack in both sides is warmer than the boundary stone denouncing the discontinuity of the pillar. Finally, the temperature distribution shown by figure 112, clearly highlights the negative effect of the protective cap against the below pillar which is strongly stimulated. Although the elongation is minimal, its cyclic nature confirms that probably the vertical fissure crosses the whole width and that a more complex monitoring is necessary to ensure the best conservation of the monument.

5. Restoration activity

The conservation of the monuments is due to several activities that involve both the restoration and the intervention on the environment aiming to control the degradation mechanisms. However, ordinary maintenance activities are necessary to guarantee the best conservation of the restored monuments, mainly in not isolated environments, such as the Mayadevi Temple and Sacred Garden compound.

The restoration activity started on 2011 and involved the three main monuments in the area: Marker Stone, Nativity sculpture and Ashoka Pillar and Capital, and directly involved five members of the Lumbini Conservation Team. The same team participated in the restoration of a limited area of the masonry in 2012.

The practical restoration activity started on April 6th 2011 on the Ashoka Pillar, where scaffolding was built to reach the top of the Pillar. Initially, the scaffolding was not suitable to carry out any restoration work because of the lack of walking planks and the shaking that occurred when people got on them. However, it was made secure to ensure safety during the restoration work (figure 113). On April 7th, the protective box of the Marker Stone was removed in order to verify the results of the biocide treatment and to continue the restoration. Nevertheless, the restoration activities suffered a consistent delay because of the lack of

materials that were transferred from Italy on April 11th because of the long delay time at Italian customs. But, purchasing solvent and necessary products in Butwan and Bhairawa made it possible to carry out the restoration.

Restoring the Ashoka Pillar prompted the decision to dismantle the Capital, which was assembled with cement concrete; the exhibition was also changed, while a cast of the inscription was prepared as well, in order to obtain replicas to exhibit to the visitors aiming to reduce the impact on the original.

The activities carried out are summarized in the following chapter, but they are detailed in the Conservation Cards (Annex 19). In Annex 6 all restoration procedures are described, while Annex 7 contains both the technical and the safety cards of the chemicals used for the restoration.

5.1. Nativity Sculpture

On April 11th a service scaffolding was built to enable the conversation team to reach the Nativity Sculpture; as figure 114 shows, the safety is relative, but the restoration activity started immediately.

The distribution of the damages has been verified and compared with the data acquired during the training. Then, the soft deposit of powder was removed by dry soft brush, collecting the material for lab analysis (Sample NS-1). Preliminary cleaning tests allowed the team to verify the presence of organic layers (namely PVA, according to the information given by Mr. Bidari) that should be removed by using the 2A mixture (Acetone/Alcohol 1:1 v/v). Nevertheless, several red coloured layers, presumably made of epoxy resin, have been identified on the stone surface. Using 2A solution and cotton carried out the cleaning: the superficial layer of PVA was completely removed, but the insoluble red layers still adhere to the stone's surface. These layers are very hard, water-repellent and difficult to remove because the resin penetrates the stone porosity (maybe the restorer intended to consolidate the stone).

Furthermore, all areas where this degradation pattern is present show (figure 115) that the hard scales are detached from the substratum that is locally powdered. The cleaning test performed using Ammonium Carbonate 10 per cent w/w solution did not work properly because of the presence on the surface of some remains of PVA and of the red resin layers. Using a 2A solution applied by toothbrush, new tests were carried out, aiming to definitively remove the organic layers. Figure 116 shows how the original colour of the stone has changed owing to the colours applied on the surface, while the sandstone was originally pale yellow with both red iron oxide and grey chlorites veins. Cleaning was completed on April 16th except for the lowering of the epoxy plaster applied to glue the separated part of the statue.

All activities were stopped on 18 April for the Maya Festival and part of the scaffolding was dismantled and the temple was opened to the visitors. The number of pilgrims was very high in that period and when on 21 Aprilthe festival completed, the appearance of the sculpture was as shown in figure 117. The lower part of the relief was painted with the purple colour, while sugars and milk were thrown up onto the Mayadevi face causing white spots to adhere to the surface. Thus, the sculpture needed new cleaning that was done through using 2A solution (applied by toothbrush) and a scalpel to remove the adhering sugars. Applying ESTEL 1100 (CTS – Italy), which is a mixture of ethyl silicate and alkoxy-silane, performed the final protective treatment. The choice of this chemical was justified by the necessity to

contemporary develop strengthener and waterproofing properties in order to control the degradation processes.

The monitoring of the microclimate carried out from February allowed the use of both of PVA (Poly-Vinyl-Acetate) as a restoration protective and epoxy resin as an adhesive, the main causes of the stone degradation in the presence of high values of the relative humidity. The differences in the superficial temperature of the stone from the bottom to the top of the statue may induce that humidity condenses causing damage to the stone. The main degradation pattern observed is in fact the scaling of the surface, which is hardened by the polymers applied during the restoration, while the beneath stone powders. The treatment stops the degradation because the chemical reaction that the chemicals develop originates a new polymer, whose structure stops the absorbance of the liquid water, while the compactness of the stone matrix increases. Figure 118 shows the Nativity Sculpture after the restoration treatment.

5.2. Marker Stone

Once the protective box has been removed, the Marker Stone appeared wet and browngreenish in colour owing to the patina that homogeneously covered the surface (figure 119). The ground powder not adhering to the surface was removed by using a dry soft brush and collected for analysis (Sample MS-1). Thus, a measured sketch of the area was taken in order to support the definitive projecting of the new protective box (Figure 120). To definitively remove the brown-green patina, the Marker Stone was cleaned by using Ammonium Carbonate 20 per cent w/w solution, softly acting by toothbrush in order to completely remove the organic remains from the natural cavities of the stone. Washing with distilled water and drying by soft synthetic sponge removed the potentially dangerous residual chemical products. To reduce the threat that biologic attack develops again, the biocide Biotin T 3 per cent v/v solution was sprayed on the Marker Stone and its surroundings.

During the restoration of the Nativity Sculpture, a wooden frame was applied to protect the Marker Stone, but microclimate monitoring continued to record the effects of this temporary protection.

On April 18th, the start of the Maya Festival enforced the temporary termination of the restoration of the Nativity Sculpture and the temple was opened to the visitors. Part of the scaffolding was then removed and the Marker Stone was temporarily protected with a transparent box to enable the pilgrims to view it. Figure 121 shows the situation after three days of the Maya Festival. Several kind of offerings cover part of the box and contaminate the surroundings, increasing the organic pollution and the risk that biological attack develops quickly.

The restoration of the Marker Stone restarted on April 27th, when the Nativity's restoration had been concluded, and consisted in the mechanical cleaning of the surroundings, followed by the chemical cleaning by compress of 1:1 mixture of EDTA and Ammonium Carbonate 10 per cent w/w solutions. The compress act lasted for three hours and then the area was rinsed with fresh water. Using a 1:1 mixture of hydrogen peroxide and ammonia liquor aimed to remove organic remains and to eliminate the biologics enduring into the stone porosity, performed the final cleaning of Marker Stone (Figure 122). Before it was protected with the transparent box, a biocide solution of Biotin T 3 per cent was sprayed on the Marker Stone's surface and surroundings. A monitoring of the microclimate was restarted as well.

5.2.1. Building the new protective bow

According to the LDT, a new box able to protect the Marker Stone aimed to enlarge the protected area and optimize the visibility of the relic (figure 123). The box consists in three different boxes made of a metallic frame and covered by a bulletproof glass (figure 124) which are connected by iron pins. The assembled bow was allocated over the area of the Marker Stone and supported on a flat perimetral ring of new brick. The perimeter was sealed by lime mortar to avoid offerings entering the protected area.

The lightning system consists in eight warm-white led lamp located two to each side in order to homogeneously light the entire area. Unfortunately, owing to the unsuitability of the electric power, when the system was connected with the power, all the lamps emitted a violet light, whose colour intensity slowly decreased in time (figure 125). However, eight new lamps were purchased, but they were not placed because of the lack of suitable electric power. Also the two UV lamps applied within the box to help in the reducing the risk of biological growth are not functioning because of the peculiarity of the electric system.

5.3. Ashoka Pillar

The cleaning of the stone cap protecting the top of the Pillar was performed by using dry brushes and Ammonium Carbonate 20 per cent w/w solution applied with a toothbrush. The cleaning removes both the black patina and the lichens. Washing by water to extract the remains of the saline solution concluded the cleaning. Figures 126, 127 and 128 show the sequence of the actions made for cleaning.

The restoration of the Pillar starts with the mechanical removal of the plaster that connects the cap with the top of the column. The plaster is coarse grained and powdered and appears as a pre-mixed mortar containing gypsum and cement (Sample AS-100). On the contrary, the external surface consists of a thin compact and elastic layer (figure 129) that seems to be constituted by a synthetic.

The plaster was mechanically removed to eliminate the greater quantity of cement from the external layers (figure 130). The cement mortar was then substituted by a traditional hydraulic mortar made by mixing lime, sand and brick powder in the report 1:1:1 (figure 131). The external layer of mortar was made by mixing lime, sand and brick powder in the report 2:3:0,75; the colour of the stone has been approached by adding the necessary quantity of yellow ochre (figure 132).

The external surface of the pillar was cleaned using 2A acetone/alcohol 1:1 solution with cotton in order to remove the thin film of Paraloid B72 applied during the last restoration. In the western side some yellow layers adhering to the stone appeared after the cleaning. The aspect, the compactness and the insolubility in acetone allowed the team to hypothesize that these layers are composed of epoxy resin that may be casually applied during the last restoration. Once the waterproofing layer is removed, the cleaning continues by using a 1:1 hydrogen peroxide/ammonia liquor (HP/AL) solution that acts on organic compounds like fats and oils, which transform in soluble salts removable by water.

Alternating the cleaning with 2A and HP/AL solutions allowed the team to remove most of the organic deposits adhering to the surface. However, the surface became slightly patchy because of the difference in the composition, degradation and age of the absorbed materials. The Pillar has been in fact exposed many years – more than one century according to the authors of the most recent publications on Lumbini (Bidari, 2009 and Rai, 2010) – to the public and this has resulted in the situation in which the pilgrims have applied several organic

materials on it as religious offerings. These saturate the porosity of the stone and degrade the surface, changing both the colour and chemical composition, but allow constituting the original patina of the Ashoka Pillar. According to the universally accepted criteria for conservative restoration (Brandi, 1964), the cleaning must remove from the surface the potentially dangerous materials, while preserving the patina. As a consequence, the cleaning aimed to eliminate the externally layered materials without removing the absorbed ones, which contribute to form the patina. This will cause the colour of the Pillar to change from the brownreddish at ground level to the pale yellow-grey at the top. The cleaning process also revealed that the sandstone was differently degraded by the weathering and by the past restoration interventions as the chemical corrosion of the south exposed face shows. The degradation starts under the circular mark of the metallic belt, due to the absorption of the iron corrosion products and affects the vertical section of the Pillar along the stone deposition planes. The degradation increased the porosity and caused a pitting corrosion that decreased the compactness of the stone. Thus, a strengthener treatment using ESTEL 1000 (CTS – Italy) was locally applied to improve the mechanical properties of the stone. The treatment temporarily changes the colour of the substratum owing to the long time that the polymerization needs and that may increase in a hot and dry climate (like that of Lumbini in this particular season). Nevertheless, the colour will fade in time until the original colour of the stone is reached (figure 133).

The restoration also included the cleaning of the vertical fissure, which develops from top to bottom in the West and East sides of the Pillar and this was filled with a yellow epoxy resin. The removal of that epoxy resin aimed to inspect the fissure and to fill it with a new highly resistant epoxy, normally used in restoration to glue separated or fissured stone blocks. The epoxy plaster was then removed by using scalpels and the stone edges were definitively cleaned by micro-motor and carborundum burs. The filling was carried out using an epoxy plaster made of epoxy and sand; the addition of sand increases the mechanical resistance of the mortar, and reduces the shrinkage so that the resulting structure is more resilient. The plaster was then covered by a traditional hydraulic mortar made of lime, sand, brick powder and yellow colour, whose function is both to protect the epoxy from the UV rays and to approach the colour of the stone. The addition of a small quantity of fluorinated waterproofing to the mixture will also increase the resistance of the mortar to water penetration.

The area where the inscription was scratched was cleaned very carefully because of its objective value and of the apparent erosion that some letters show. The offerings cover the scratches allowing diminishing the deepness of the characters (figure 134), but also dirty the surface due to the pouring of milk and other liquids sprayed by the pilgrims. Comparing figures 135 and 136 allows verifies the efficacy of the cleaning and the good conservation of the inscription despite the appearances. The removal by 2A solution and HP/AL mixture eliminates the organic layers and gives to the inscription a new legibility. However, the patina originated by the absorption and degradation of the organics is safe and preserved.

The restoration also involved the metallic belt; starting from the lower, both belts were removed, cleaned and painted. To avoid corrosive products caused by contact with water that affect the stone, a thin layer of silicon rubber was inserted between the belt and the Pillar. Figures 137, 138 and 139 illustrate the sequence of the intervention on the belts. The cleaning of the inside face of the belts was carried out mechanically and by acetone in order to remove all remains of the corrosion products. Then, an anticorrosive varnish was applied to the belt aiming to protect the metal from the corrosive action of the rainwater and humidity.

Indeed, the portion of the Pillar in contact with the belt was heavily affected by the presence of hydrated iron oxides produced by the metal corrosion. Therefore, there was a need to clean the stone both mechanically, to remove the thick deposits, and chemically by applying paper pulp compresses with ETDA 10 per cent w/w solution for a minimum time of three hours. Combining both methodologies allowed the conservationists to reduce the intensity of the red coloured spots, even if the penetration of the iron compounds is too deep to be removed with this chemical only. The stone surface was then cleaned by applying the 2A solution and then with HP/AL mixture to remove all remains of resins and organics from the surface. The waterproofing treatment with SILO 111 concluded the restoration.

In order to isolate the metallic belt from the stone, a layer of pre-polymerized silicon rubber 2 mm thick was inserted between the belt and the Pillar surface. Screwing the belt blocked the rubber, which acted as a washer, preventing the corrosive substance which results from the chemical reaction of the belt with rainwater entering into contact with the stone. Refining the varnishing of the belt concluded the treatment.

5.3.1. Restoration of the Capital

The restoration of the Ashoka Pillar also involved the restoration of the Capital and its exhibition. The restoration of the Capital imposed the dismantling of the existing exhibition because of the massive use of cement and the damage that the stone suffered. Indeed, liquid cement was used to fill the hole that originally allocated the metal pin joining the Capital with the Pillar, and also to connect the two elements composing the Capital (figures 140 & 141). The dismantling was carried out using chisels of different size carefully operated in order to avoid damaging the stone. The remains of cement concrete, adhering to the inner face of both fragments, were cleaned by using a chemical mixture 1:1 of ammonium carbonate and EDTA 10 per cent w/w solutions, applied by compress for 12 hours. The chemicals dissolve part of the concrete and softened the remnant enough to be easily removed by scalpel. Washing with fresh water eliminated all remains of both concrete and chemicals.

The external surface of the Capital showed several layers of organic matter strongly adhering to the stone and sometimes deeply penetrating its porosity. The cleaning was done by paper pulp compresses saturated with the mixture 1:1 of Ammonium carbonate and EDTA 10 per cent w/w solutions. The minimum contact time was 12 hours, but after that time, sponge and water removed most of the black remains. However, many black spots penetrate the external porosity and the superficial lack of material, changing the appearance of the stone. Applying the 1:1 v/v mixture of Hydrogen peroxide and Ammonia liquor (HP/AL mixture) performed the cleaning. This mixture, in fact, reacts with oils and fats, originating water-soluble compounds that may be simply removed with a tooth-brush and wet sponge (figure 142).

The new exhibition aimed to enhance the original shape of the Capital and to show it at the same height of the lost terminal part of the Pillar. Thus, a quarry pillar was built, inserting into it a plastic pipe with the same height and diameter of the original (figure 143) to be used as a vertical support. The cavities inside both fragments of the Capital were protected with a layer of silicon rubber. Matching the fragments allows individuating the point of contact where metallic pins are inserted to safeguard the stability of the Capital. The top of the support was then rounded to reach the same diameter of the flat seat at the base of the Capital (figure 144).

The positioning of the Capital was very difficult because of the weight of the fragments and the lack of necessary tools, but with the help of some levers and ensuring the security with a rope, the first element was properly located (figure 145). Inserting two pins and using an epoxy resin added with paper pulp and sand to increase its viscosity, made it possible to match correctly the second fragment to the first (figure 146). In both cases, the previous application of silicon rubber to the support increases the adhesion between the stone fragments and the support and the stability of the whole structure. The fissure that separates the fragments was filled with hydraulic traditional mortar in order to increase the compactness of the element. Then, the fissure was closed with the same mortar used to fill the vertical fissure of the Pillar, also applied on the round terminal part of the support (figure 147). The state of conservation of the stone and the threat of damage that the Capital suffers due to the frequency of the pilgrims required the need to protect the external surface by using the ESTEL 1100 (CTS – Italy) strengthener, which develops waterproofing properties as well (figure 148).

5.3.2. Casting of the inscription

With the aim to avoid the pilgrim's offerings which directly affect the conservation of the monument, the replica of the inscription was made, according to the wishes of LDT. The surface was treated with a vegetable soap solution (figure 149) in order to makes it possible that the mould separates from the stone surface. The use of soap instead of the commonly used products was preferred because of the necessity to apply on the scratched letters a silicate strengthener compound, which might react with the silicon rubber, causing the mold to irreversibly adhere to the stone. The cast was then produced applying two layers of silicon rubber (figure 150) both by brush (the first layer is liquid to make the best replica of the surface) and by spatula the second layer is made of silicon rubber charged with paper pulp to increase the viscosity. Finally, a tissue was applied to the silicon rubber in order to prevent the mould because of the verticality of the surface. The mould was detached after 24 hours (figure 151) and the surface was cleaned with acetone to remove the residues of the silicon oil contained in the rubber. The cast was then transferred to the laboratory and prepared to obtain a flat copy of the inscription (figure 152).

5.4. Pottery

The final restoration activity of the year 2012 concerns two pottery items recovered by the archaeological team from the village and the monastery. Both pots were preserved by the soil and wrapped with tissues (figure 153a) to preserve their shape during the drying of the soil. Removing the tissues caused the soil to slightly collapse (figure 153b), but all the fragments remained in piece, so that all of them may be correctly located during the cleaning process (figure 153c). Athough the pottery items have been well recovered, the state of conservation of the VATA pottery (LMS -12 tr1 (3032) <6088>) appeared unsatisfactory. Indeed, the original smoothed surface was lost and the body tended to powdering; furthermore, the pot was fragmented and covered by dust.

On the contrary, the state of conservation of the GHAINTO pottery (LVS -12 trP (?) <?>) was good, and the original surface was preserved, although the pot was fragmented and each fragment was covered by dust. The mechanical cleaning was performed through the use of a soft brush and toothbrush in order to remove the dust before washing the fragments with pure water. In order to make it possible manage the fragments without increasing their degradation, their consolidation was performed. All fragments were immersed in 1,5 per cent v/v

Mowital¹/alcohol solution for a maximum time of two minutes to attain the surface and body hardening.

After the consolidation of the fragments, the reconstruction of the pots was necessary before gluing (figures 153d, 153e). The gluing of the fragments was achieved in two steps: firstly the joints were connected by using UHU Plus epoxy resin in limited areas, than filling the joints with Mowital resin (10-20 per cent v/v in Isopropyl alcohol) definitively glued the fragments. The integration of the fissures and of the lack of material was performed by applying gypsum plaster, which was smoothed after the hardening. Natural earth colors mixed with acrylic binder were applied on the gypsum plaster by spotting technique in order to agree the restored parts with the original surface colour. The protection of the ceramic surface was undertaken by using a 1,5 per cent v/v Mowital alcoholic solution, which allowed the conservationists to achieve the final restoration (figure 153f).

5.5. Masonry

The mission of the year 2013 aimed to complete the monitoring of the Mayadevi Temple and to identify the best solution for the restoration of the masonry. Thus, the restoration took into account the limited section corresponding to the northern side of the South wall (figure 154); the base of the same wall till the walkway; and the walls of the Trench C7.

5.5.1. Describing the degradation of the masonry

Preliminary to the restoration intervention, all information about the degradation of the masonry and the distribution of the degradation patterns were recorded, generating the maps like those of figure 155, where biologic attack, deposits of dust, the presence of efflorescence, brick scaling and powdering were reported. Observing the figure confirms that while dust mainly deposits on the exposed surfaces, the biological patinas, which refer to green algae, moss and cyan-bacteria, probably develops at the ground floor level where the water content is the highest. Efflorescence appears in the vertical surfaces, which are mostly exposed to air circulation and preferably dry; the same is for scaling and powdering that mainly concentrate at the edges of the masonry where drying and evaporation probably occurs. Several small animals (mice, hornets, millipedes and insects in general) settled down in the holes affecting the masonry where the bricks collapsed and the mortar was destroyed.

The original orange patina of the bricks is lost in all the areas worked on by the team during the periodical cleaning of the archaeological remains, while it is preserved in the protected areas

Furthermore, all restored areas showed a high mechanical degradation – probably due to the use of an improper quality of mortar, which in some cases contains cement. The walls of the Trench C7 appear to be better preserved, but scaling and fissuring of the bricks caused a loss of material and a risk of collapse of part of the upper and middle rows (figure 156).

5.5.2. Restoration of the masonry

The first step of the intervention consisted in the mechanical removal of dust from the surfaces by using soft brushes. This action aimed to remove both the remains of the pilgrim's offerings, and the fine powder deposited by the wind and people dispelling the dust through human

¹ Mowital B60HH is the commercial name of a poly-vinyl-butyral supplied by Kuraray America, Inc.

movement (figure 157); the last was necessary to increase the efficacy of the chemical cleaning. The chemical cleaning was necessary to remove all dust deposits adhering to the brick surfaces and this was achieved by using ammonium carbonate 5 per cent w/w solution applied by brush and toothbrush according to the compactness of the layer to be removed.

Indeed, the complete cleaning of the walls of Trench C7 needed to be repeated five times, while in the case of the South Wall, the cleaning was applied twice only. The strongly adhering residues were removed by using a scalpel and spatula. Final washing with pure water helped to eliminate residuals from the surfaces of the chemical products (figure 158). Where algae and cyan-bacteria had produced a well adhering green patina, the cleaning was performed applying a 1:1 mixture of ammonium carbonate 10 per cent w/w and biocide Biotin T 2 per cent v/v solutions, and acting mechanically with a toothbrush until the patina softens. The application of a soft natural sponge and pure water allowed the complete removal of the biological patina.

Applying this methodology, the base of the South Wall reaching the central walkway was cleaned in a very short time and this has produced good results. (figure 159). At the end of the cleaning process, all fissures and cracks produced by degradation into the brick surface became evident (figure 160), while emptying two holes individuated in the plan of the inner platform revealed the base of two different poles, which were probably used to support a tent. With the aim to increase resistance to the degradation and the collapse of the masonry, all fissures were filled with a lime plaster (figure 161) made by mixing sand and brick powder with hydrated lime in the ratio of 1:1:1. The same plaster was also used to repair and join some broken bricks (figure 162) and to fill the mortar between the bricks as well. After two days of natural drying, all surfaces were sprayed with a protective solution obtained by mixing four parts of the (40+60) per cent v/v Silo 111/Estel 1000 solution, with six parts of the (40+60) per cent v/v White Spirit/Isopropyl alcohol solution (figure 163). Due to the chemical reactions involved, this peculiar mixture will obtain the double result of strengthening the surface of the bricks, avoiding the powder within, and waterproofing the surfaces (figure 164), thereby reducing the absorbance of water from the environment in the cold season. However, in case of strong capillary from the soil, water may evaporate freely as well.

5.6. Criteria for the long-term conservation

Since the environment plays a very important role in the activation of the degradation mechanisms, owing to the variability of the parameters that characterize the site, all archaeological finds and remains actually protected by the shelter named Mayadevi Temple need continuous routine maintenance in order for them to be preserved in the best possible conditions.

As regards the Marker Stone and Nativity Sculpture, the recommendations to carry out regular maintenance were given after their restoration. Similar procedures were defined for the preservation of the Ashoka Pillar and its capital, which are only protected by the fence. However, is to be noted that the long-term conservation of the Pillar depends both on the influence of the aquifer on the basement of the column, and on the levels of air pollution and how high they adversly affect the structure.

As for the brick masonry, part of the original temple, the conservation is strictly related to the quality of the environment included within the shelter - specifically the microclimate and the level of the aquifer. Thus, intervention to deal with these two elements is a priority.

6. Future activities

Taking into account all information collected during the three-year work span and the last work completed, the following activities should be carried out over the time frame of the next three years project:

- · minimizing the negative impact of the aquifer;
- · restoring the brick ancient masonry;
- · optimizing the shelter;
- · monitoring the stability of the Ashoka Pillar.

6.1. Minimizing the negative impact of the aquifer

The necessity to realize the need for an efficient drainage system within the Mayadevi Temple comes from evidence provided through physical monitoring exercises and intensive studies carried out, both inside and outside, the temple. The drainage system serves to lower the water level of the aquifer inside the area protected by the shelter. The functioning of the drainage system is in fact preliminary to the restoration of the masonry. The following activities need tobe carried out:

- a) Inserting water-pumps inside the external wells;
- b) Connecting all external wells by using 3/4 inch pipes in order to transfer the water to the pond by excavating a small canal to insert the evacuation pipes;
- c) Connecting each component of the drainage system to the electric power system;
- d) Connecting the water evacuation system to the general management system.

6.2. Restoration of the Mayadevi Temple masonry

According to the general conservation plan, the restoration of the masonry will be carried out in order to complete the conservation of the whole area in three years. The restoration of the masonry needs all of the chambers to be emptied and excavated in order to allow the drying out of the masonry. The restoration will be carried out in parallel sectors, starting from the East side of the Mayadevi Temple.

The conservation activity will consist of:

- a) Cleaning of the surfaces using approproate chemicals that are sensitive to the process;
- b) Strengthening treatment of both bricks and mud mortar through the use of suitable, sensitive chemicals:
- c) Gluing of the detached parts and filling of the fissures in the brick structure by using suitable traditional mortars;
- d) Structural consolidation of the walls (if necessary to guarantee their stability) by using bricks and traditional mortars;
- e) Final treatment of the surfaces according to the general microclimate conditions;

f) Analysis of brick, plaster and mortar samples taken during the archaeological excavations.

6.3. Proposal for the optimization of the shelter

On the base of the microclimate data and of the aquifer displacement in the protected area, the most favourable modification of the shelter will aim to stop the negative effects of capillary on the archaeological masonry, as well as to minimize the impact of the microclimate on the degradation processes.

6.4. Monitoring of the Ashoka Pillar

A scientific examination of the Pillar was necessary to define the possibility of exhibiting the structure's entire height. To achieve this, the following actions are necessary:

Scan laser mapping of the Pillar to obtain a 3D mathematical model that can be used to determine what action is needed to achieve the overall aim of displaying the entire structure: IR thermograph of the column:

Study through a modeling process the effects on the pillar of the thermal conditions; Study through a modeling process the effects on the stability of the pillar caused by mechanical conditions:

Instrumental analysis, using ultrasound technology, of the column to determine the ongoing effects of vertical cracks and splits caused by natural degradation and climatic conditions.

Bibliography

Tange, K. and Urtec. 1978. Master Design for the Development of Lumbini, Phase II. Final Report, New York, United Nations.

Boccardi, G. and Gupta, D. 2005. Reactive Monitoring Mission to Lumbini, the Birthplace of the Lord Buddha, World Heritage Property, Nepal. Mission Report. Paris, UNESCO.

Atzori, A. 2006. Lumbini. An archaeological perspective, in: Jenkins M. & Selter E. (Eds), *Lumbini. Present status and future challenges*. Kathmandu, UNESCO, pp. 71-100.

UNESCO. 2009. Strengthening Conservation and Management of Lumbini, the Birthplace of the Lord Buddha, World Heritage Property. Project proposal, Kathmandu, UNESCO.

Meucci, C. 2009. The Mayadevi Temple and Archaeological Conservation. Mission Report, Kathmandu, UNESCO.

Meucci, C. 2011. Strengthening Conservation and Management of Lumbini, the Birthplace of the Lord Buddha, World Heritage Property. Conservation of archaeological remains. Mission report, Kathmandu, UNESCO.

Bidari, B. 2007. Lumbini. A Haven of Sacred Refuge. 3rd edn. Kathmandu, Hill Side.

Albright, J.N. 1971. *Mineralogical Notes. Vaterite Stability, The American Mineralogist*. Vol. 56. pp. 620-624.

Coningham, R.A.E., and Acharya, K.P. 2011. Identifying, evaluating and interpreting the physical signature of Lumbini for presentation, management and long-term protection. Strengthening the Conservation and Management of Lumbini, the birthplace of the Lord Buddha. Report of the first season of field operations, Kathmandu, UNESCO.

Duggan, M.B.1988. Zirconium-rich sodic pyroxenes in felsic volcanics from the Warrumbungle Volcano, Central New South Wales, Australia, Mineralogic Magazine, Vol. 52, pp. 491-496.

Mishra, T.N. 1996. The archaeological activities in Lumbini. Kathmandu, S.K. International Publishing House.

Ricci, S. 2000. *Il biodeterioramento dei materiali lapidei*, in: B. Magrelli & C. Meucci (Eds.). Degrado e conservazione dei materiali lapidei, Roma, pp. 72-83.

Caneva, G., Nugari, M.P. and Salvadori, O. 1991. Biology in the conservation of works of art. Rome, ICCROM.

Bidari, B. 2009. Lumbini Beckons. Lumbini, Bidari, B., pp. 56-62.

Rai, H.D. 2010, Lumbini. The supreme Pilgrimage. Kathmandu, pp. 95-97.

Brandi, C. 1964. Teoria del restauro. Roma.

Figures

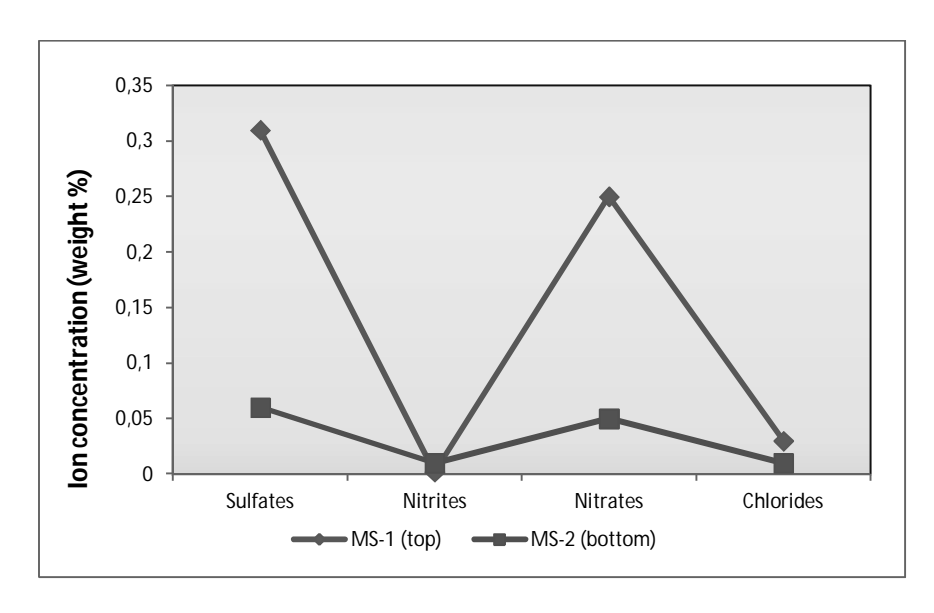


Figure 1. Trend of the salt concentrations in the Marker Stone samples.

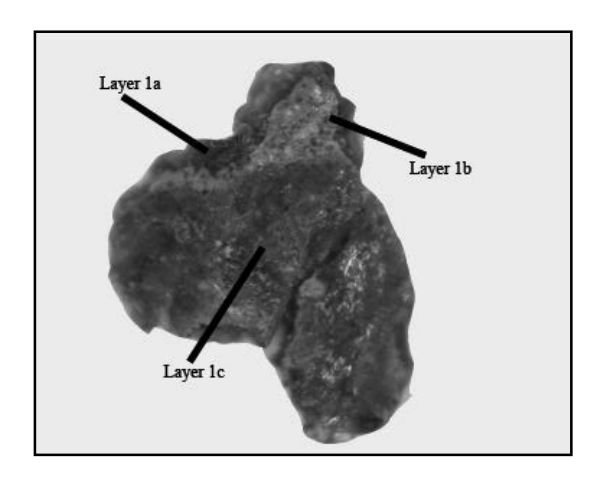


Figure 2. Sample NS3 - Location of the micro-FTIR analyses

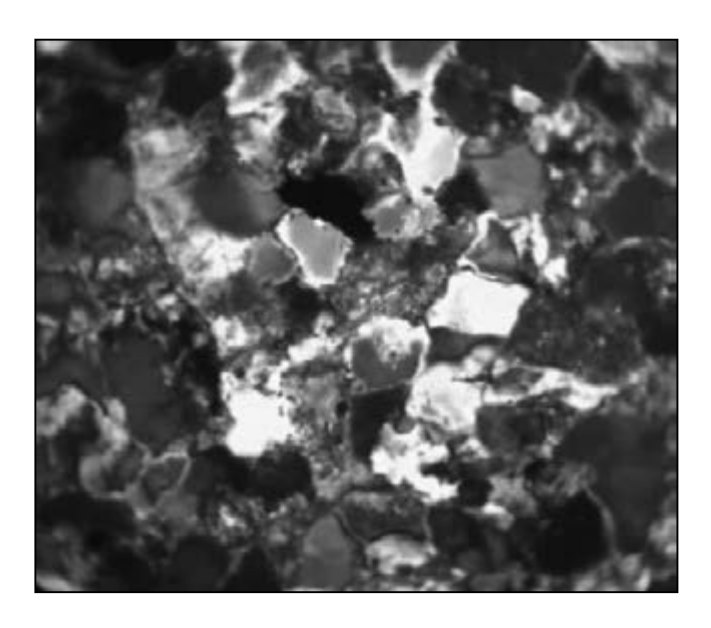


Figure 3. Sample AS1 - Texture of the sandstone (Nichols +; 100x)

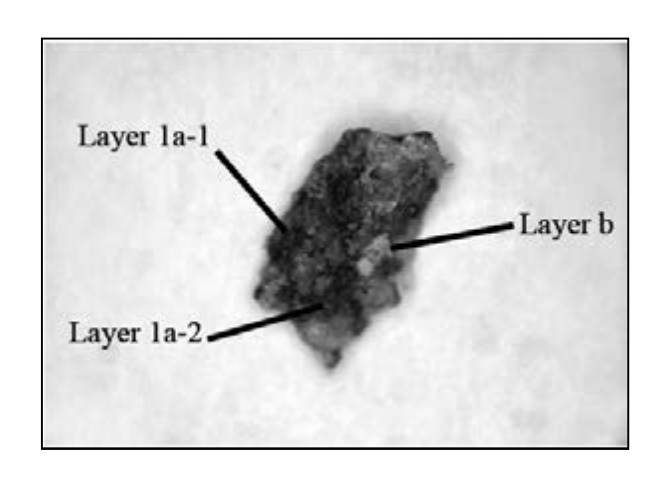


Figure 4. Sample AS1 - Location of the areas analyzed by micro-FTIR

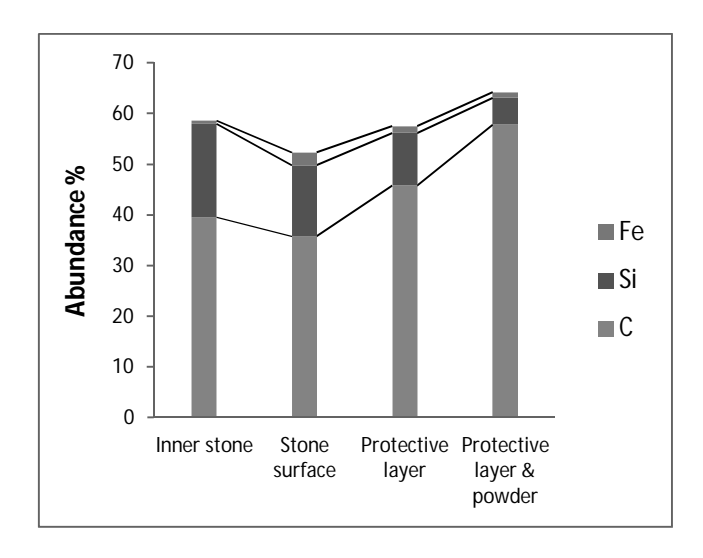


Figure 5. Distribution of the significant elements in the stratigraphy of sample AS1

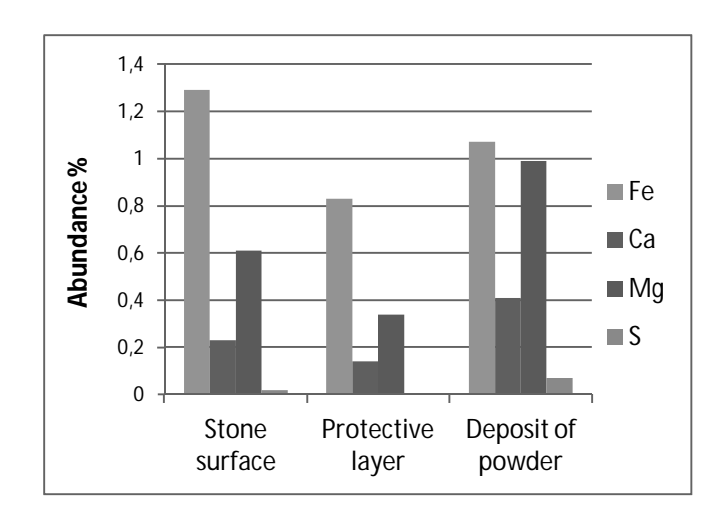


Figure 6. Sample AS1: degradation compound distribution in the stratigraphy

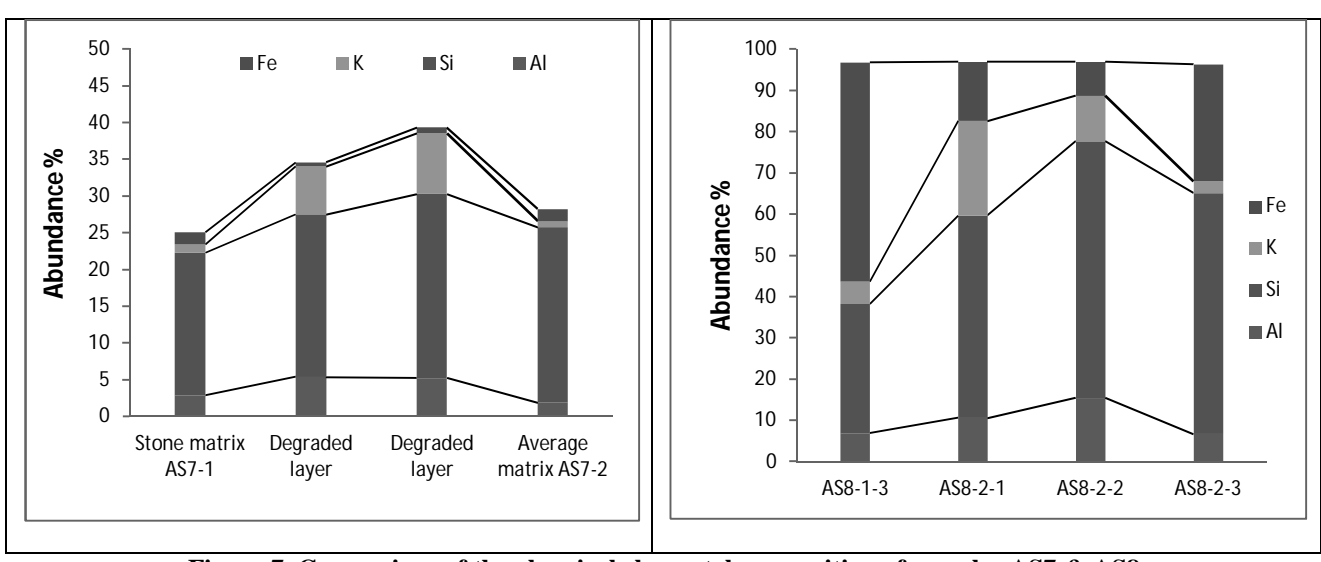


Figure 7. Comparison of the chemical elemental composition of samples AS7 & AS8

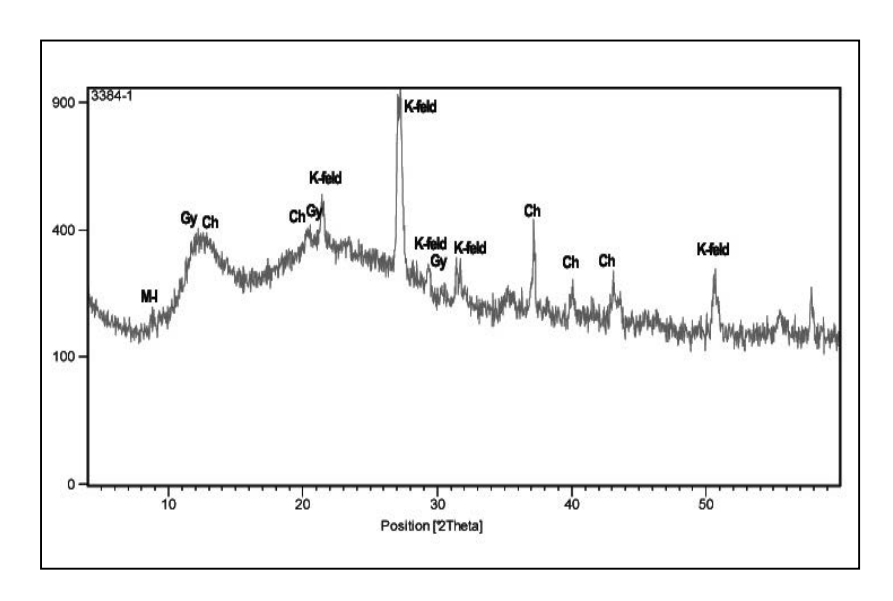


Figure 8. XRD spectrum of sample AS6



Figure 9. Appearance of the organic patinas on the capital

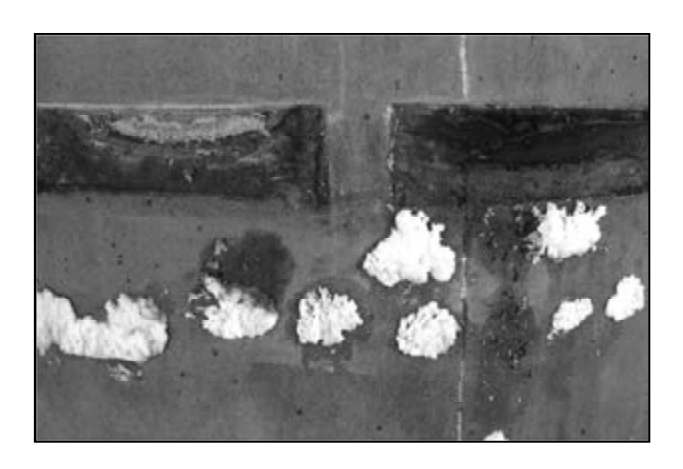


Figure 10. The surface of Pillar after the removal of the lower belt

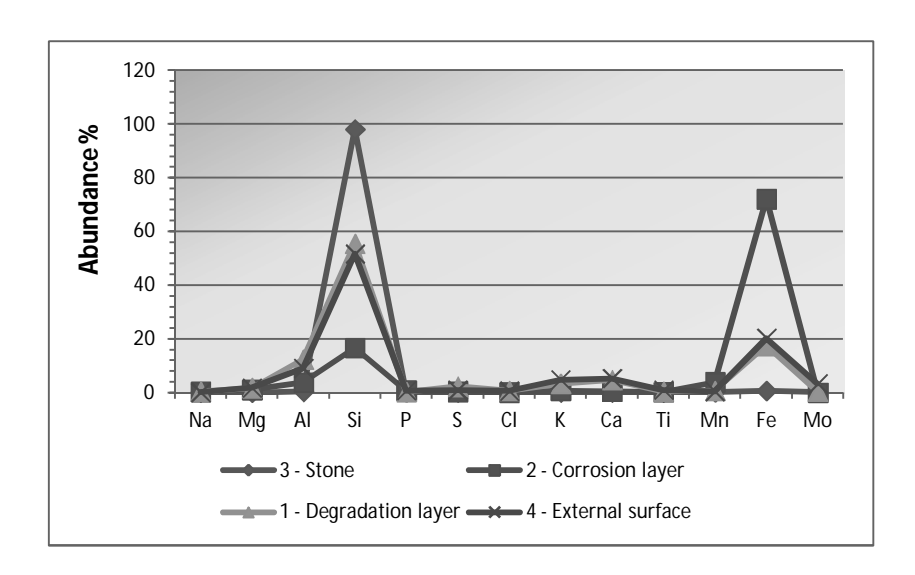


Figure 11. Distribution of component in the corrosion chip (Sample AS 9) $\,$

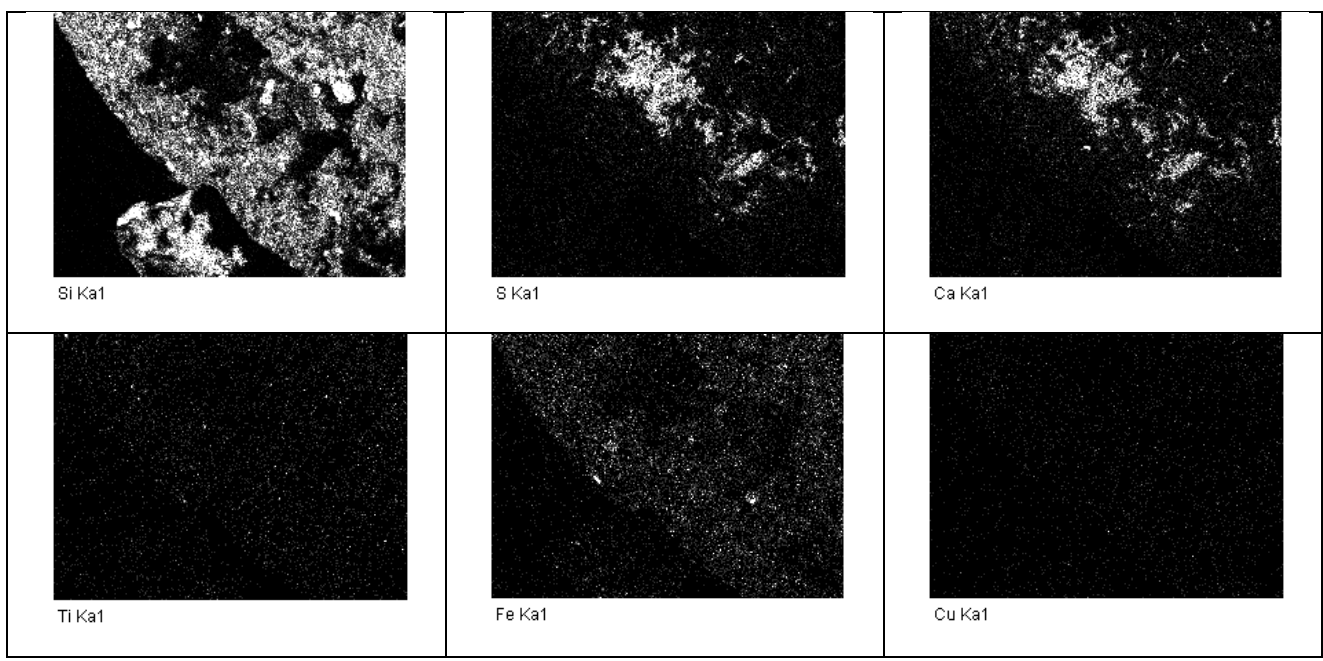


Figure 12. X-Ray distribution maps of the main elements composing sample AS9

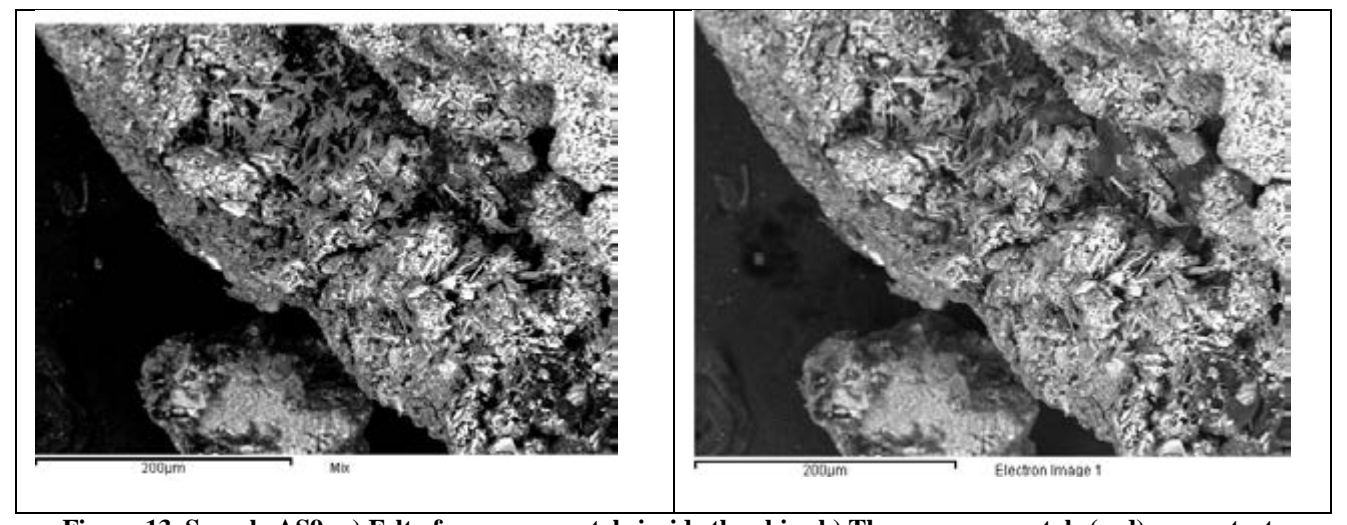


Figure 13. Sample AS9: a) Felt of gypsum crystals inside the chip; b) The gypsum crystals (red) concentrate inside the silicon matrix (white) of the ground powder

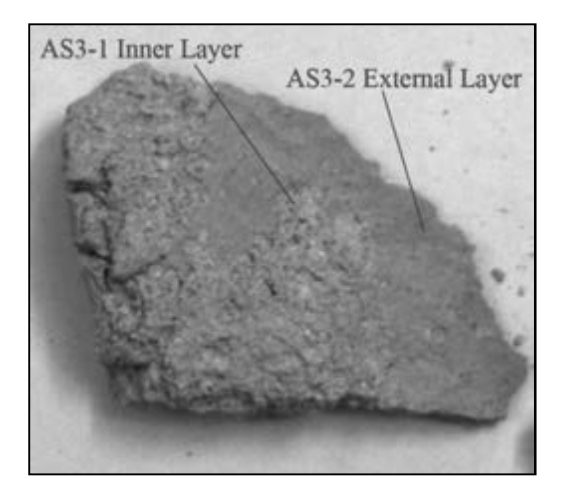


Figure 14. Sample AS3 showing the two different mortar layers

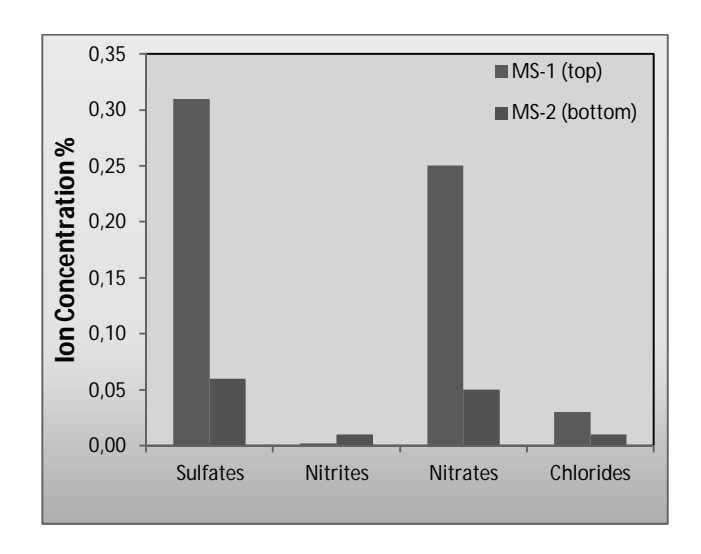


Figure 15. Marker Stone: distribution of soluble salts

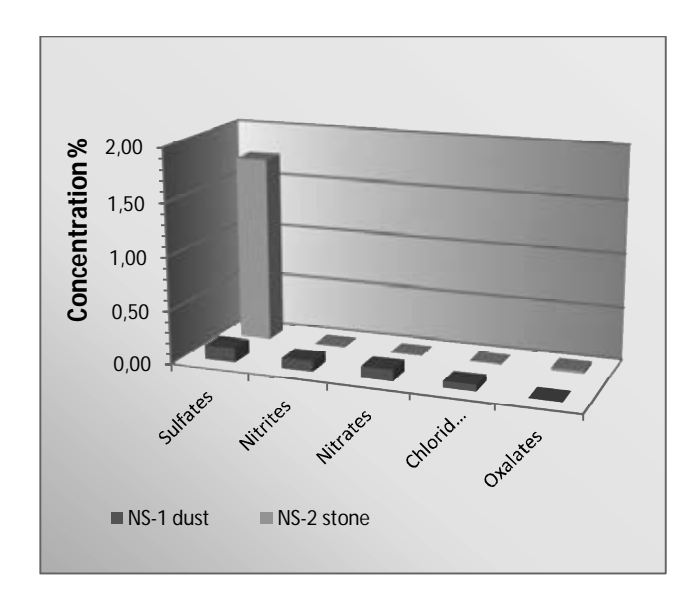


Figure 16. Nativity Sculpture: distribution of soluble salts

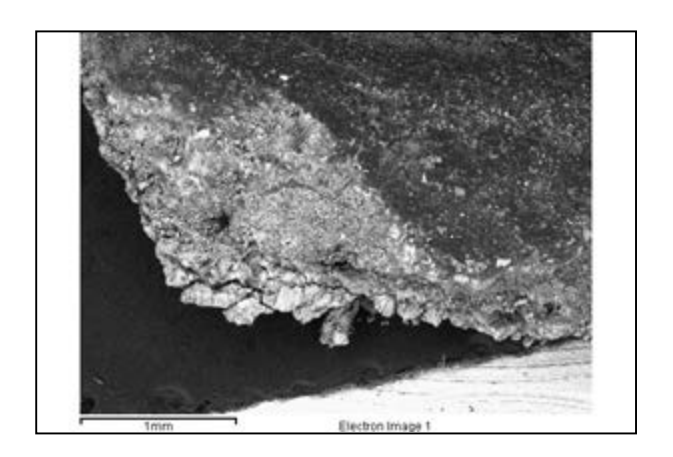


Figure 17. Sample NS2: SEM view of a chip of degraded stone

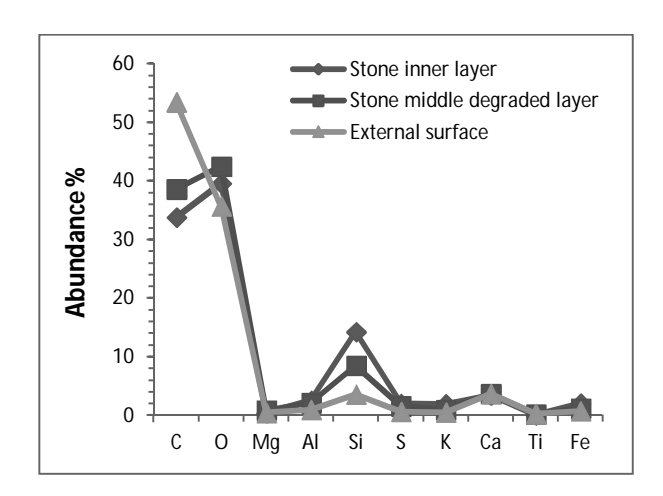


Figure 18. Sample NS2: fingerprint of the elemental chemical composition

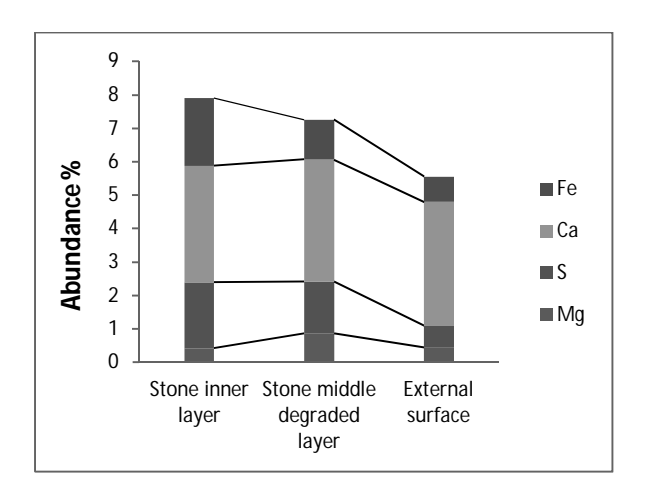


Figure 19. Distribution of degradation products in sample NS2



Figure 20. Performing XRF analyses on MD279 and MD280 bricks

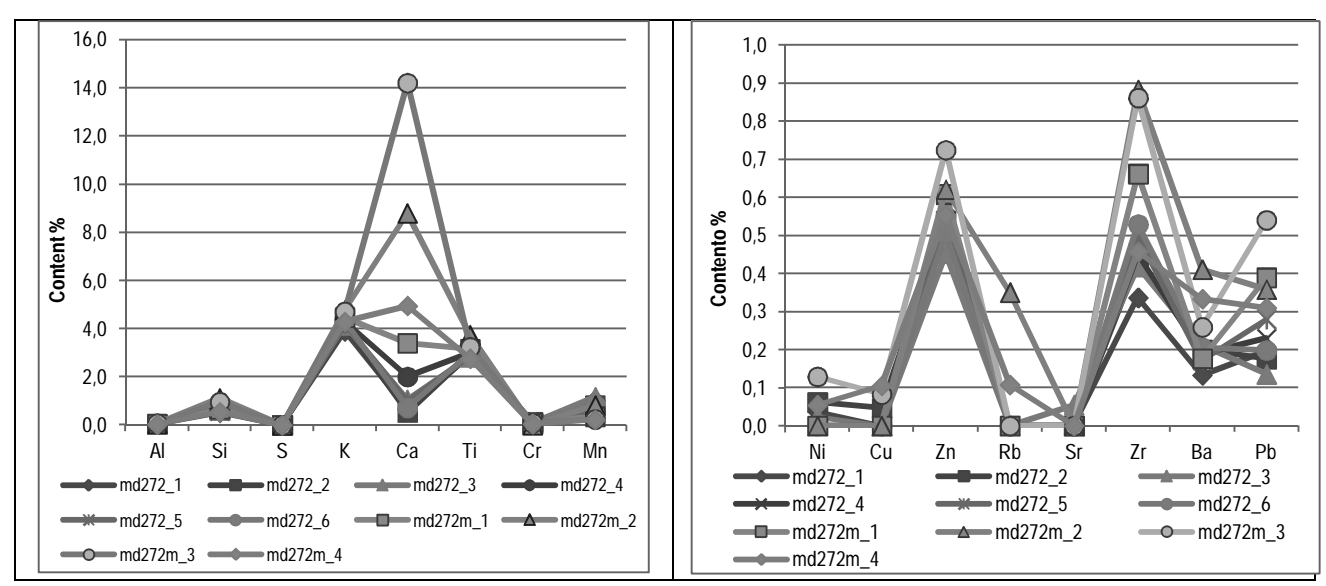


Figure 21. Fingerprint of the secondary and traces elements of sample MD272

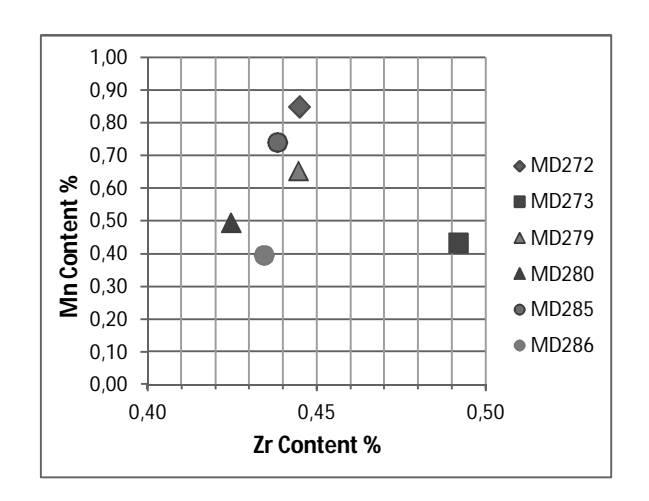


Figure 22. Pre-Asokan bricks from C5

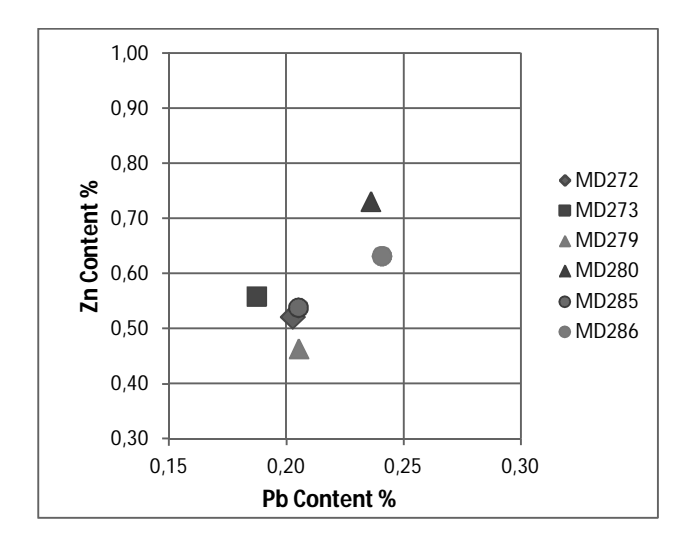


Figure 23. Pb and Zn content of pre-Asokan bricks

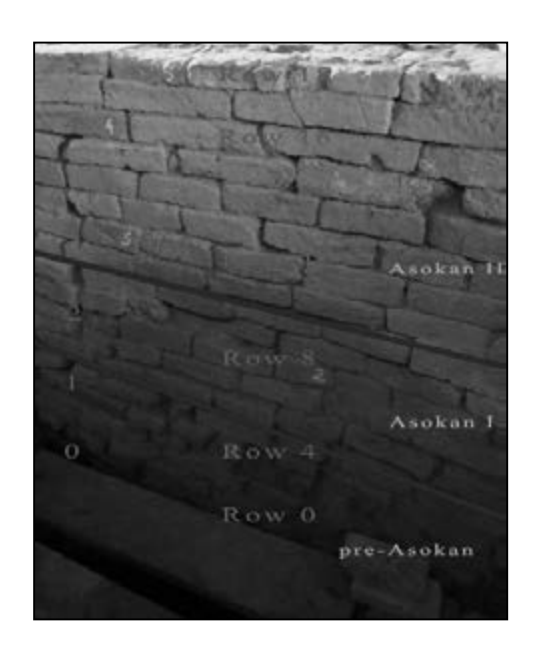


Figure 24. Brick chronology in Trench C5

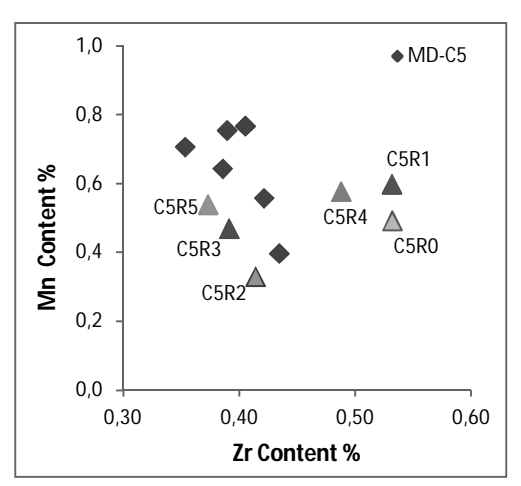


Figure 25. Fitting of C5 samples with pre-Asokan sample

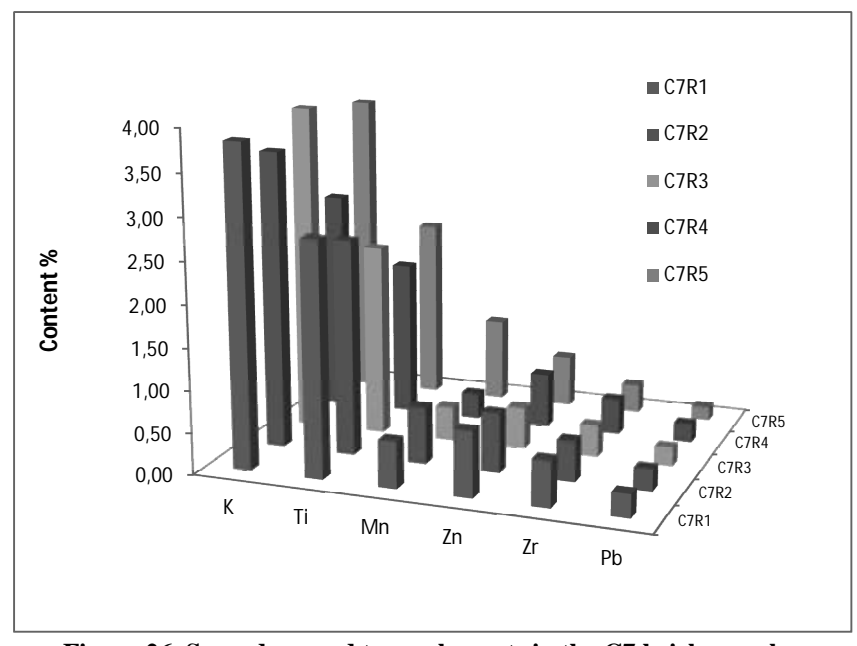


Figure 26. Secondary and trace elements in the C7 brick samples

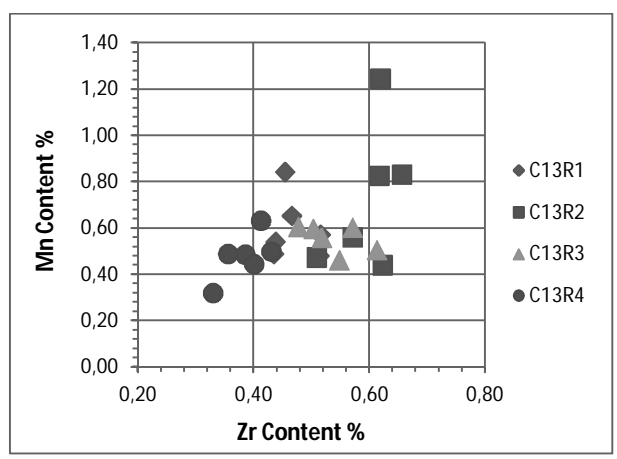


Figure 27. Distribution of the C13 samples

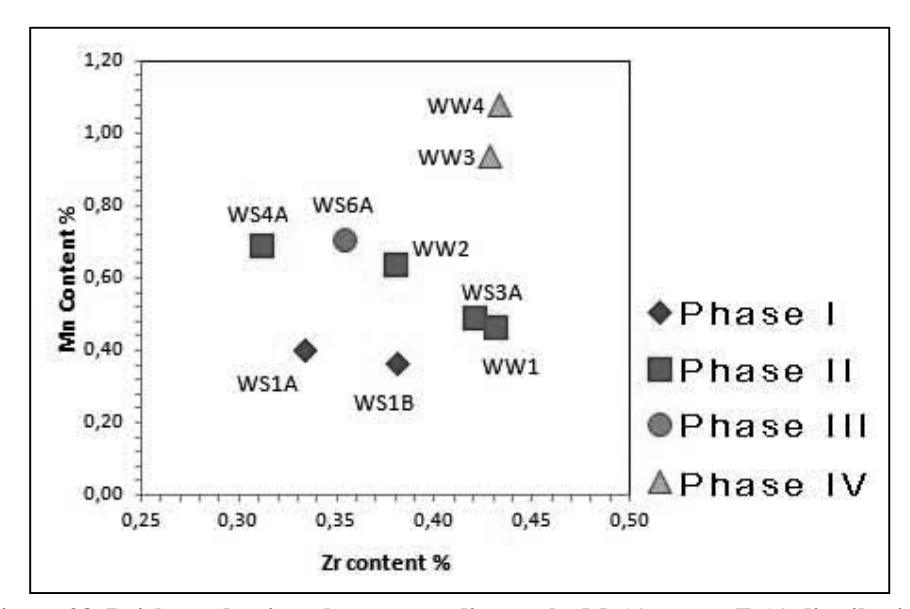


Figure 28. Brick production phases according to the Mn% versus Zr% distribution

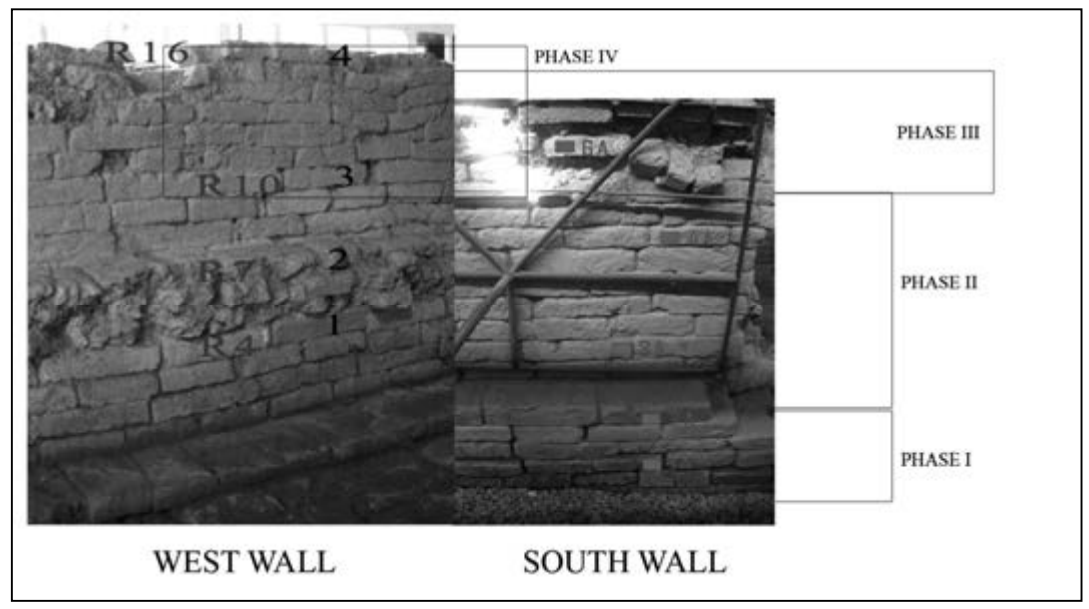


Figure 29. Comparison of South and West walls

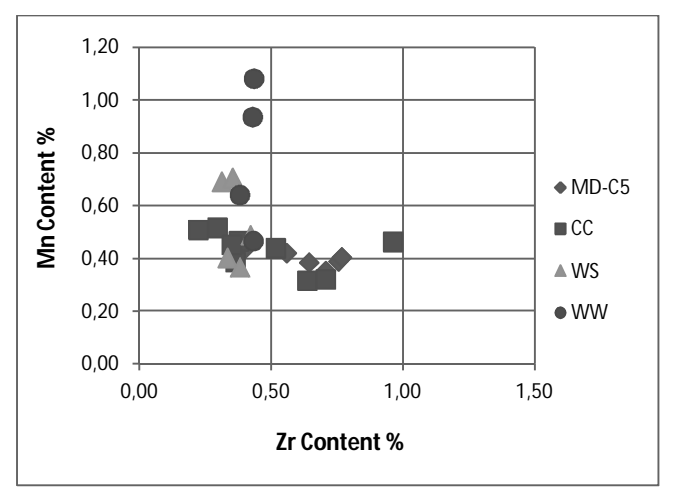


Figure 30. Distribution of the wall samples with reference to the MD bricks.

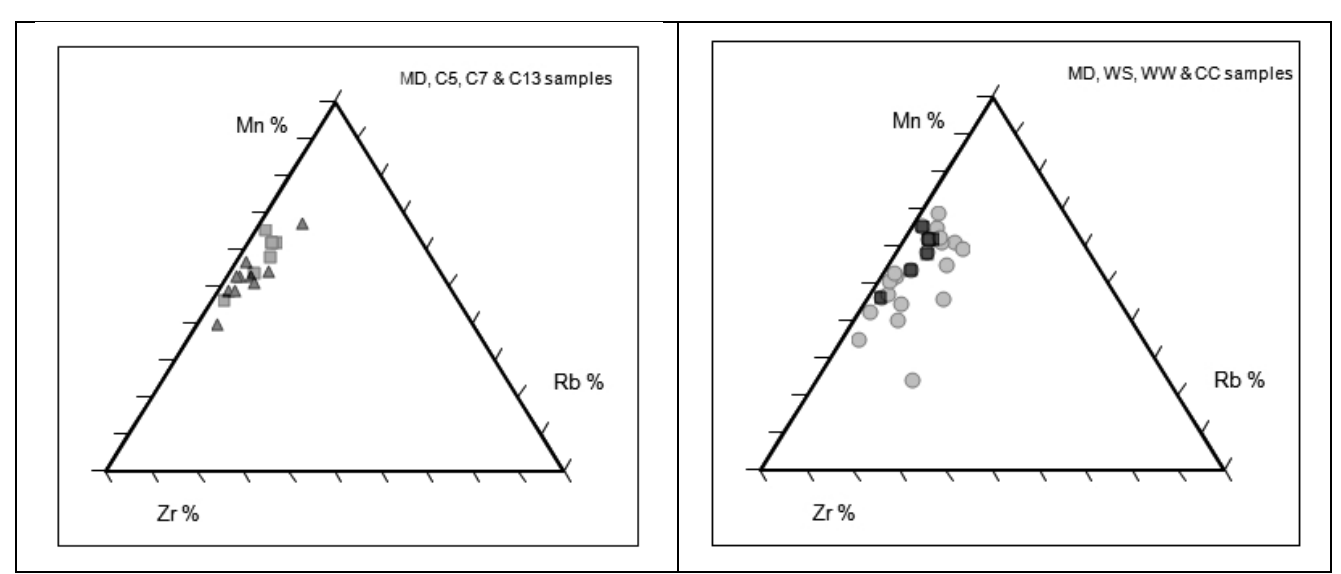


Figure 31. Distribution of the brick samples with reference to the MD-C5 samples

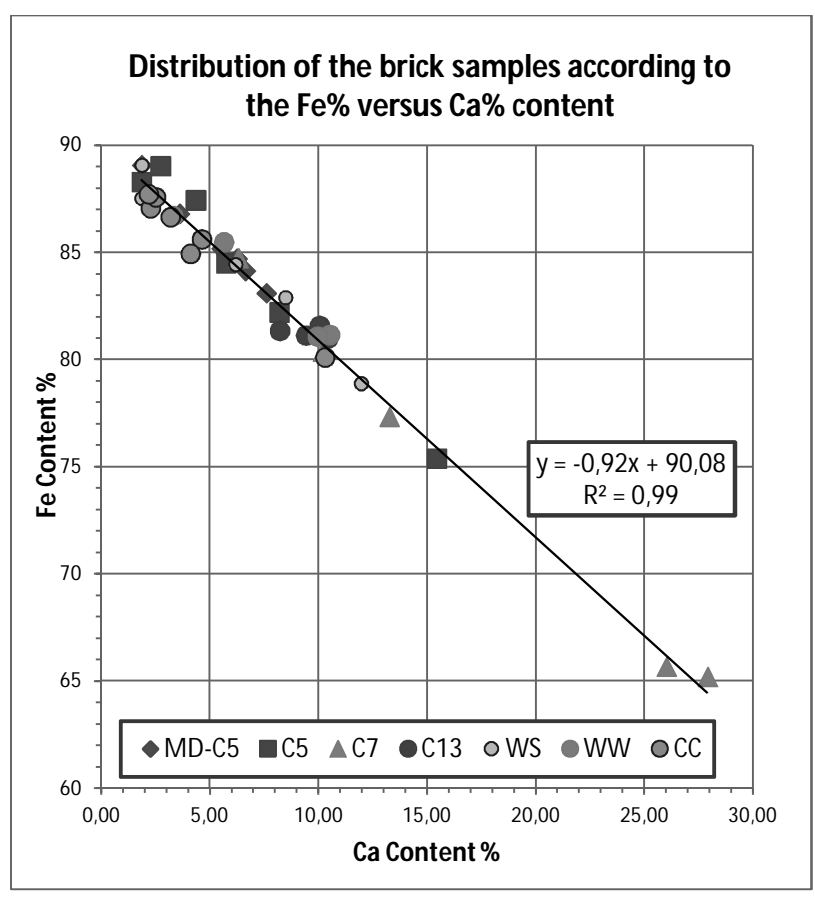


Figure 32. Distribution of all brick samples in the binary Fe% versus Ca% chart

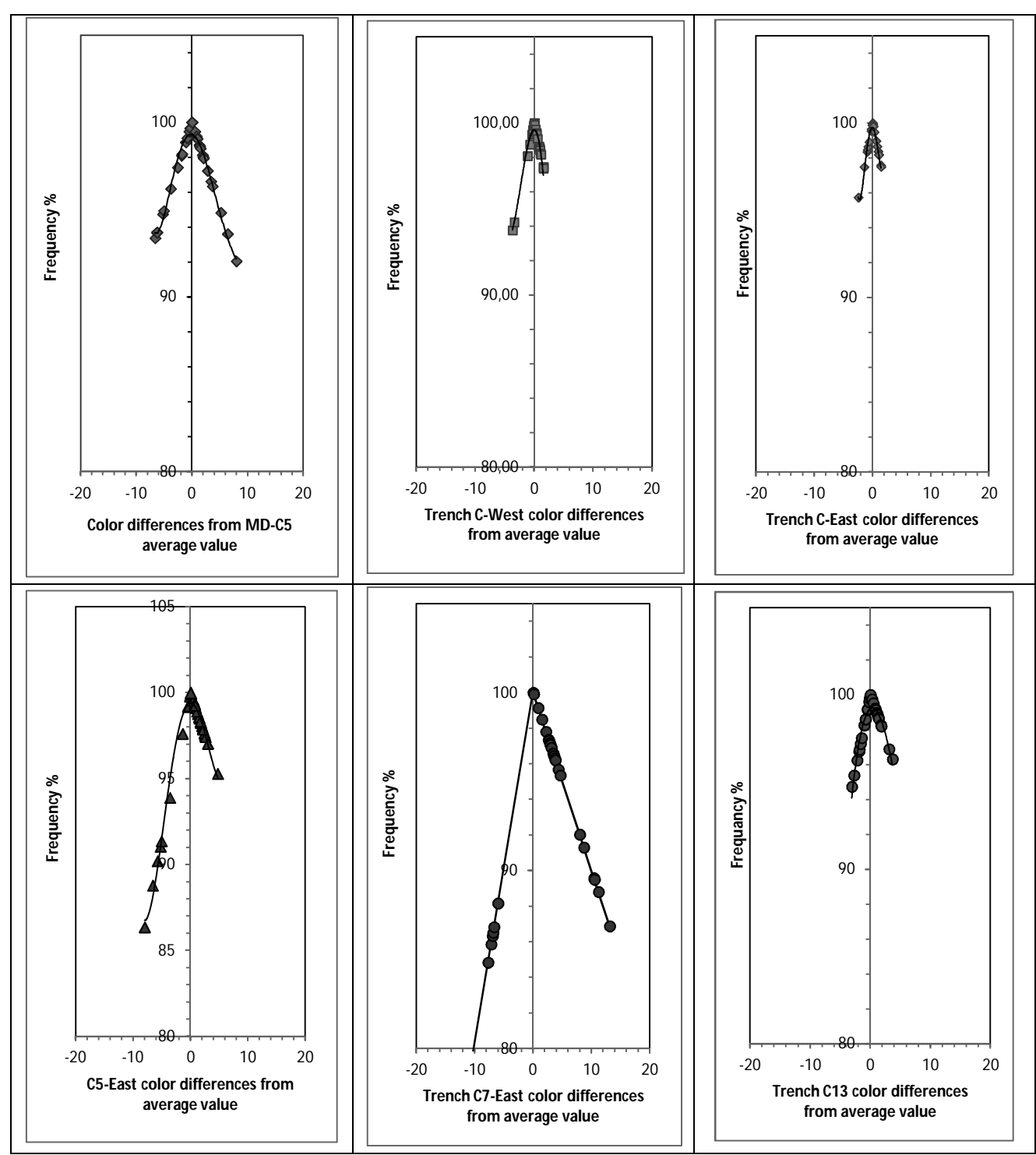


Figure 33. Variability of the color of MD-C5, and C-West, C-East, C5, C7 and C13 Trenches

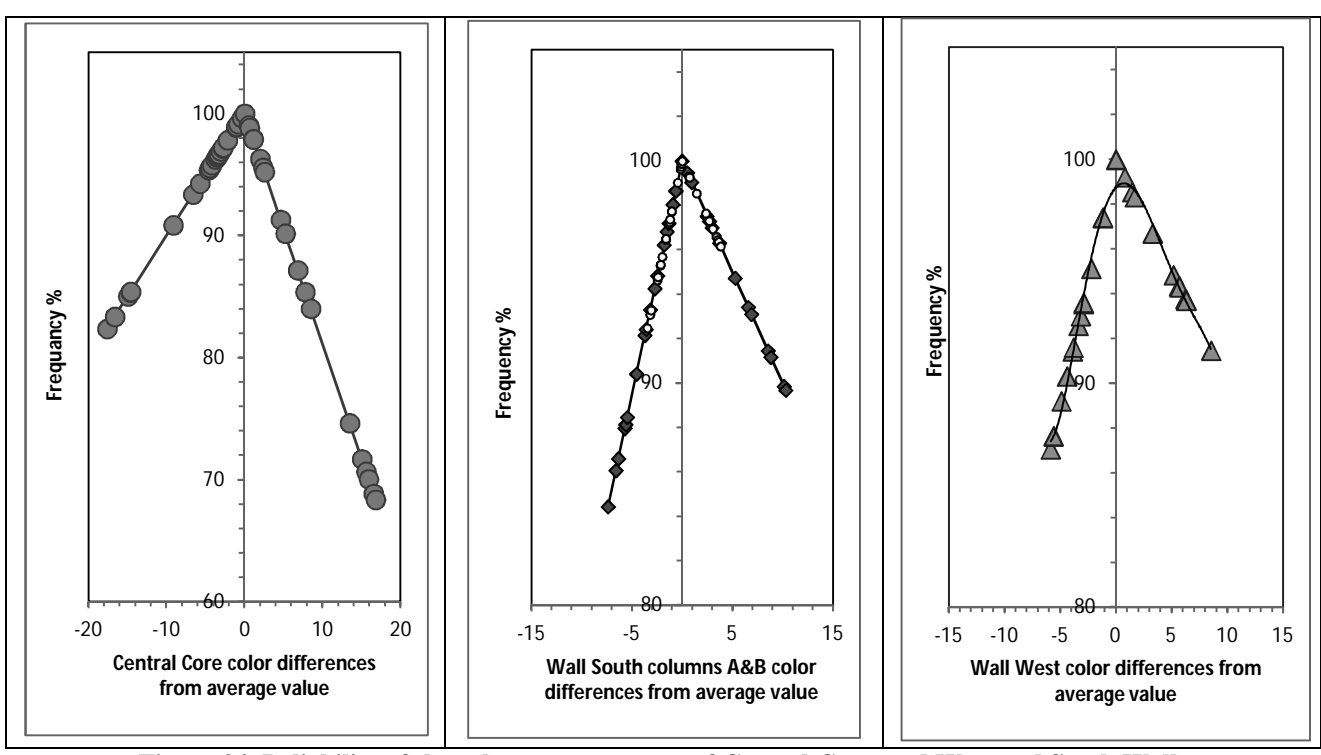


Figure 34. Reliability of the color measurements of Central Core, and West and South Walls

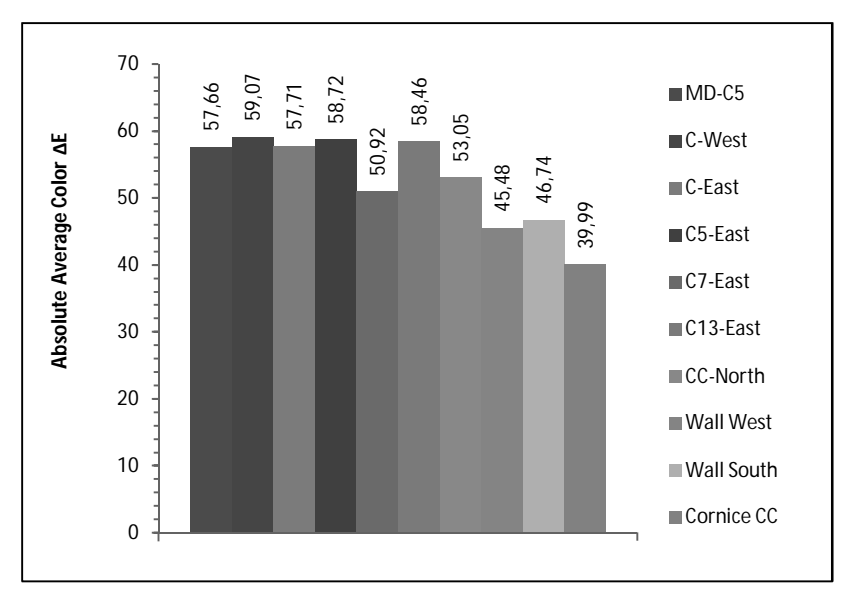


Figure 35. Absolute color of the analyzed masonries

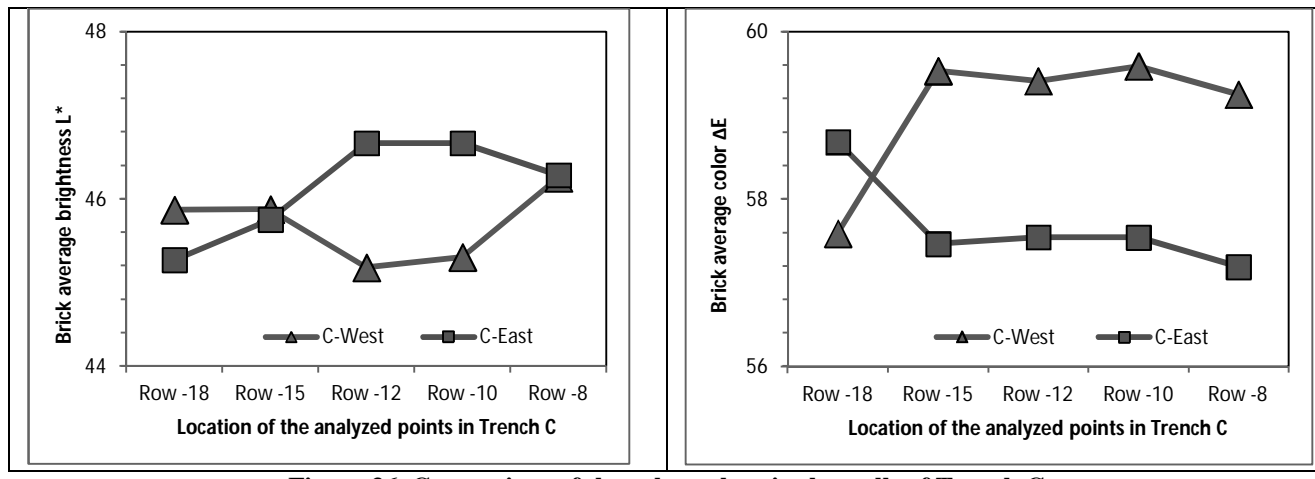


Figure 36. Comparison of the color values in the walls of Trench C

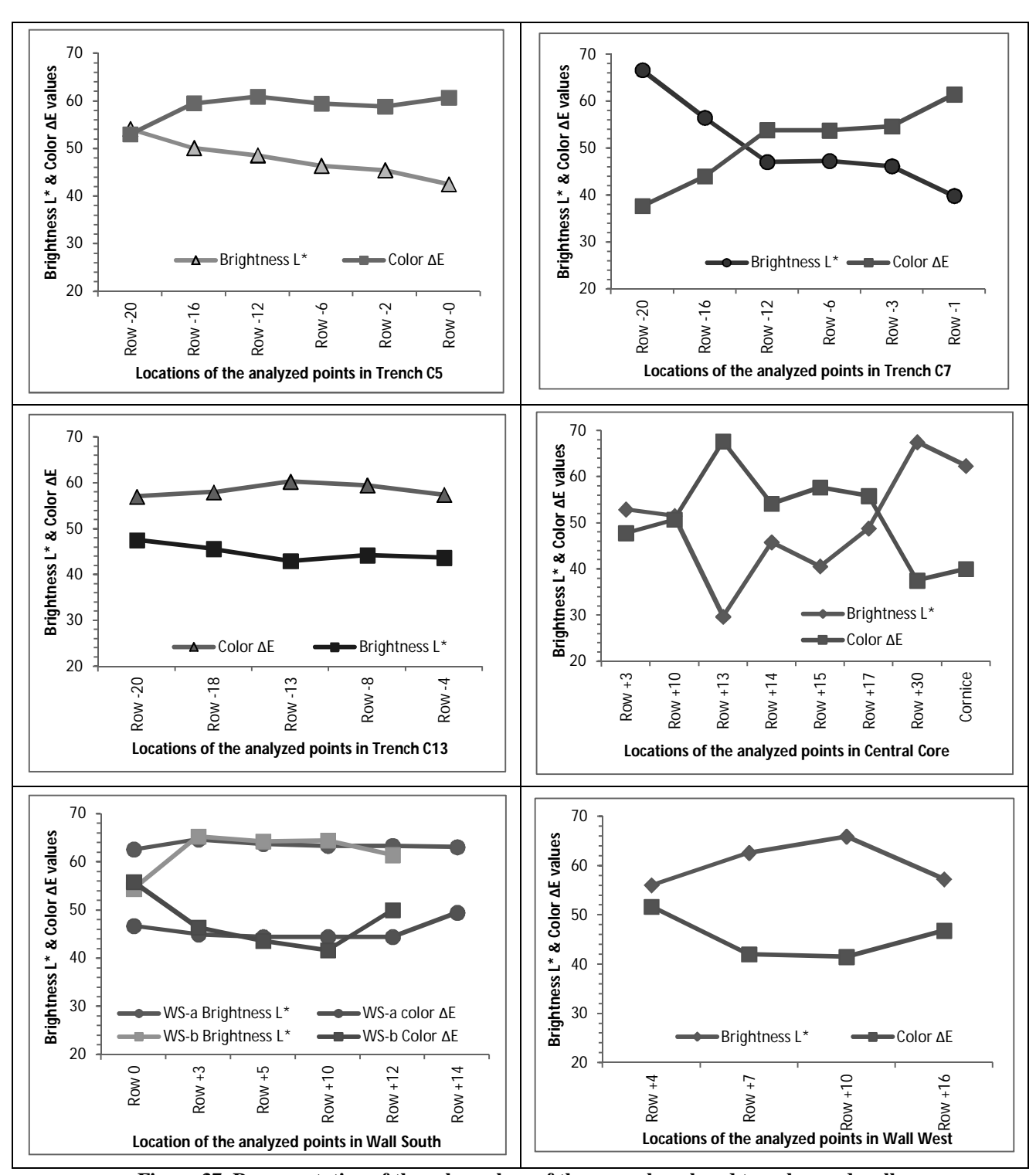


Figure 37. Representation of the color values of the several analyzed trenches and walls

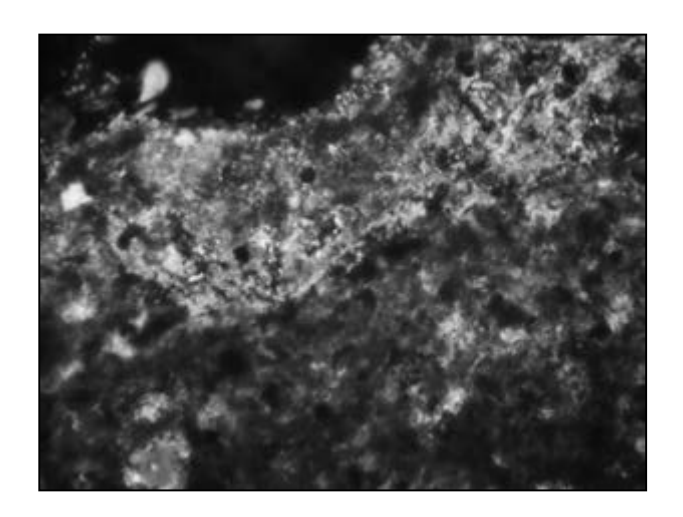


Figure 38. C5-E1, x20; Nichols#: mud mortar texture

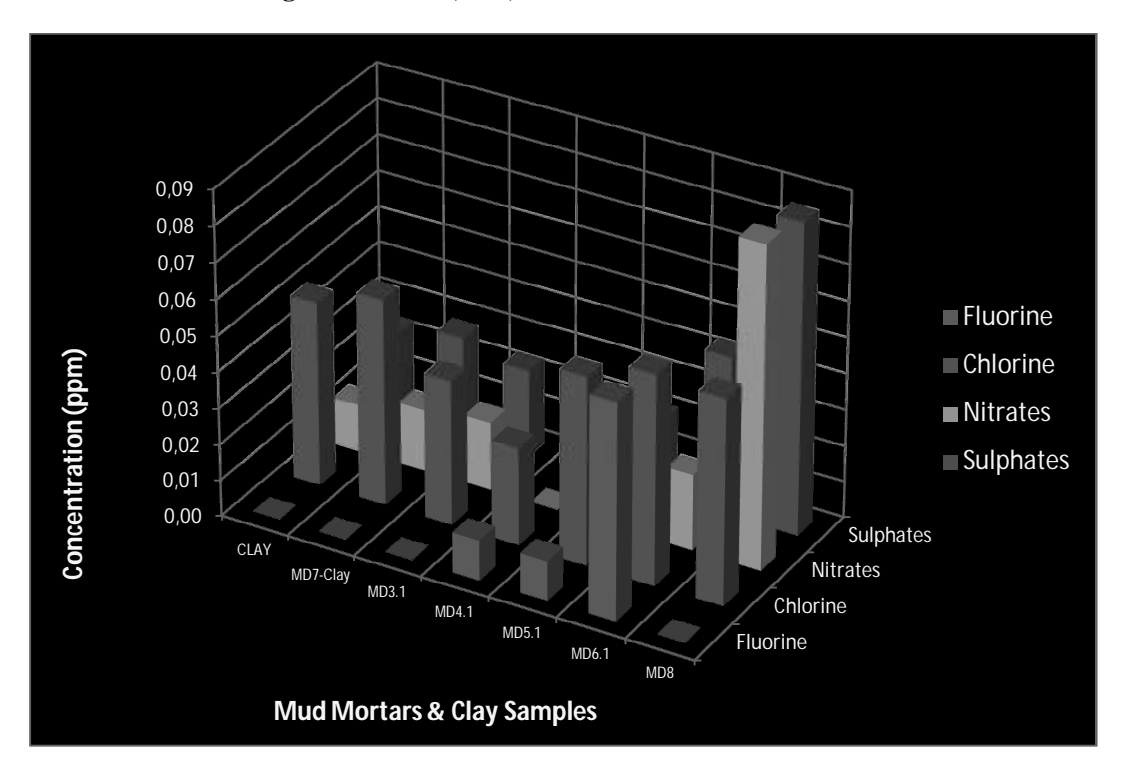


Figure 39. Trend of the salt concentrations in mud mortar $\,$

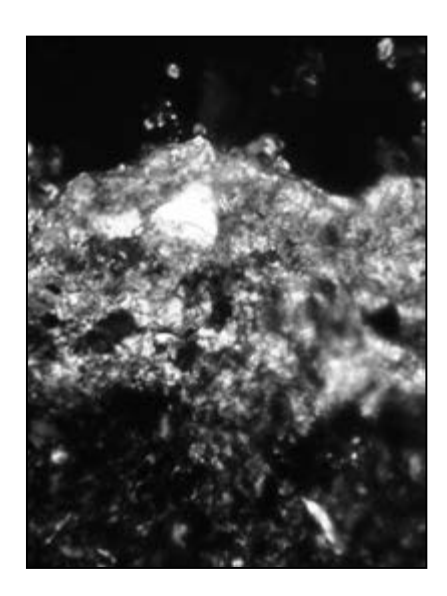
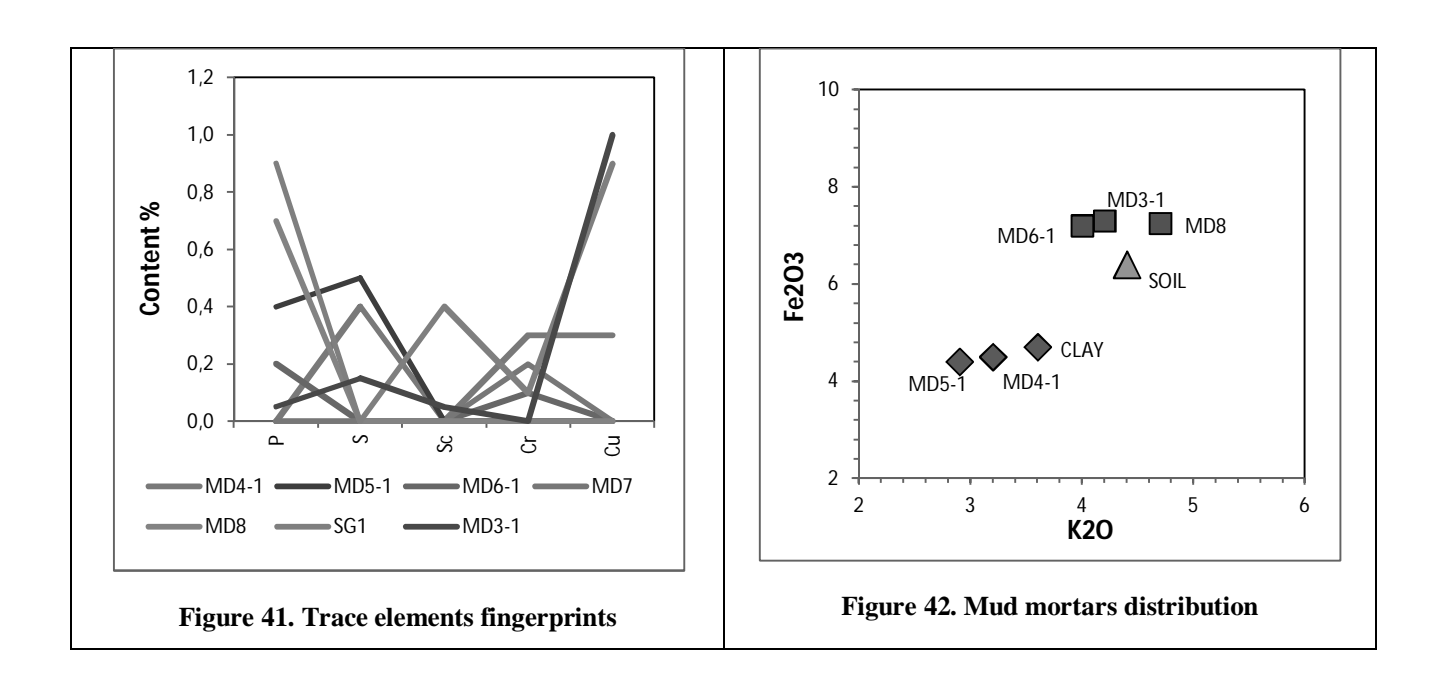


Figure 40. Sample M.D.6; x20, Nichols #: lime mortar with spatic calcite and white quartz



CHRONOLOGY	SAMPLE	Brick	PATINA	SILT	Lime Mortar	MUD
Pre-Asokan	C5-F1					
ASOKA I	C5-E1					
	C5-E2					
	C7-N1					
	C7-E2					
	MD4=C7-E6R					
	CE10=C-E2					
	WS-1a					
ASOKA II	C-W4					
	C-W8					
	C13-W4					
	CE18=C-E4					
	MD5=C7-E12R					
	MD6=C7-E18R					
	WW-1					
	WS-5b					
KUSHAN (?)	WS-6a					
	CC-4					

Figure 43. Stratigraphy of the patinas according to the chronology

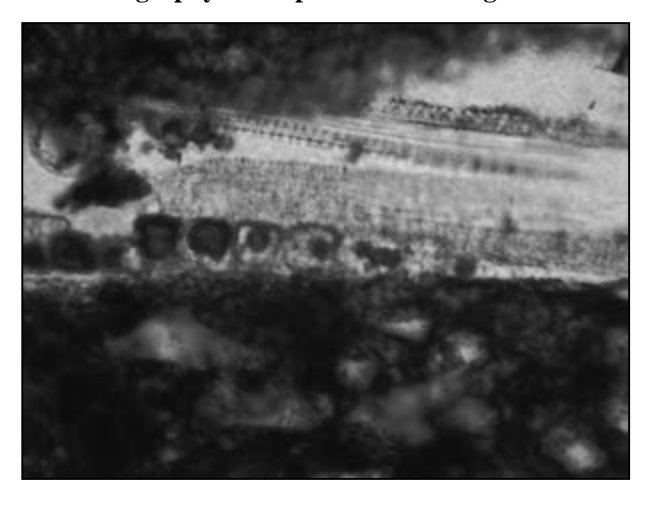


Figure 44. Sample C5-F1, x40, Nichols//: Straw remains

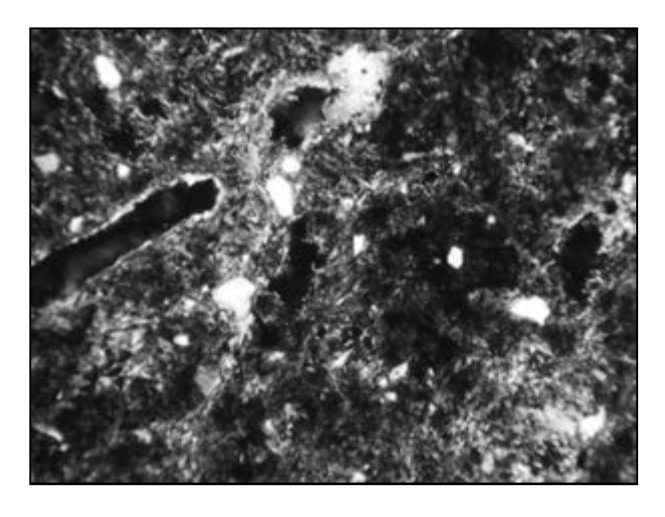


Figure 45. C7-E3, x10, Nichols#: The texture of the body shows large fissures of the straw marks

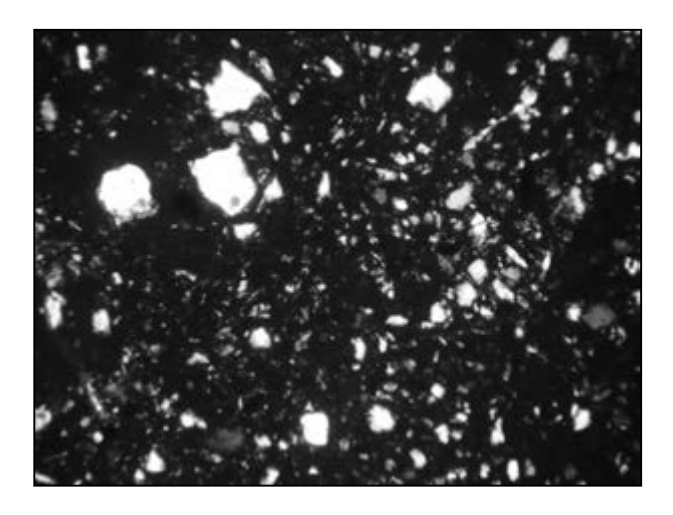


Figure 46. Temper components vary both in size and in shape

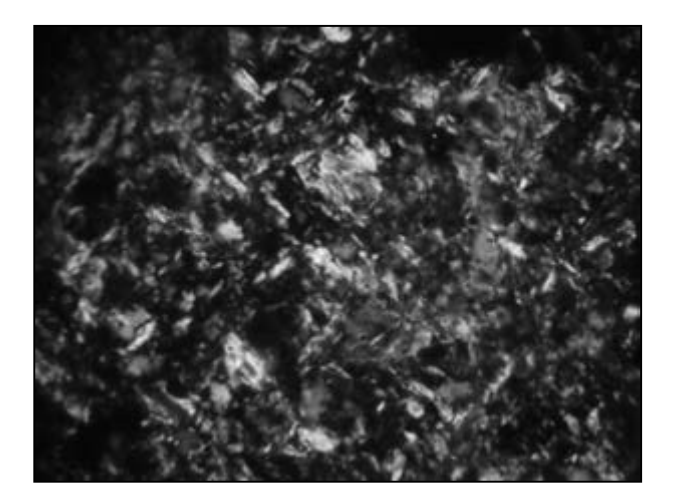


Figure 47. C-W2 x40, Nichols#: Illite-muscovite crystals characterize the matrix structure

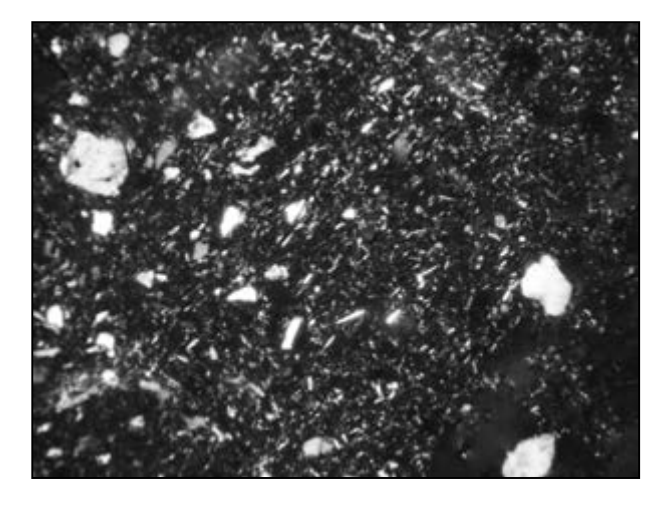


Figure 48. C-E14, x10, Nichols#: Temper is made of sub-round quartz, while acicular feldspars and angular quartz are part of the clay

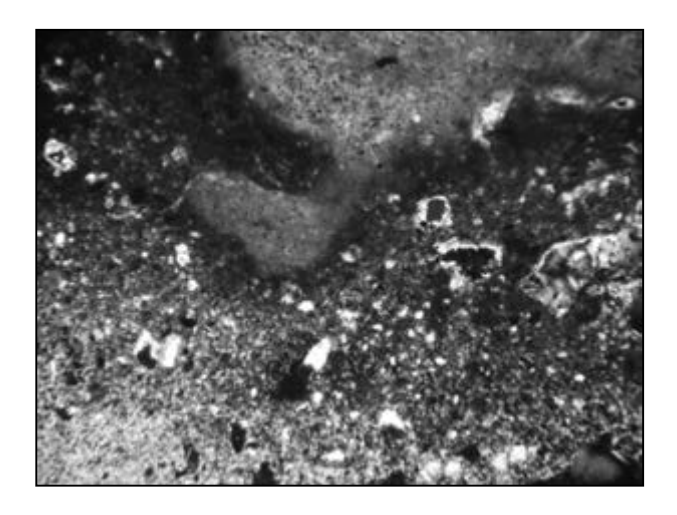


Figure 49. C5-E1, x4, Nichols#: large fragments of mudstone are component of the skeleton.

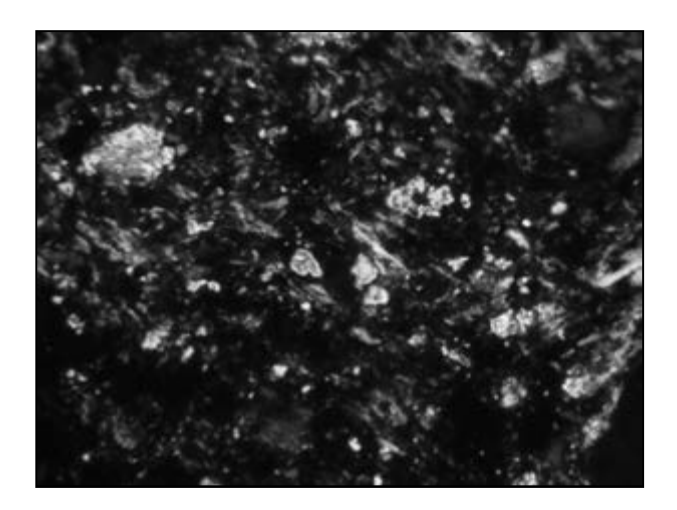


Figure 50. C5-E1, x40, Nichols#: Micro-crystals of sparitic calcite and illite minerals are dispersed in the matrix

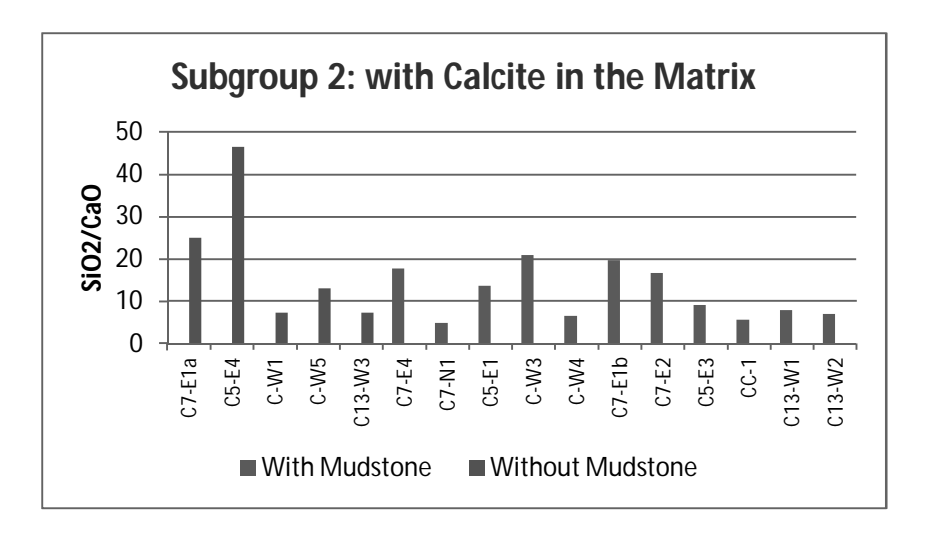


Figure 51. Distribution of the samples respect to the SiO2/CaO content ratio

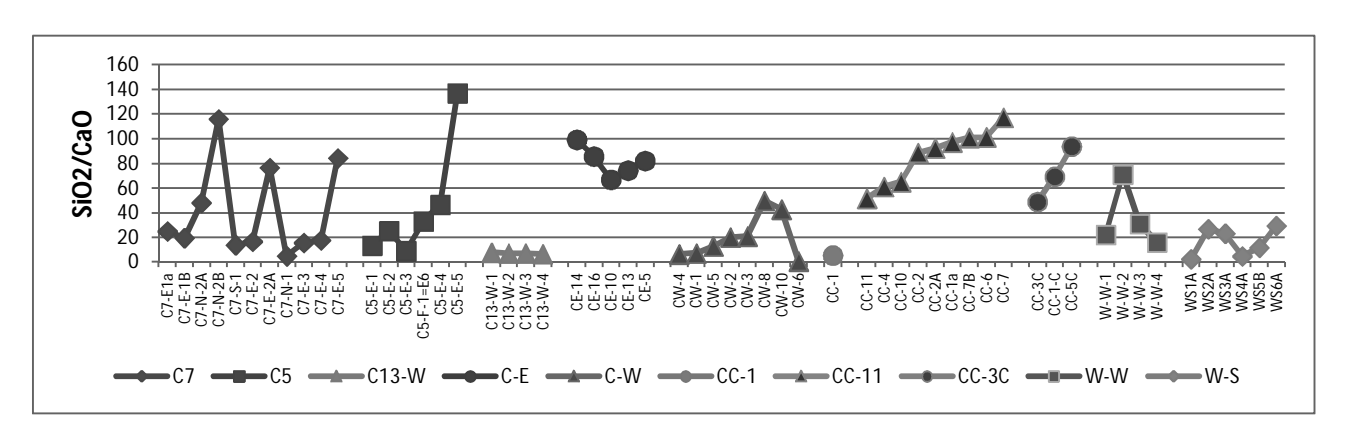


Figure 52. Samples distribution according to the SiO2/CaO ratio values

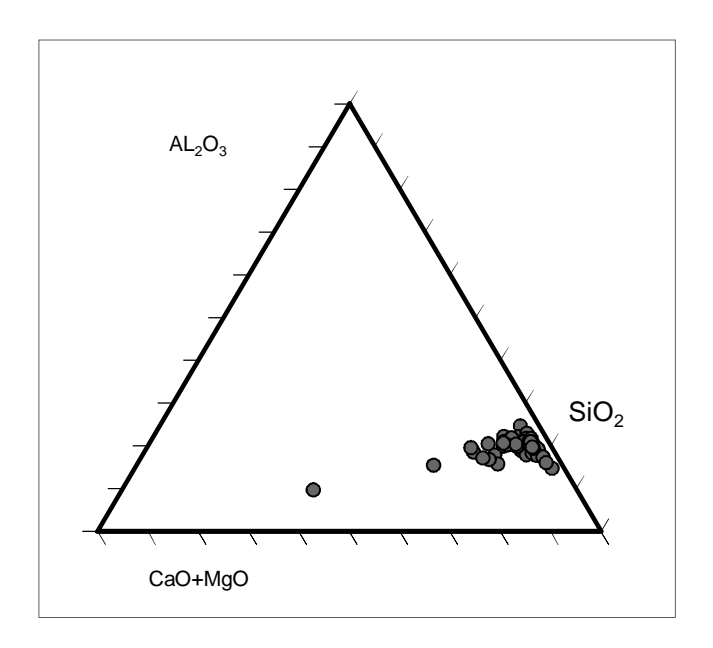


Figure 53. Samples distribution according to the silicate composition

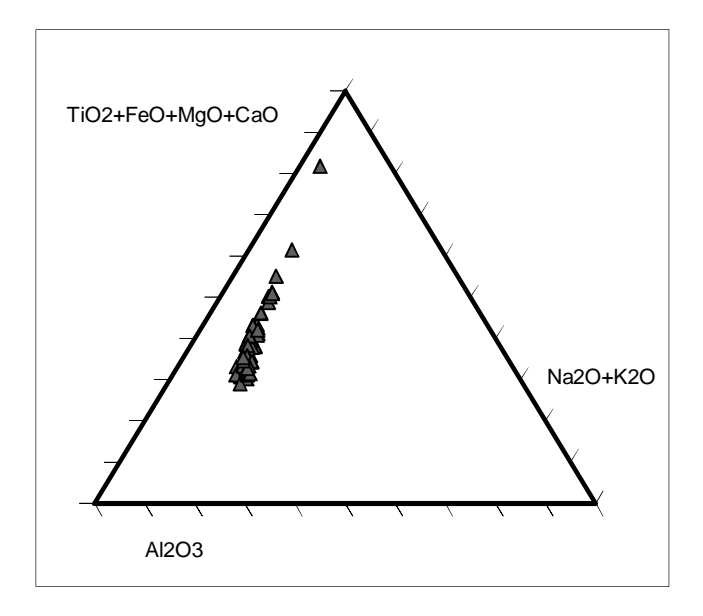


Figure 54. Distribution according to the skeleton composition

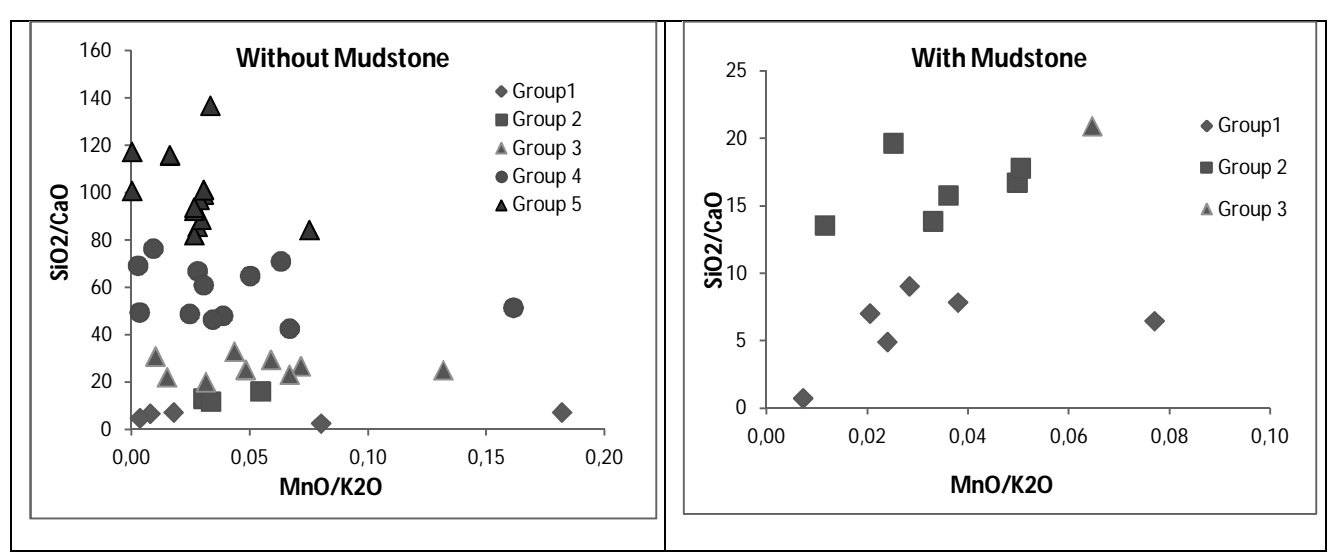


Figure 55. Comparison among the group distribution according to their petrography

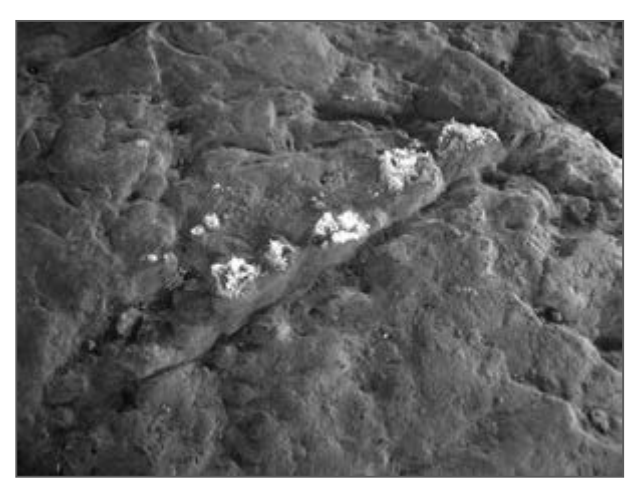


Figure 56. Salt efflorescence in the floor bricks of trench C8

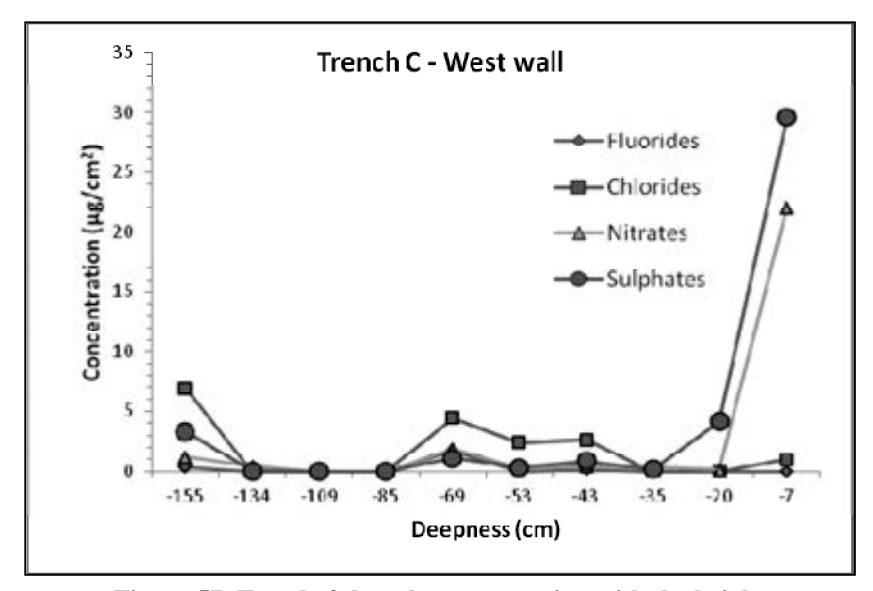


Figure 57. Trend of the salt concentration with the height

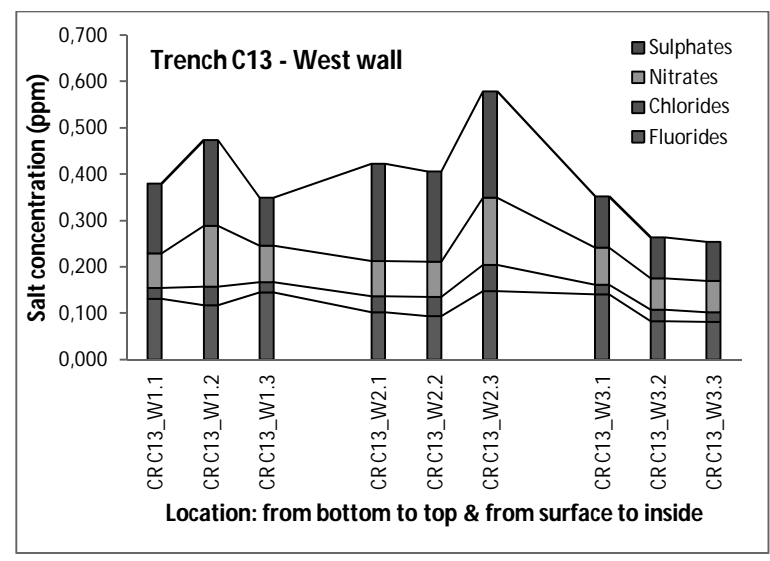


Figure 58. Trend of the salt concentration inside the masonry

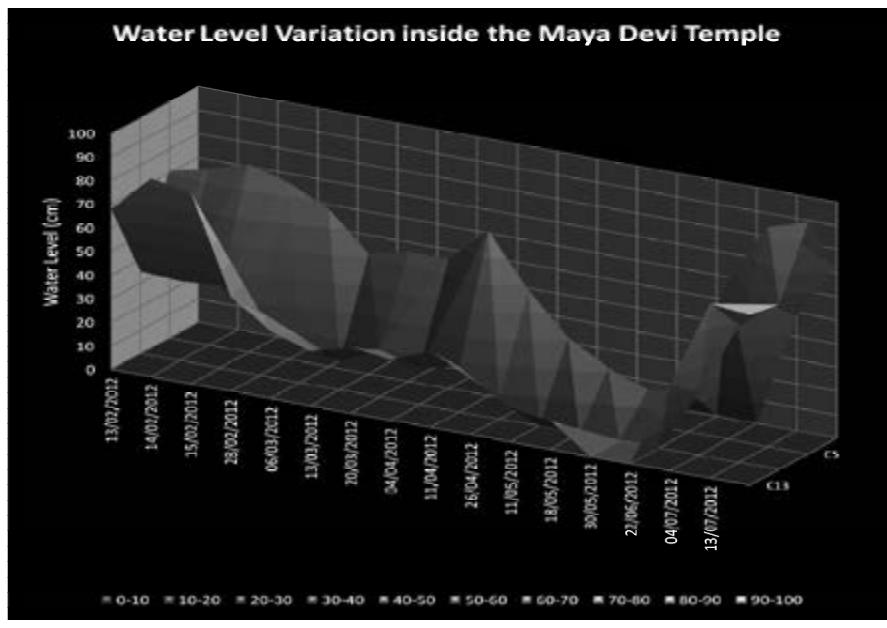


Figure 59. Variations of the aquifer level

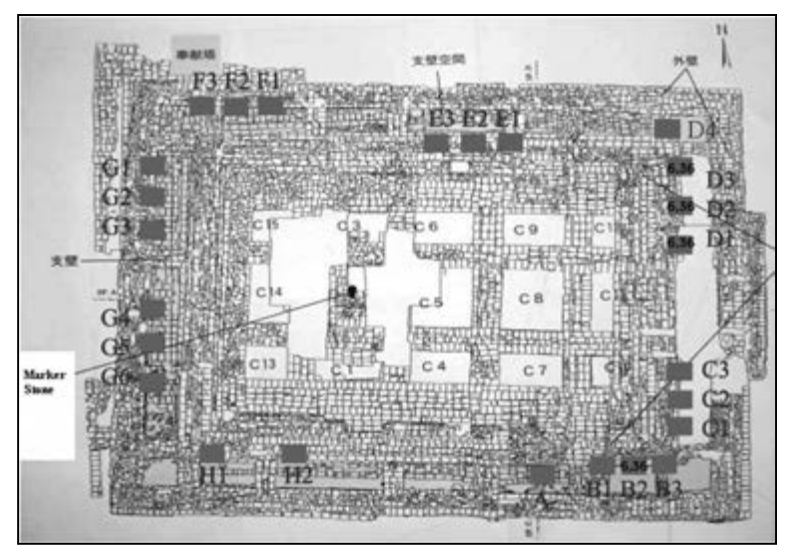


Figure 60. Location of the measurement points at under-ground level

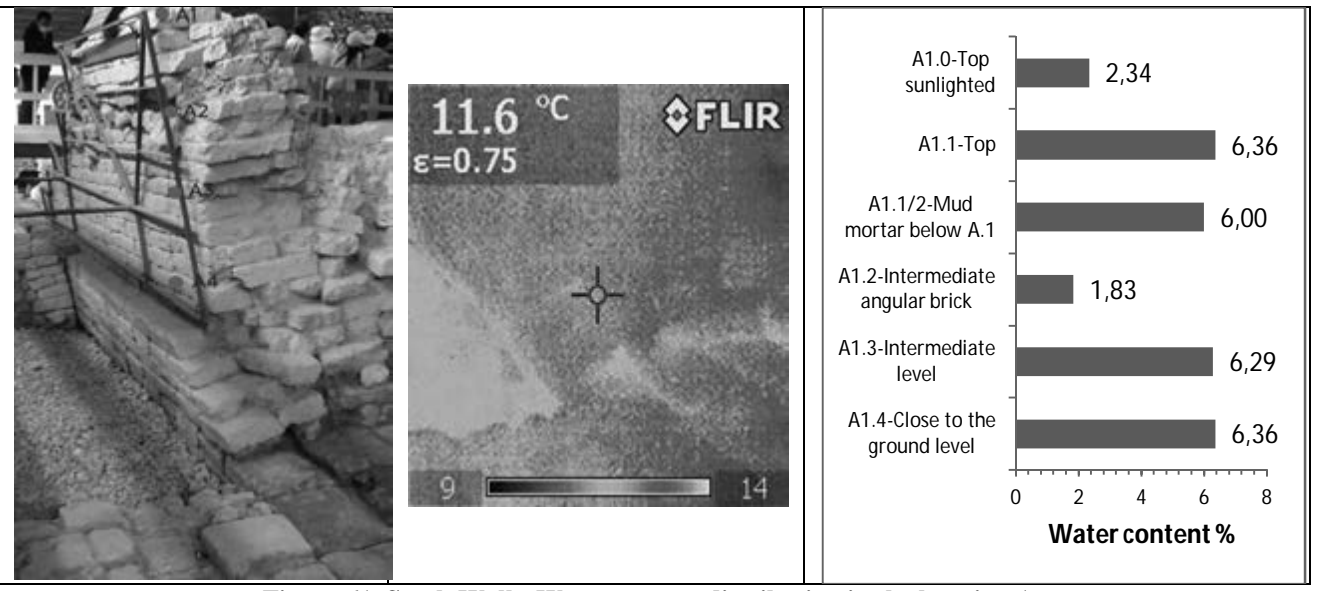


Figure 61. South Wall - Water content distribution in the location A.

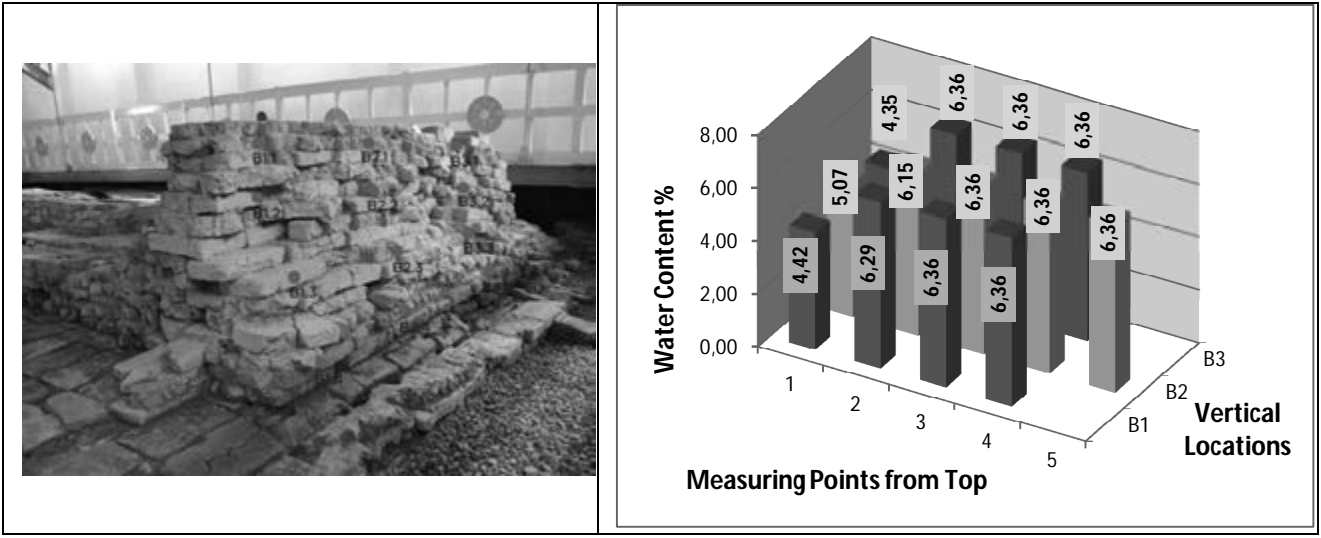


Figure 62. South Wall - Water content distribution in the location B.

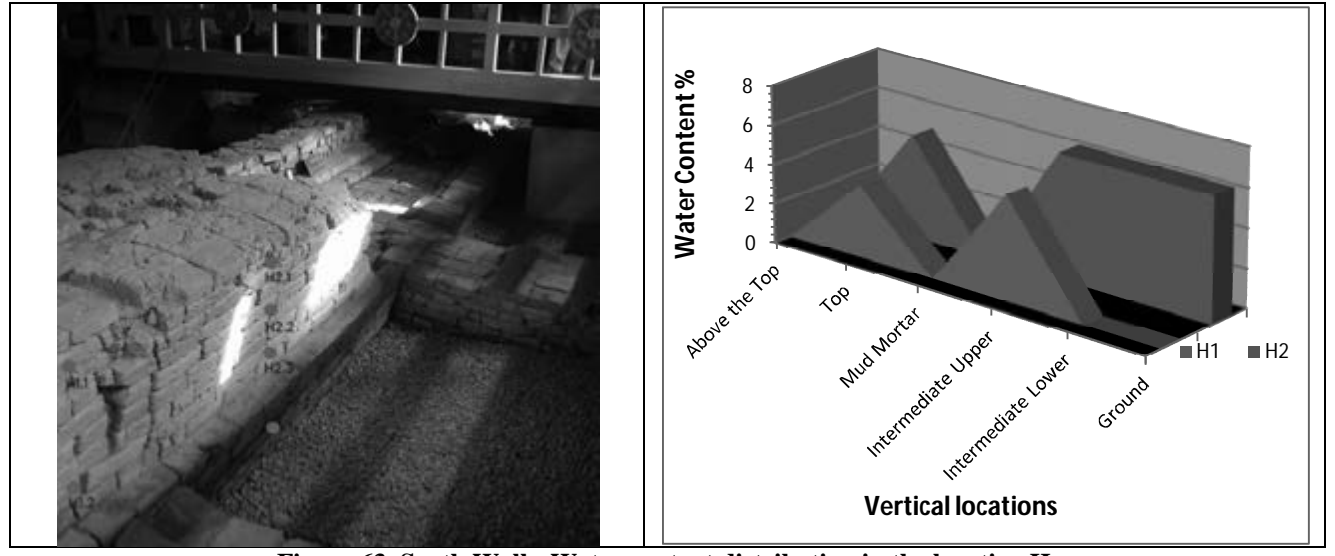


Figure 63. South Wall - Water content distribution in the location H.

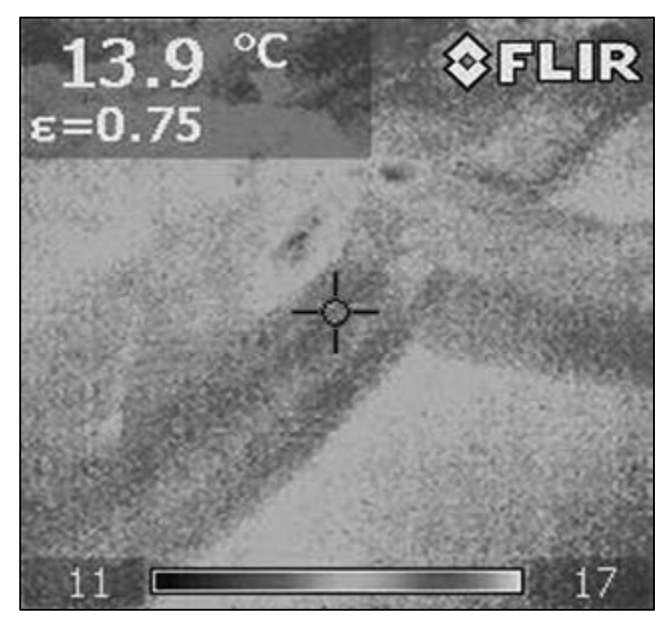


Figure 64. South Wall - Water distribution in the location H by IR camera.

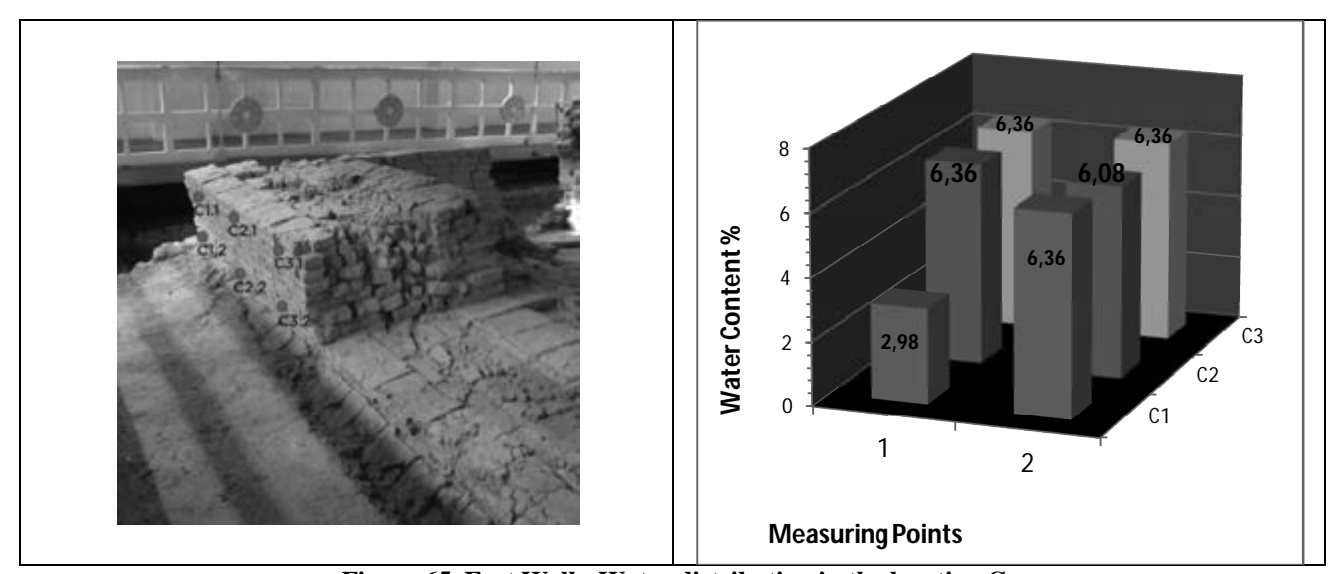


Figure 65. East Wall - Water distribution in the location C.

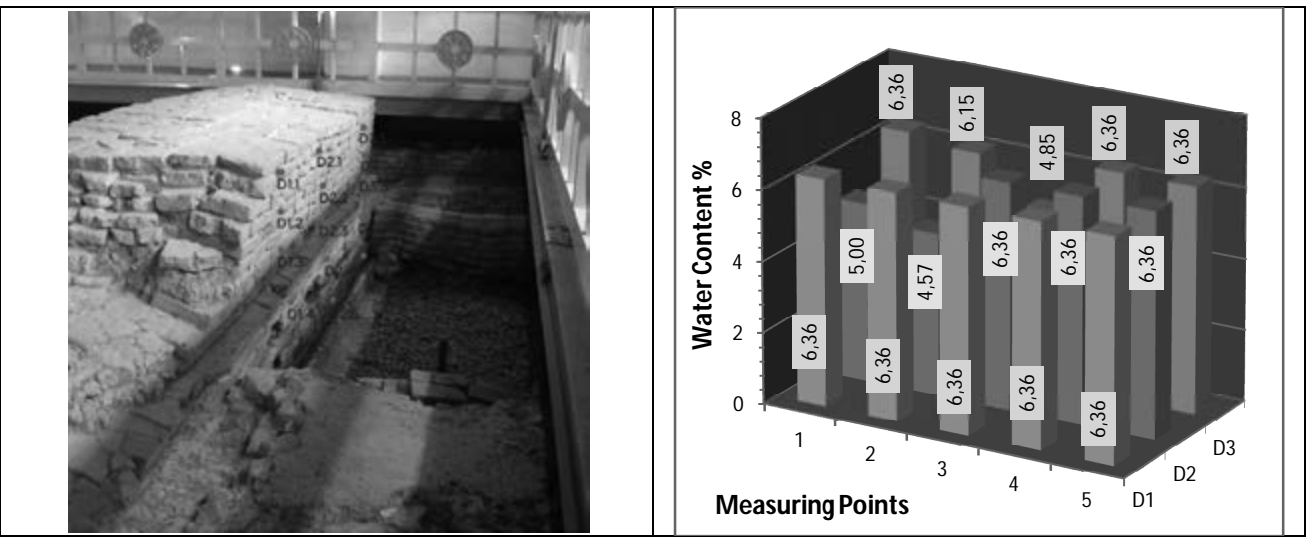


Figure 66. East Wall - Water content distribution in D locations.

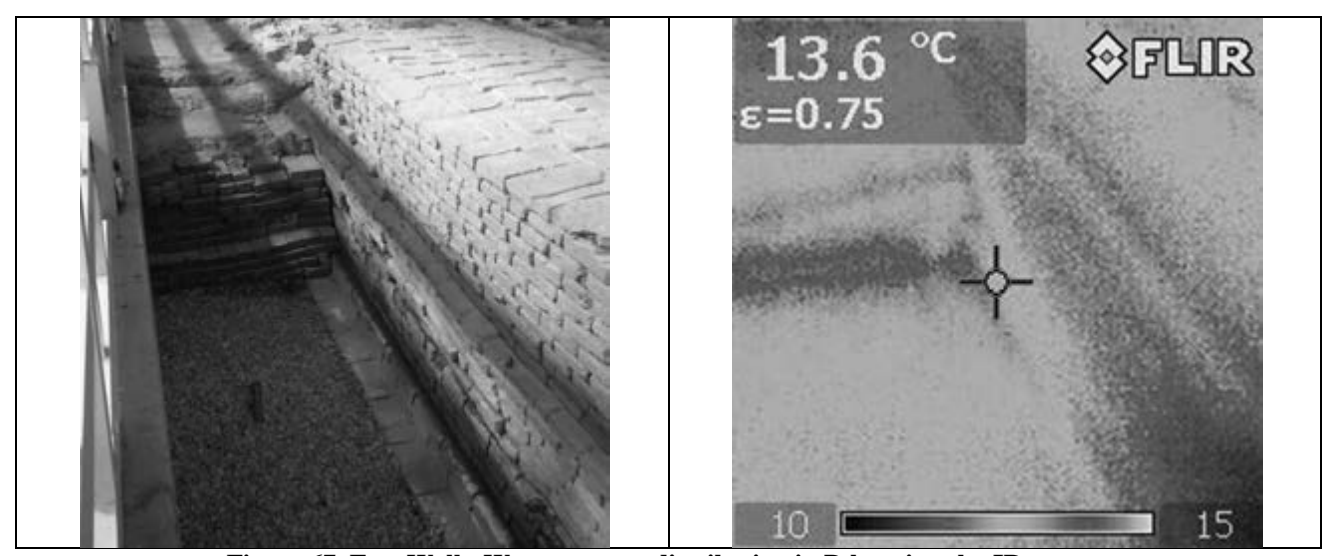


Figure 67. East Wall - Water content distribution in D locations by IR camera.

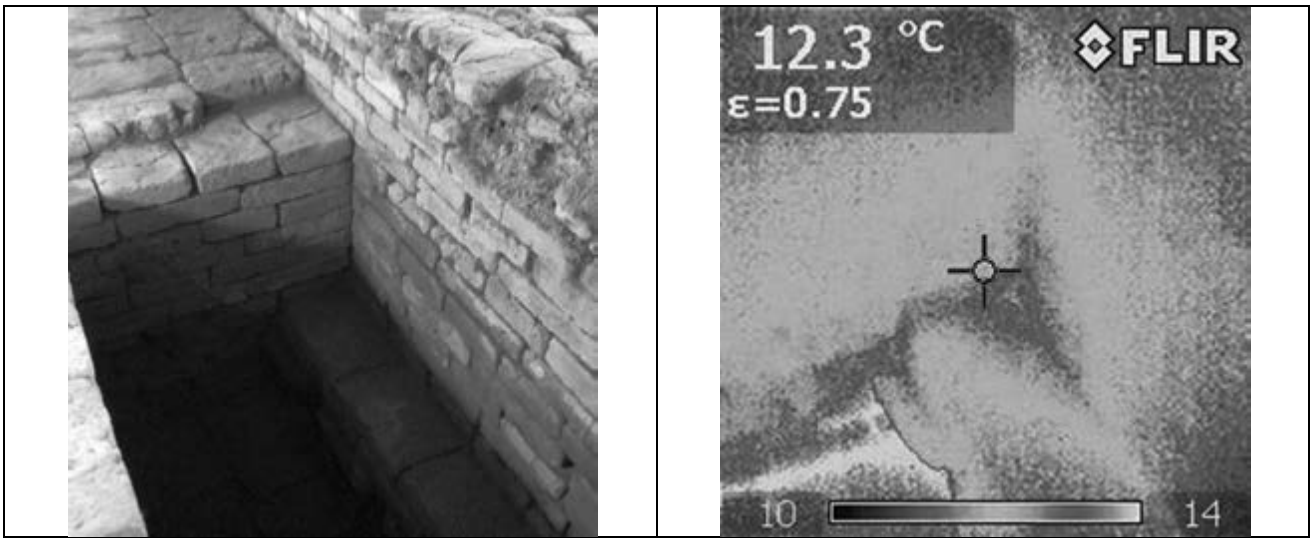


Figure 68. Trench C12 was investigated by IR camera.



Figure 69. North Wall: water content detecting locations..

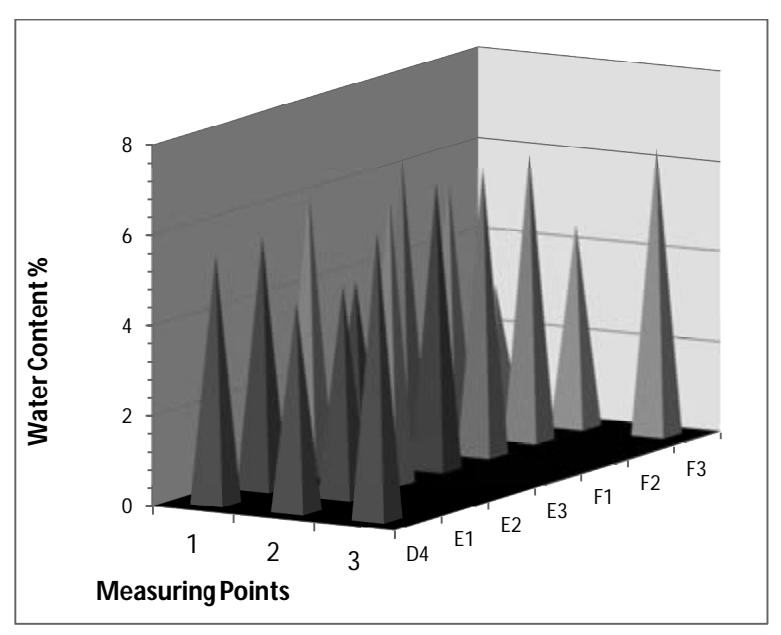


Figure 70. North Wall: distribution of the water content values.

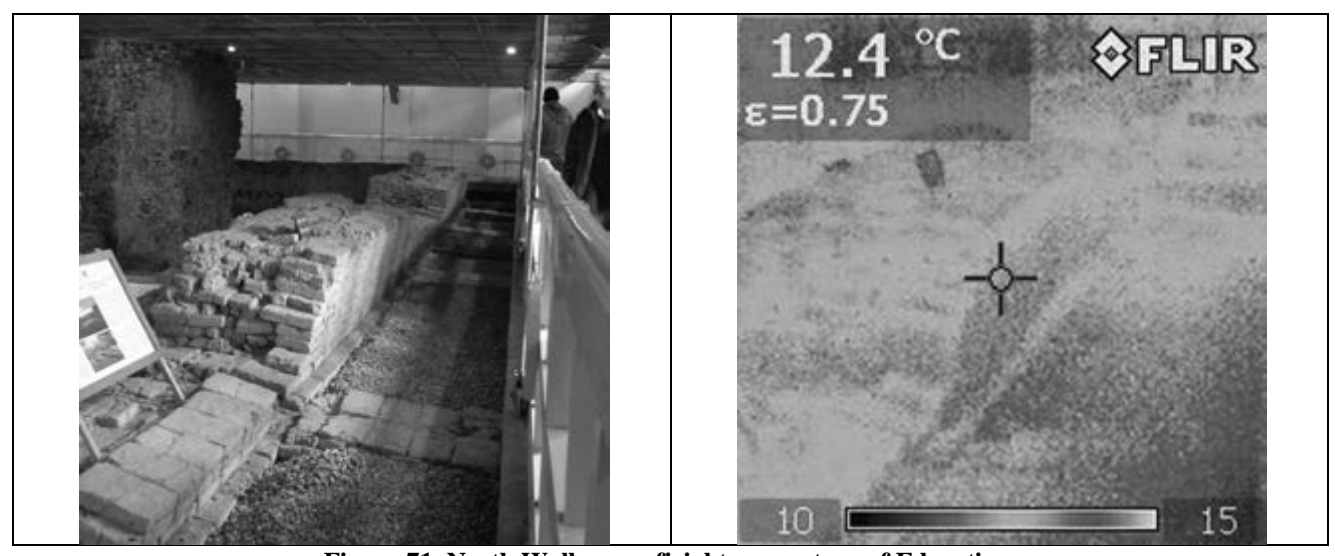


Figure 71. North Wall: superficial temperature of E location.



Figure 72. West Wall: Measuring point locations and water distribution of G4-G5-G6 locations.

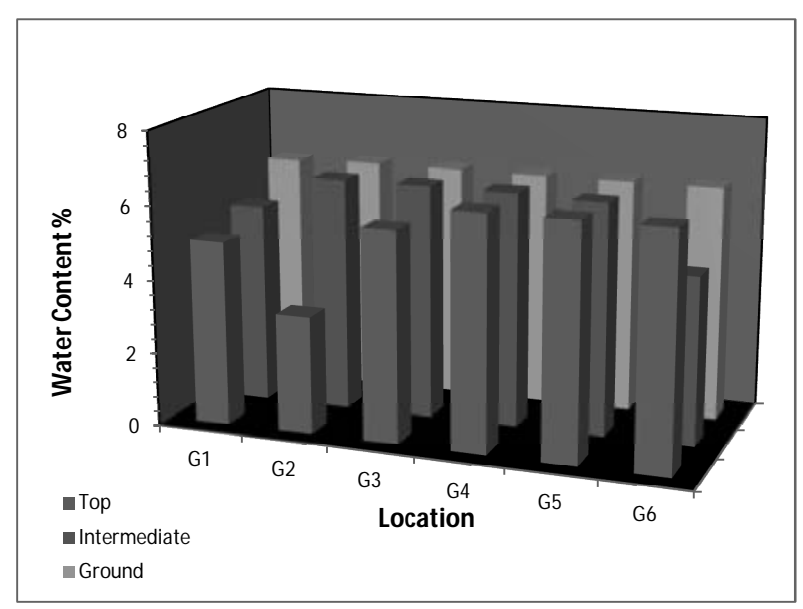


Figure 73. West Wall: Water content % in the six test locations

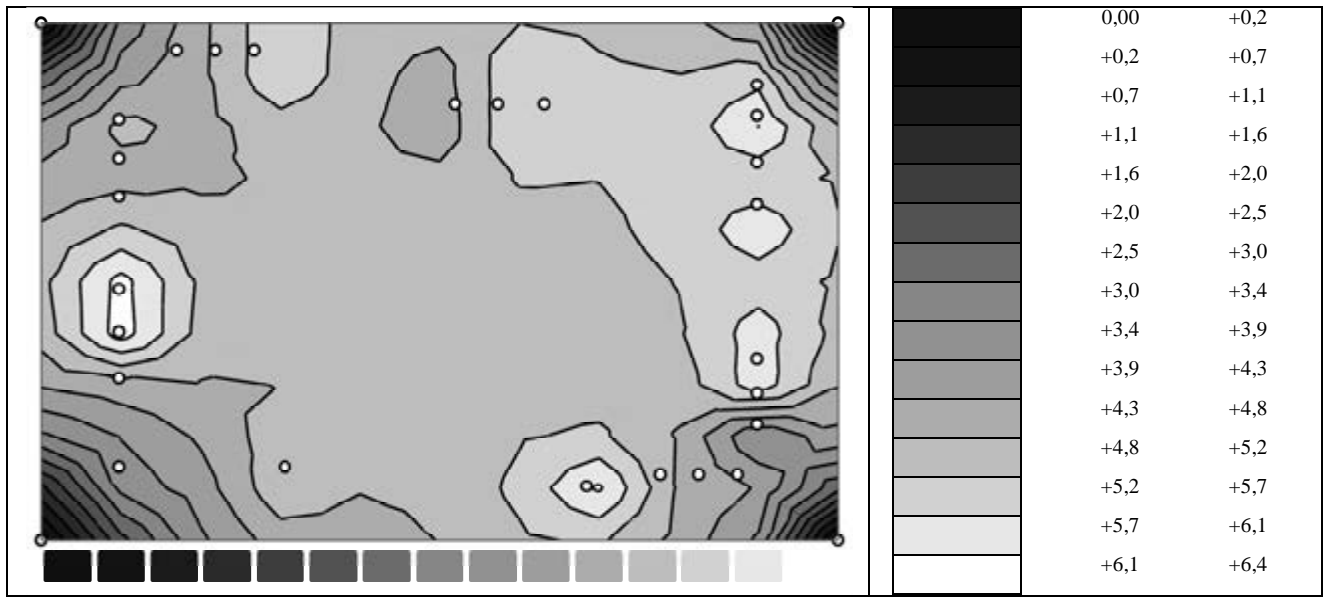


Figure 74. Water content distribution at top level of the perimetral walls

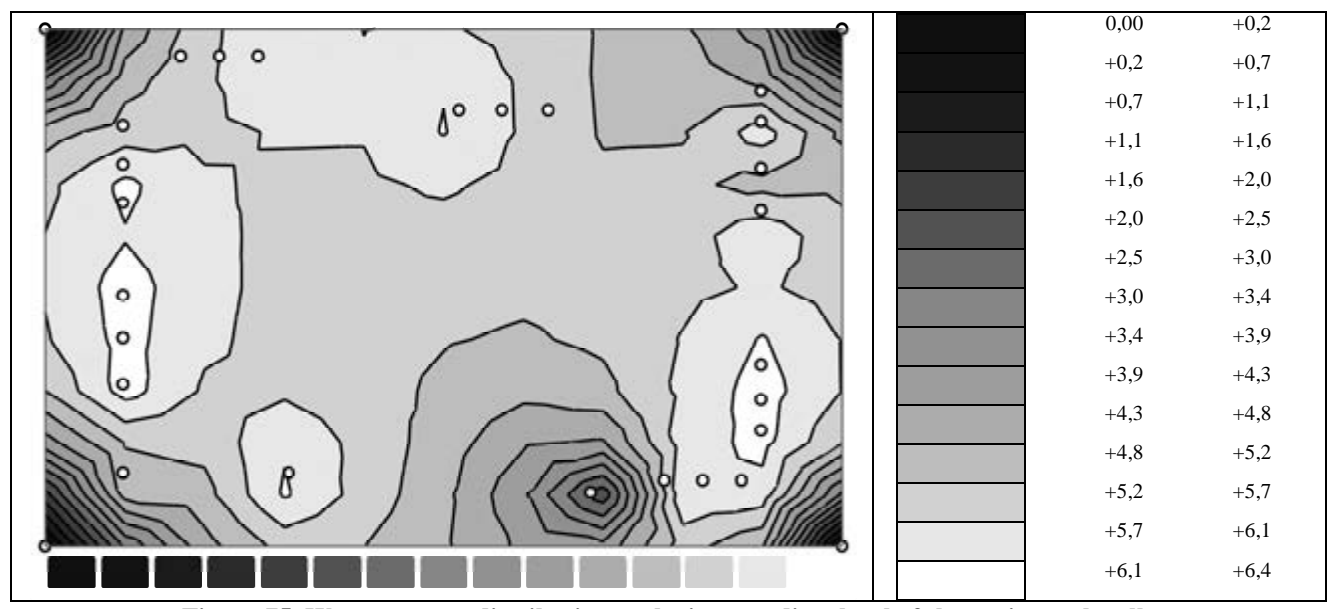


Figure 75. Water content distribution at the intermediate level of the perimetral walls

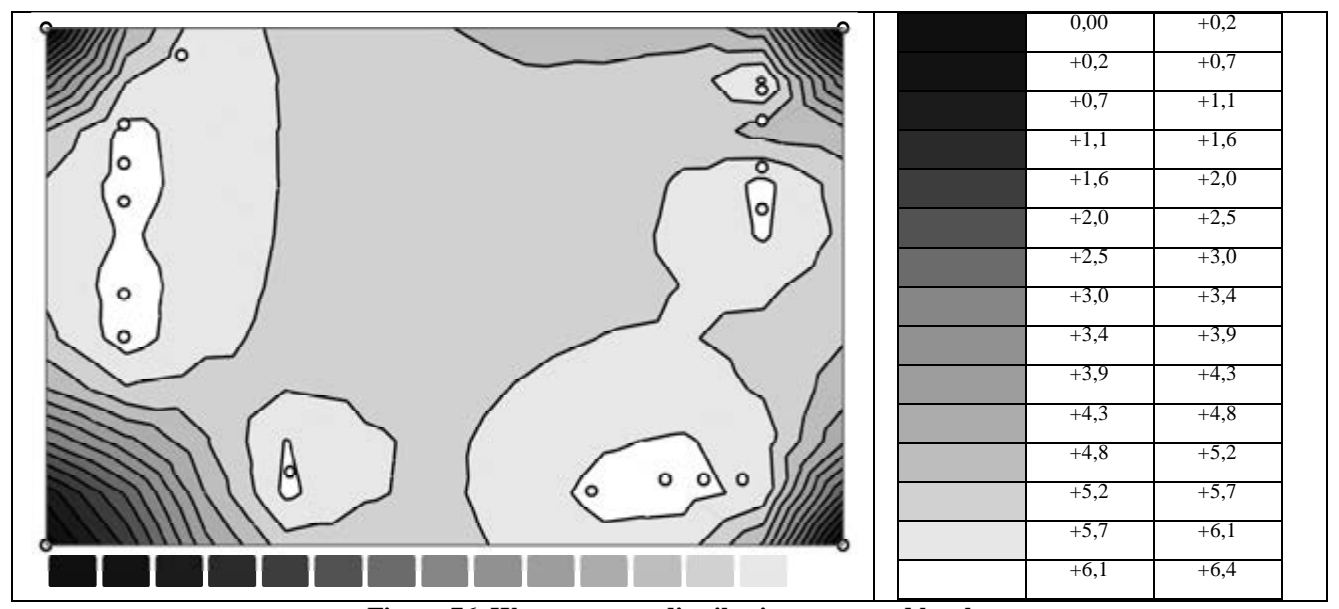
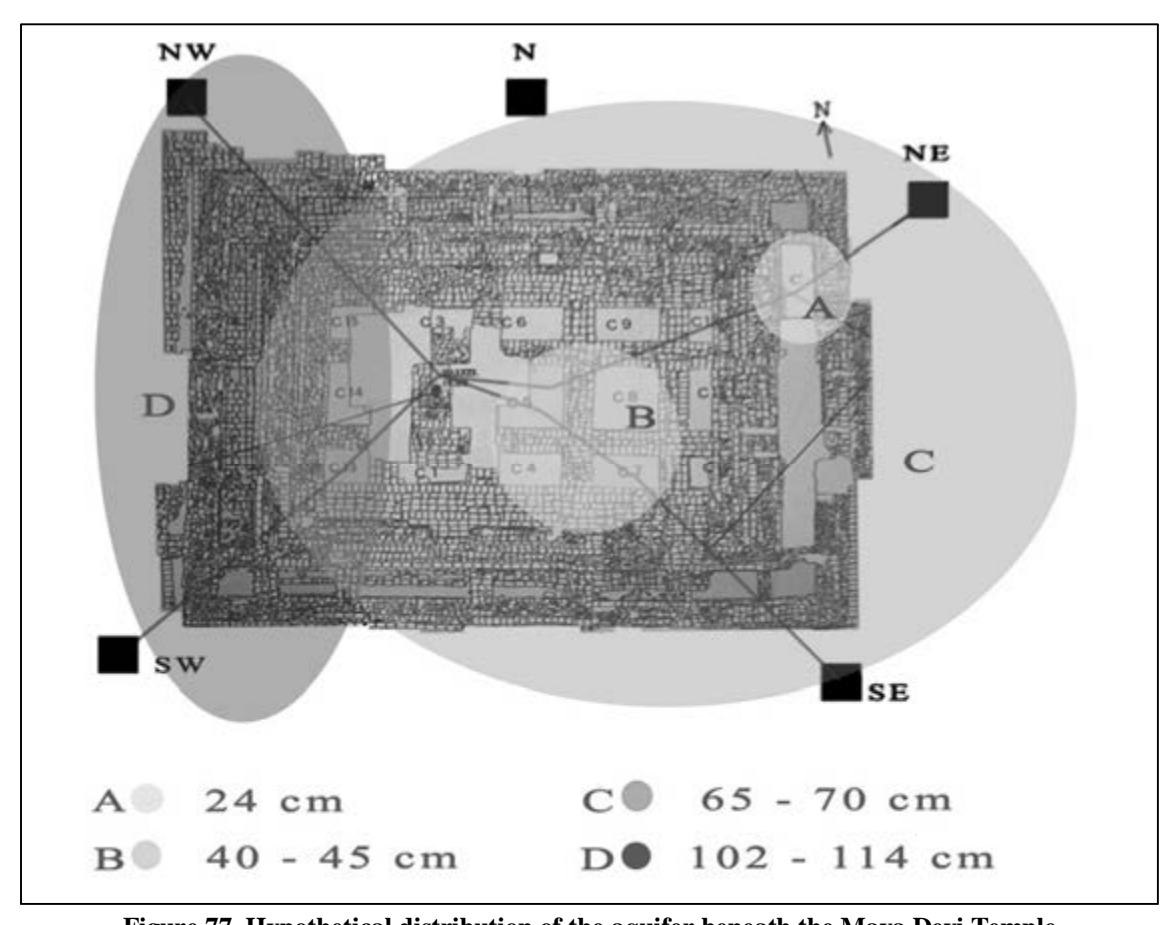


Figure 76. Water content distribution at ground level



Figure~77.~Hy pothetical~distribution~of~the~aquifer~beneath~the~Maya~Devi~Temple

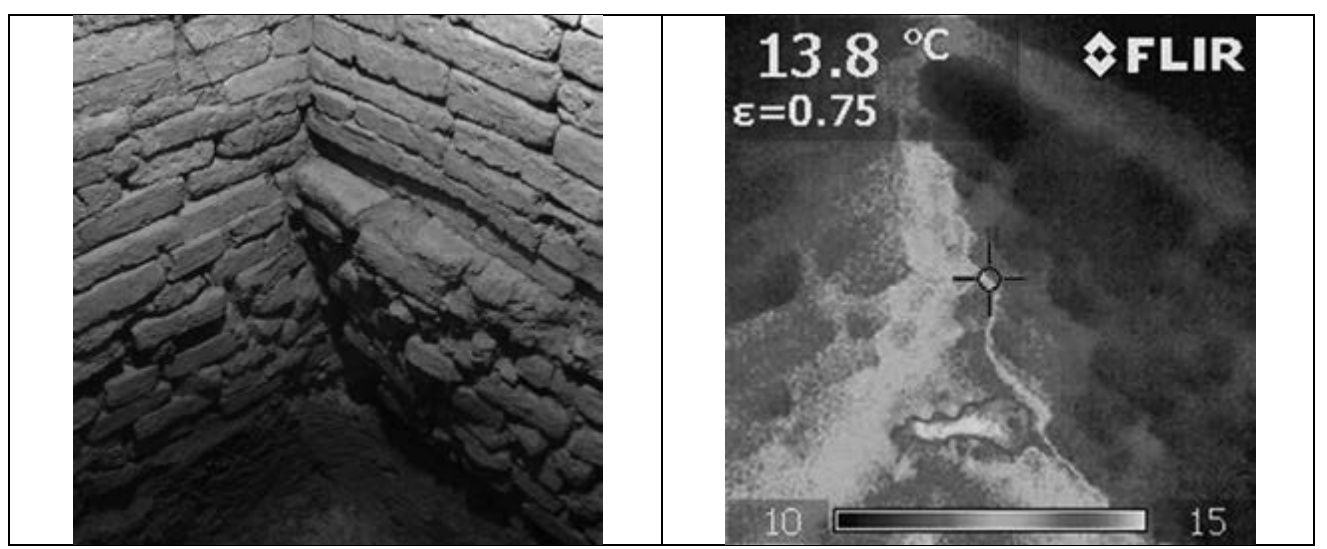


Figure 78. Trench C6: the soil at the bottom of the trench is warmer than the masonry

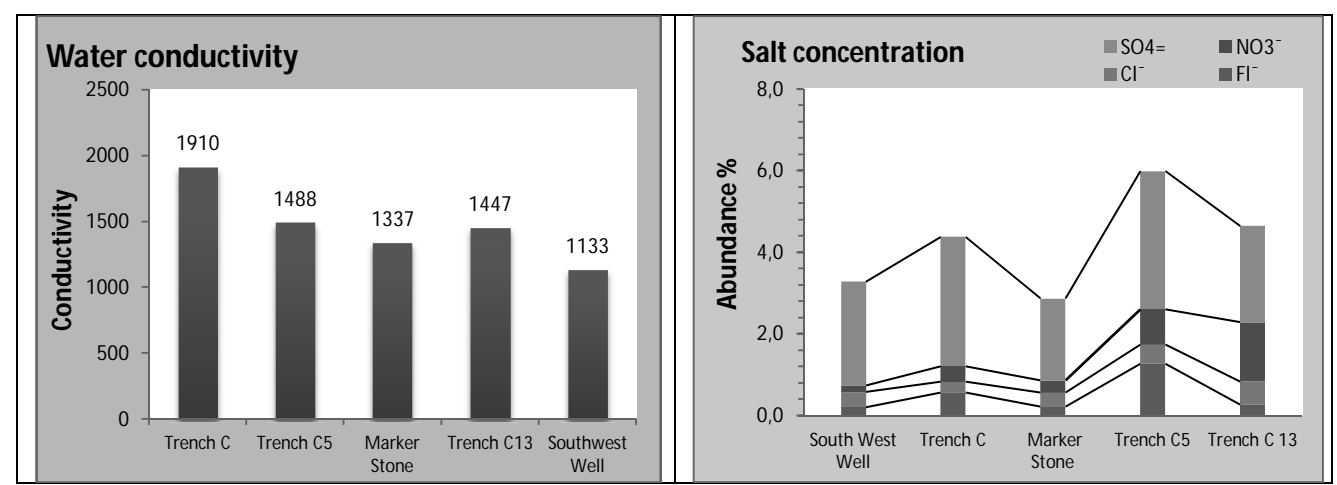


Figure 79. Quality of the water from the aquifer

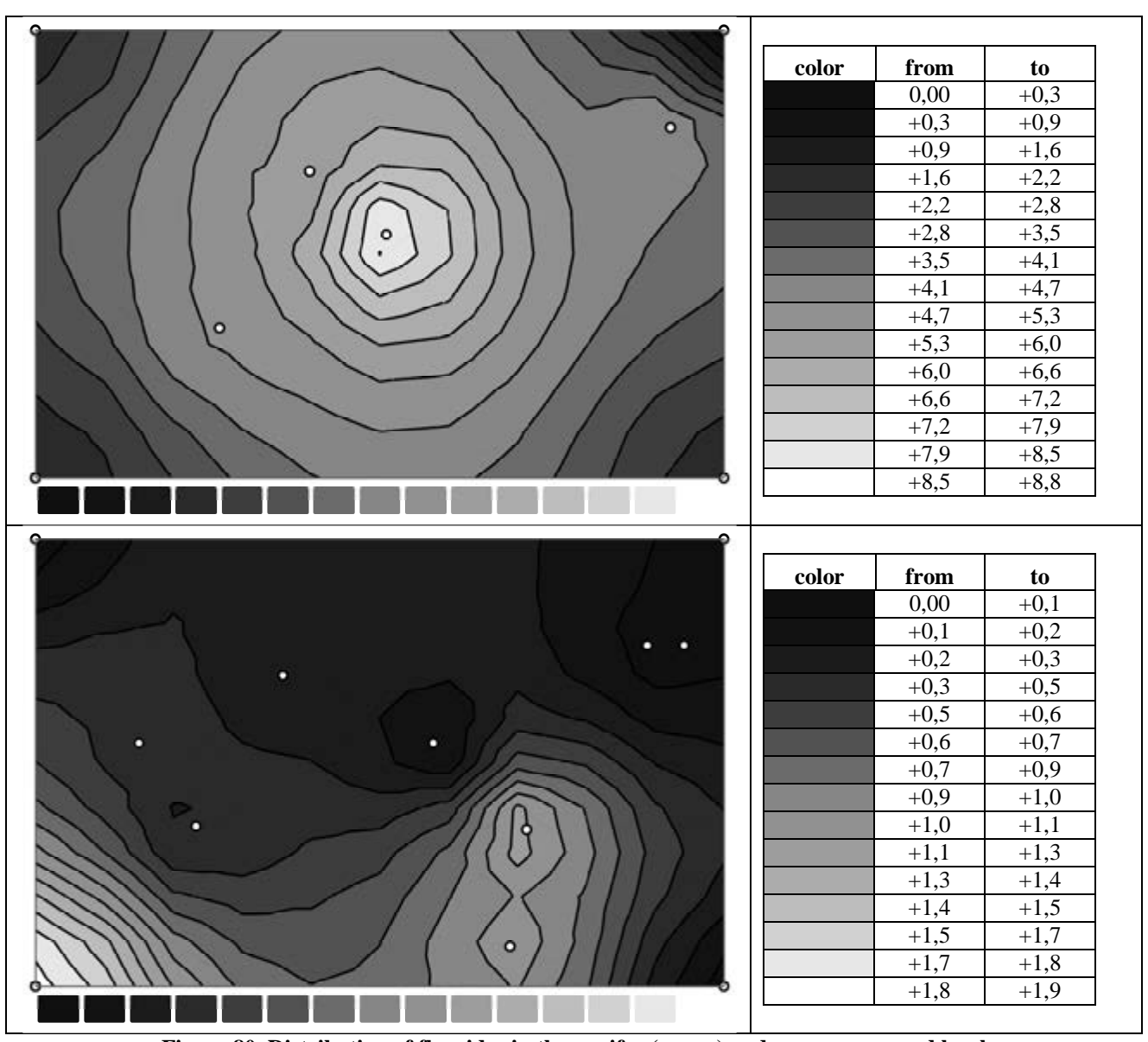


Figure 80. Distribution of fluorides in the aquifer (upper) and masonry ground level

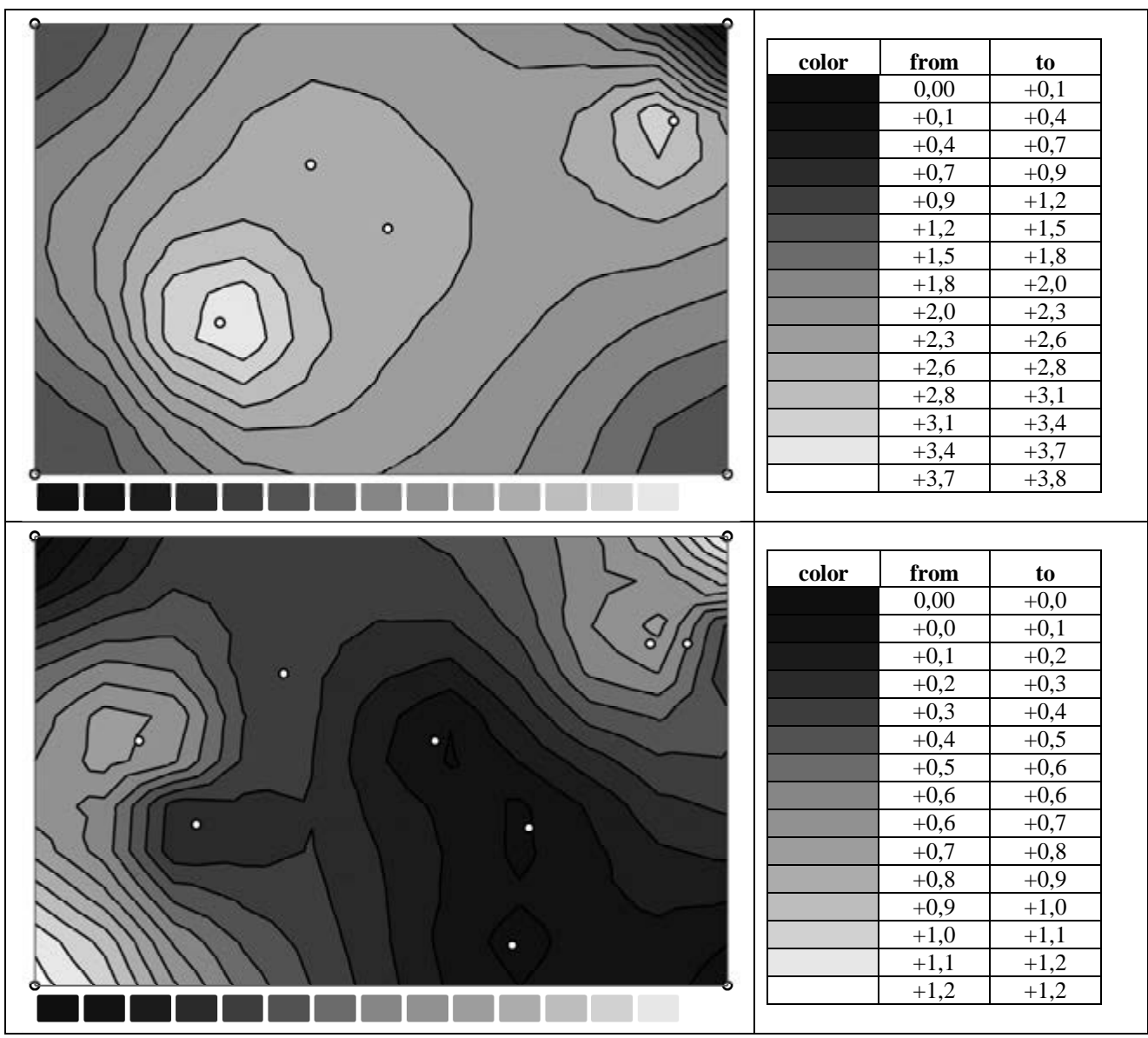


Figure 81. Distribution of chlorides in the aquifer (upper) and masonry ground level

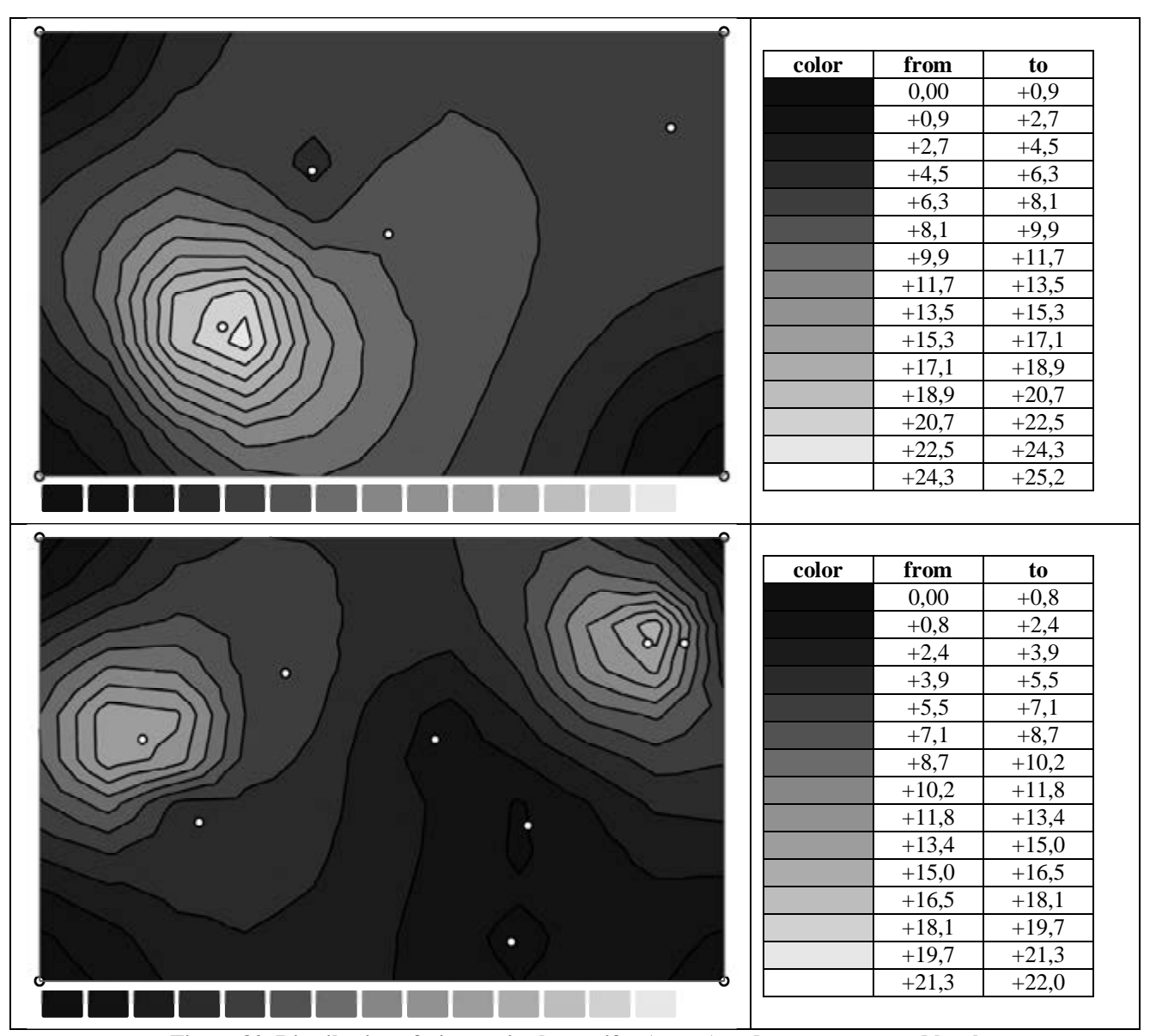


Figure 82. Distribution of nitrates in the aquifer (upper) and masonry ground level

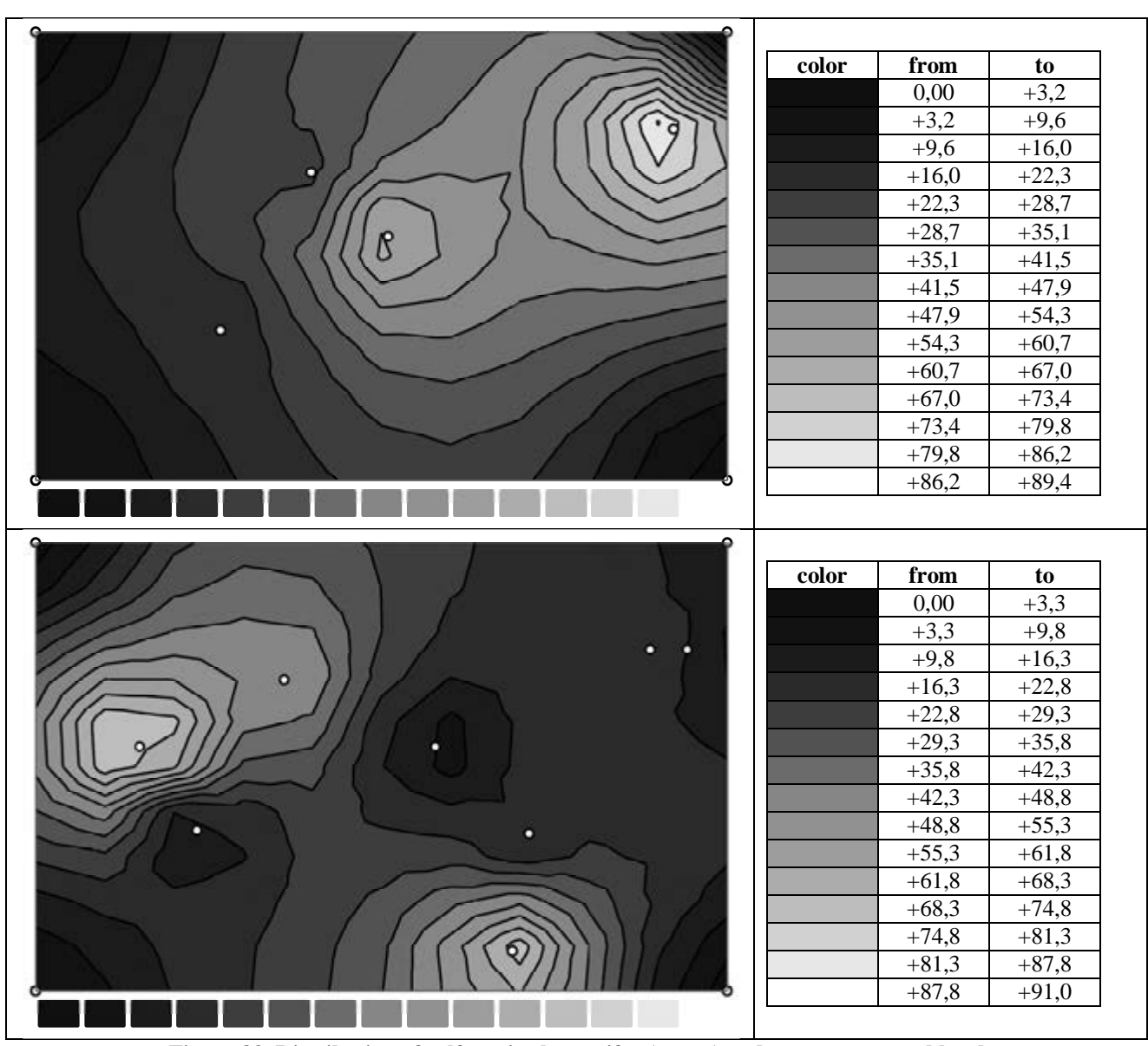


Figure 83. Distribution of sulfates in the aquifer (upper) and masonry ground level

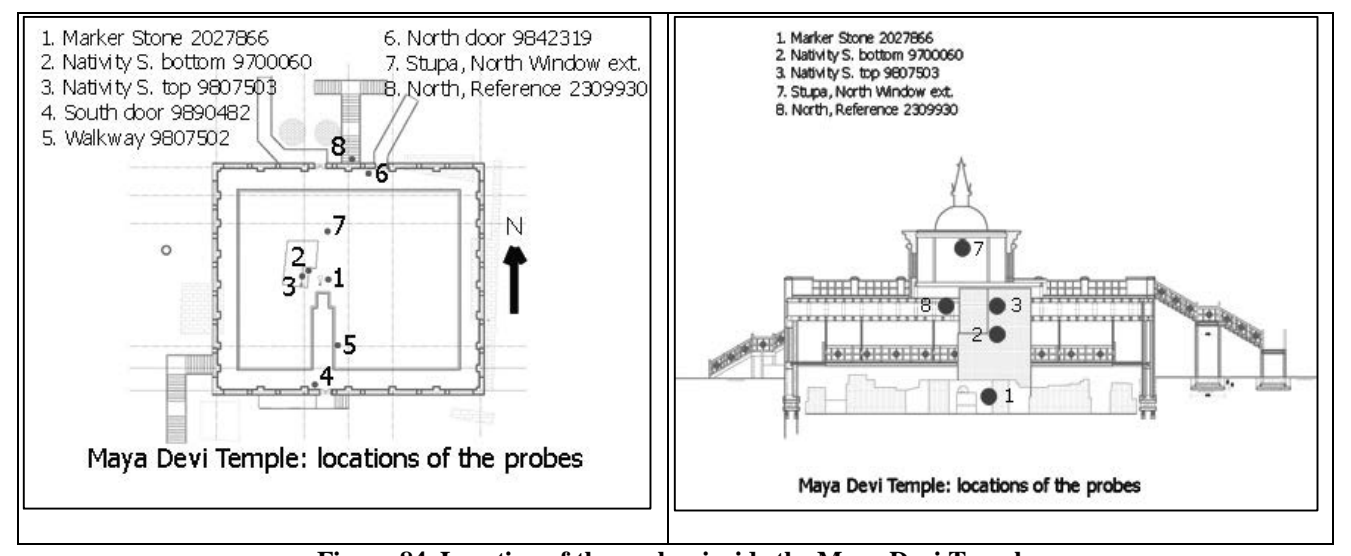


Figure 84. Location of the probes inside the Maya Devi Temple

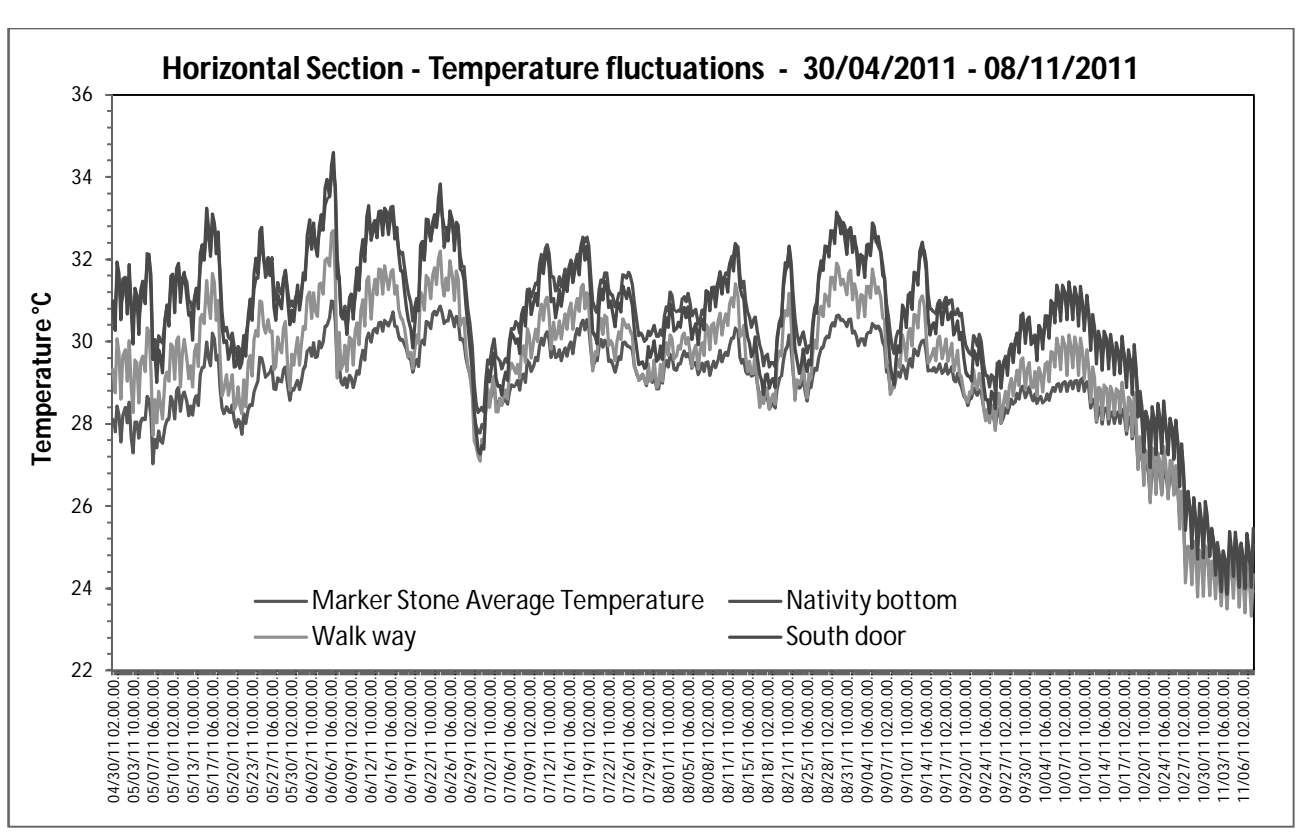


Figure 85. Trend of temperature values in the horizontal section

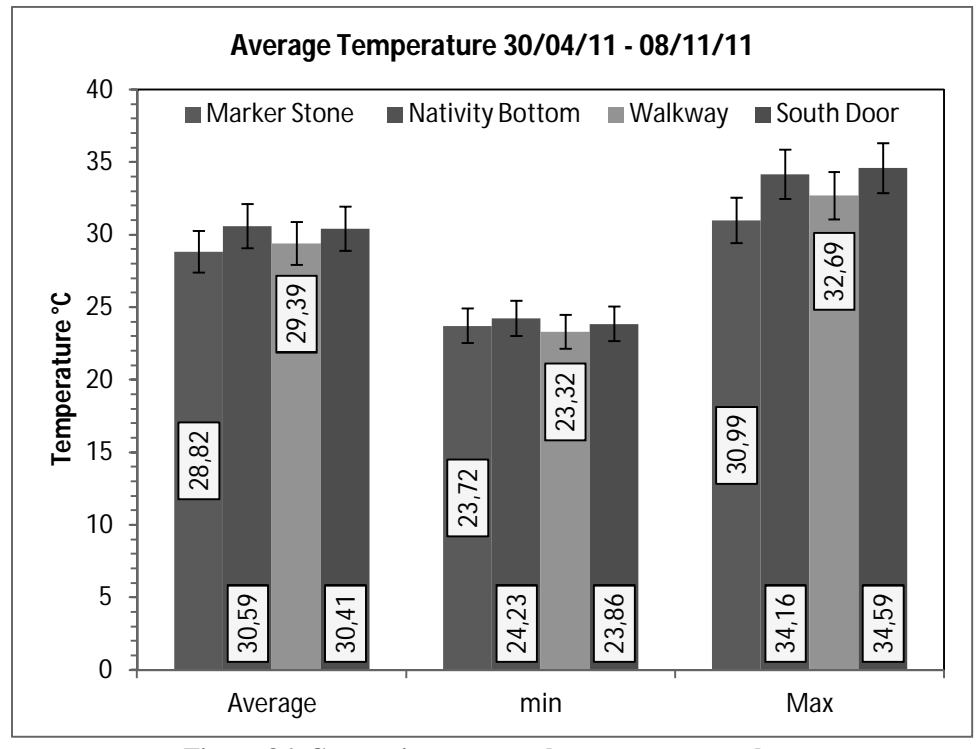


Figure 86. Comparison among the temperature values

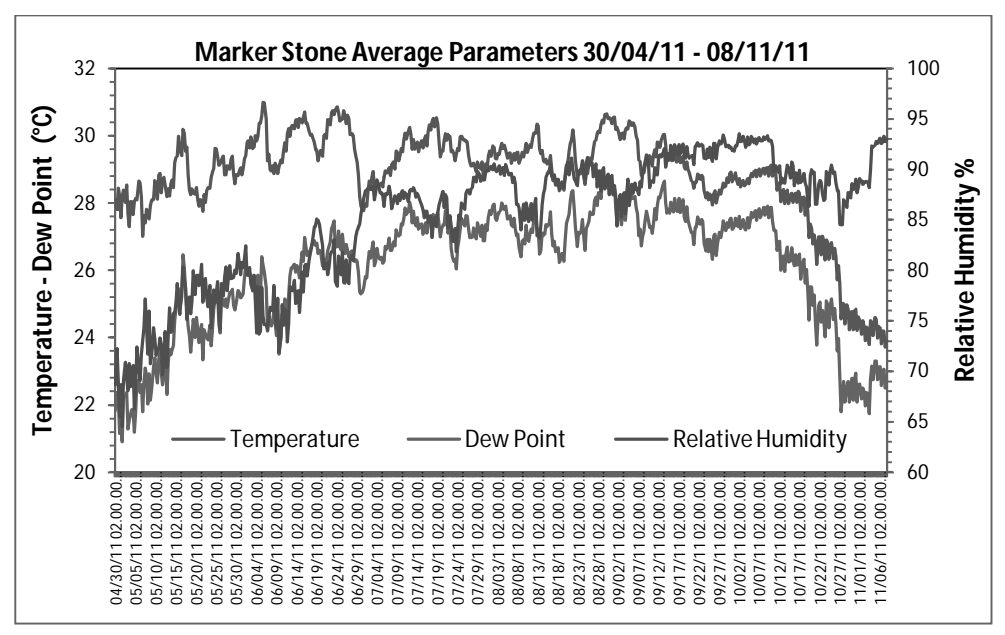


Figure 87. Microclimate changes in the Marker Stone location

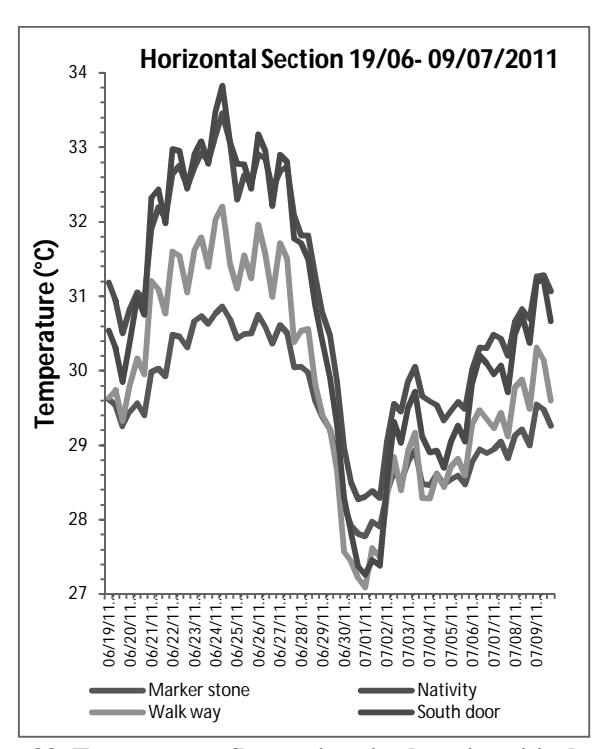


Figure 88. Temperature fluctuations in the rain critical period

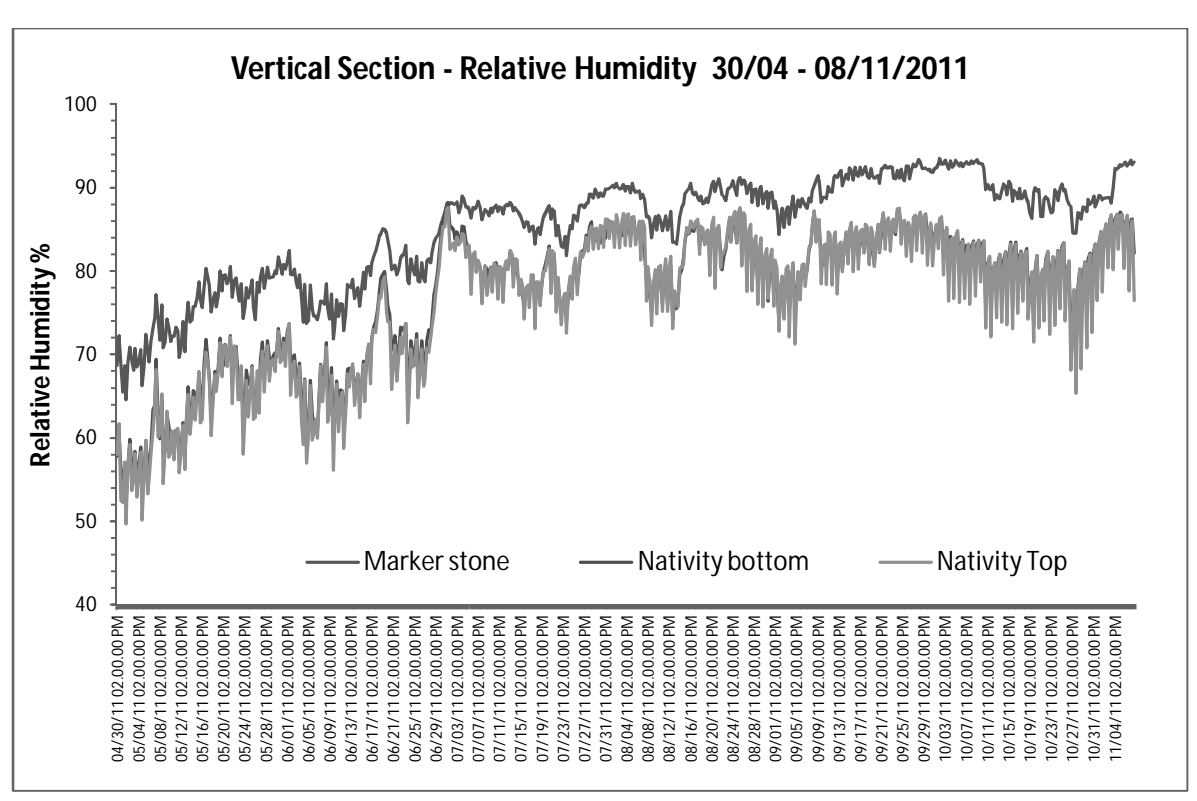


Figure 89. Relative humidity trend in the vertical section locations

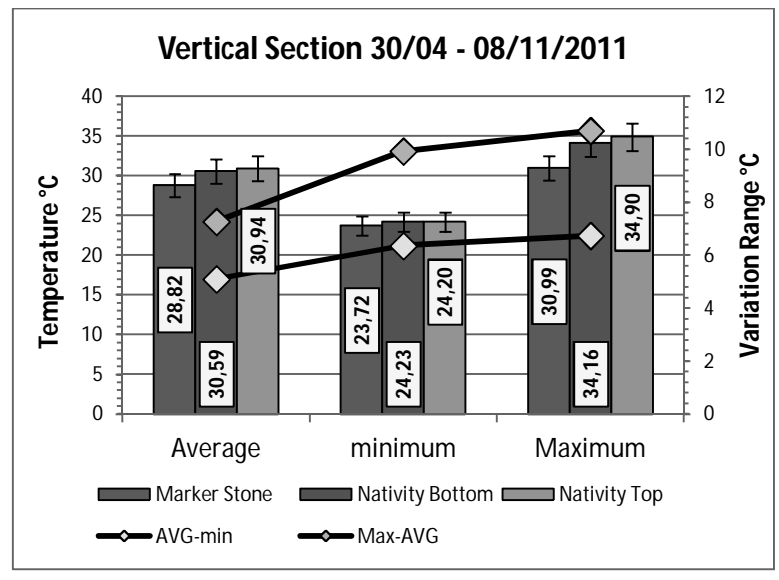


Figure 90. Temperature variations in the vertical section

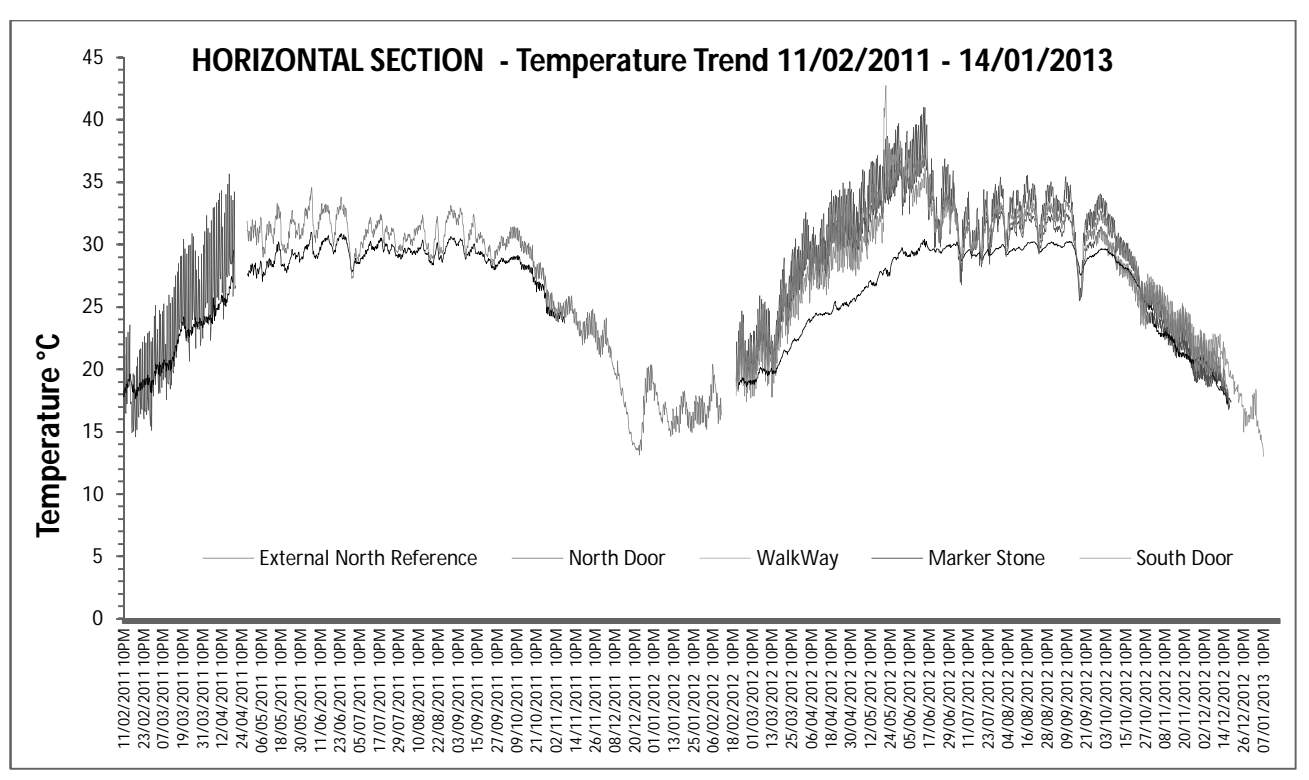


Figure 91. Full period temperature fluctuation trend

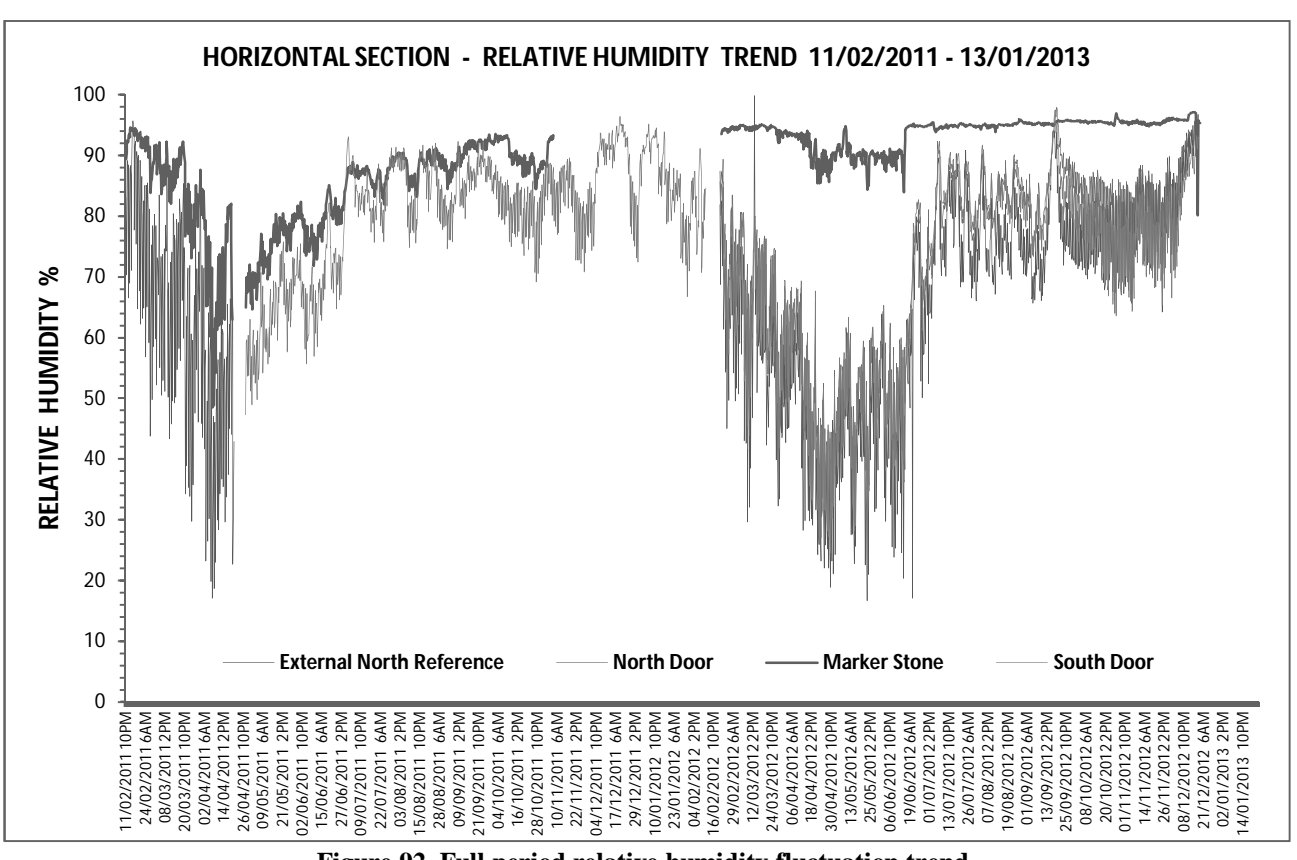


Figure 92. Full period relative humidity fluctuation trend

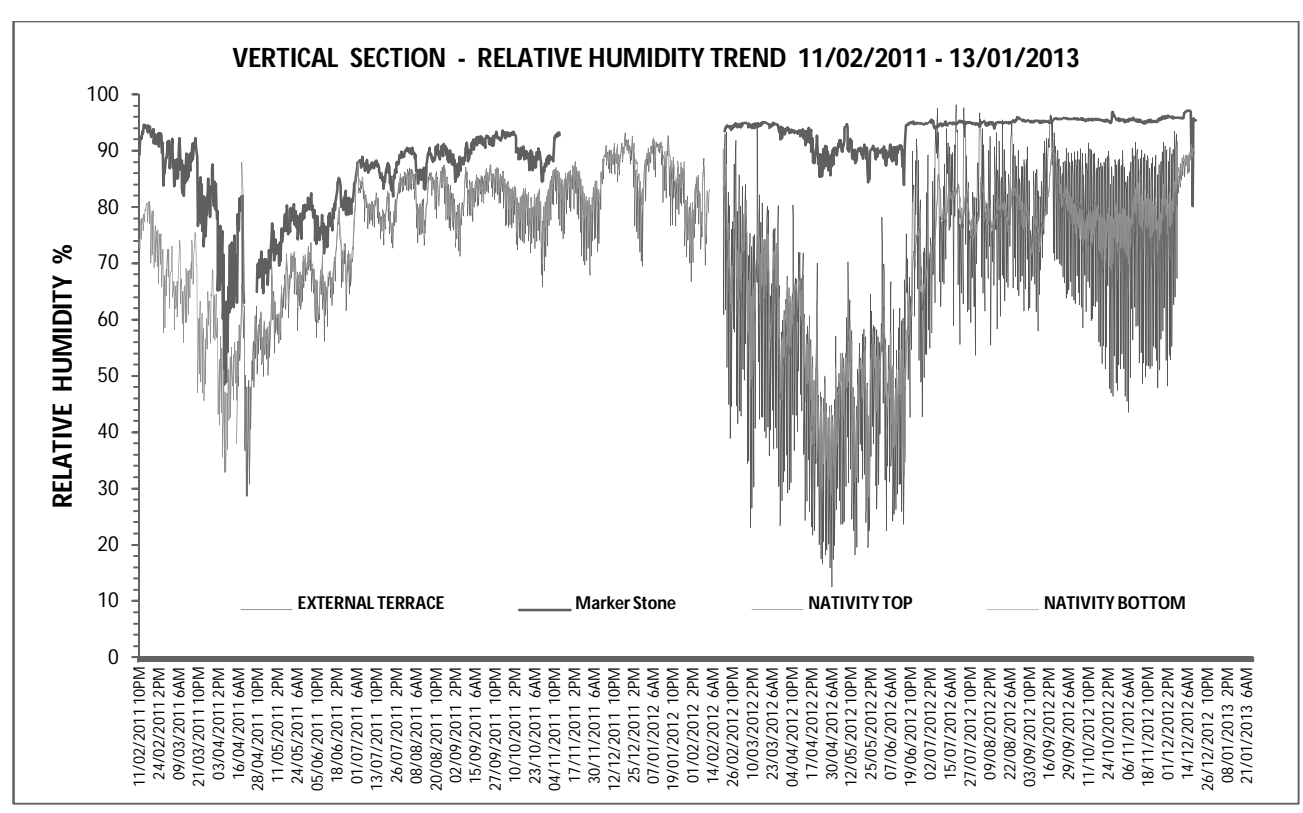


Figure 93. Vertical section: trend of the relative humidity in the whole monitoring period

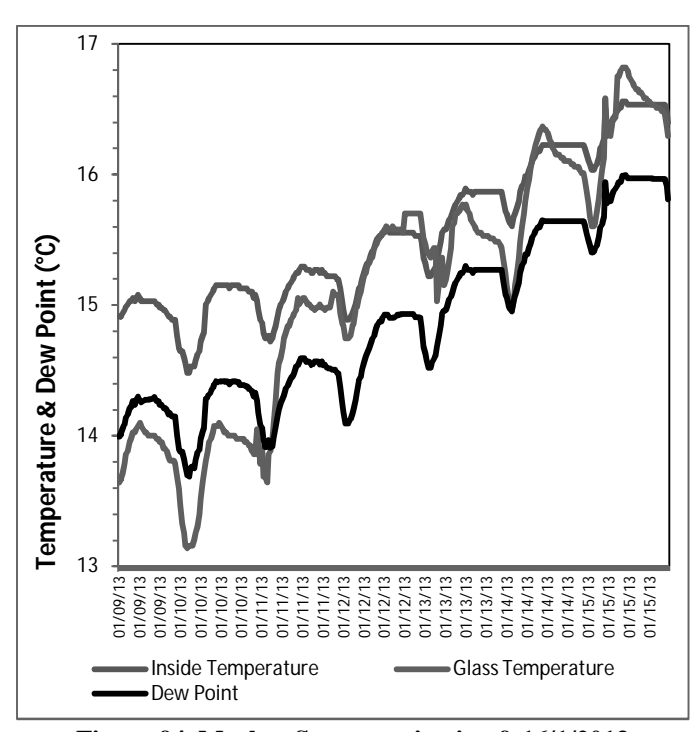


Figure 94. Marker Stone monitoring 9-16/1/2013

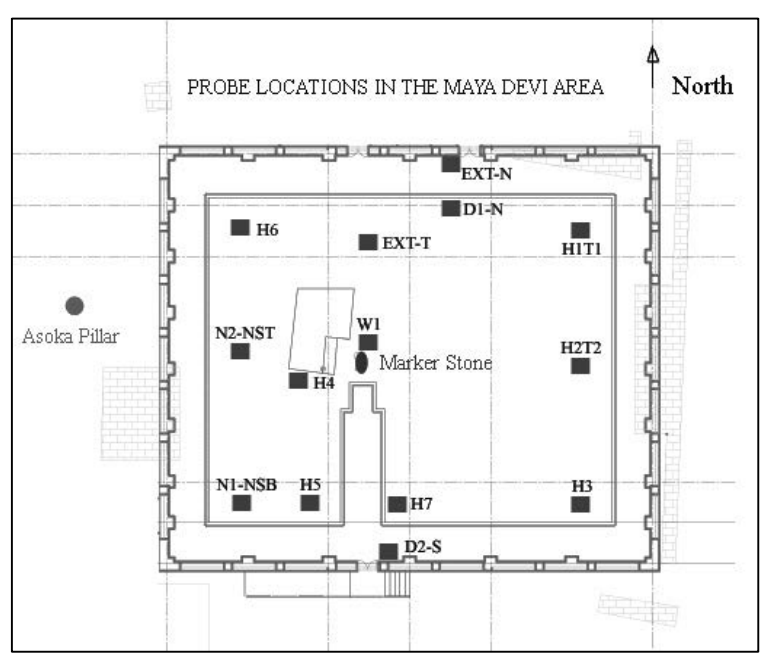
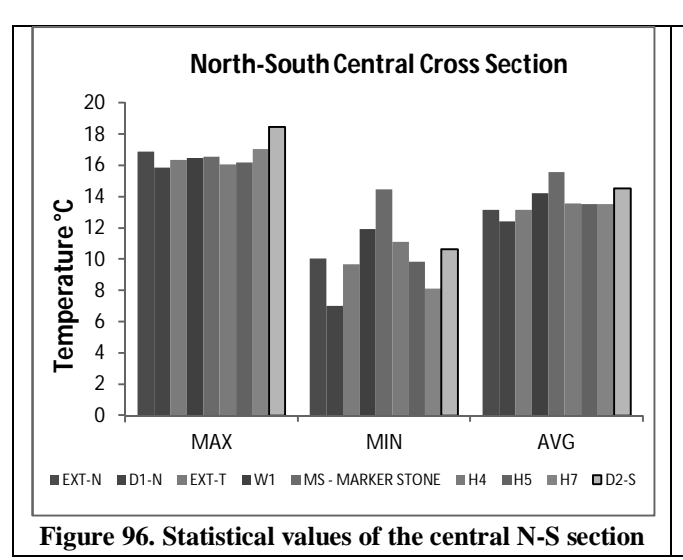
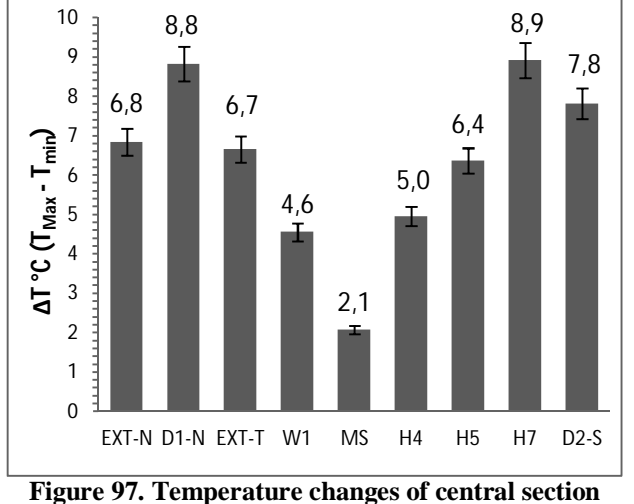


Figure 95. Location of the probes in the whole plan monitoring





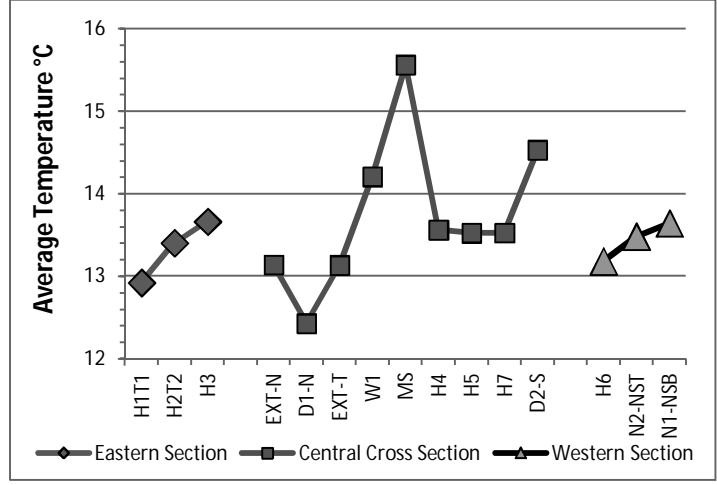


Figure 98. Average temperature changes in the three cross sections within the Maya Devi Temple

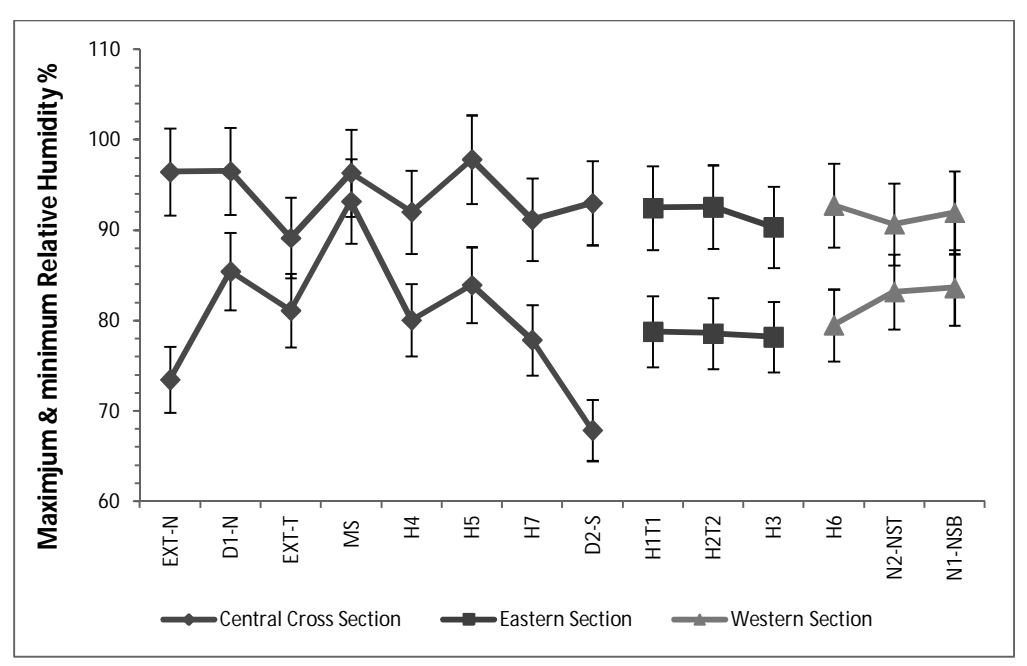


Figure 99. Relative Humidity fluctuations in the horizontal plan within Maya Devi Temple

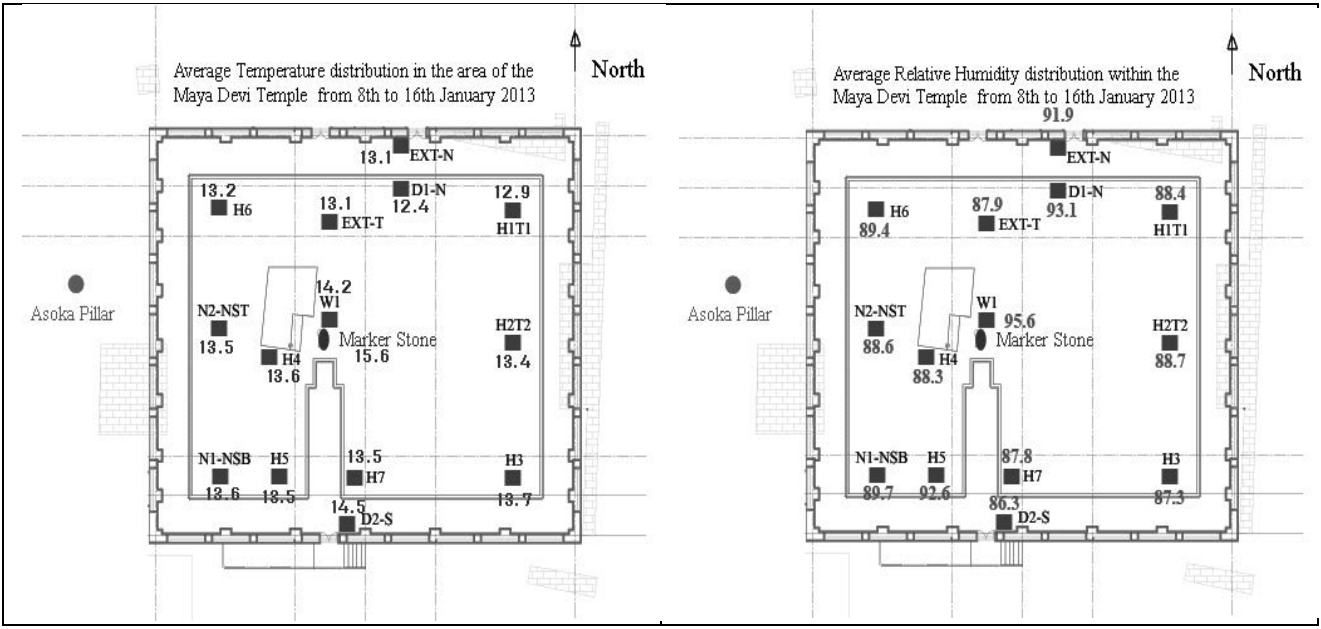


Figure 100. Distribution of average values of Temperature and Relative Humidity within the Maya Devi Temple

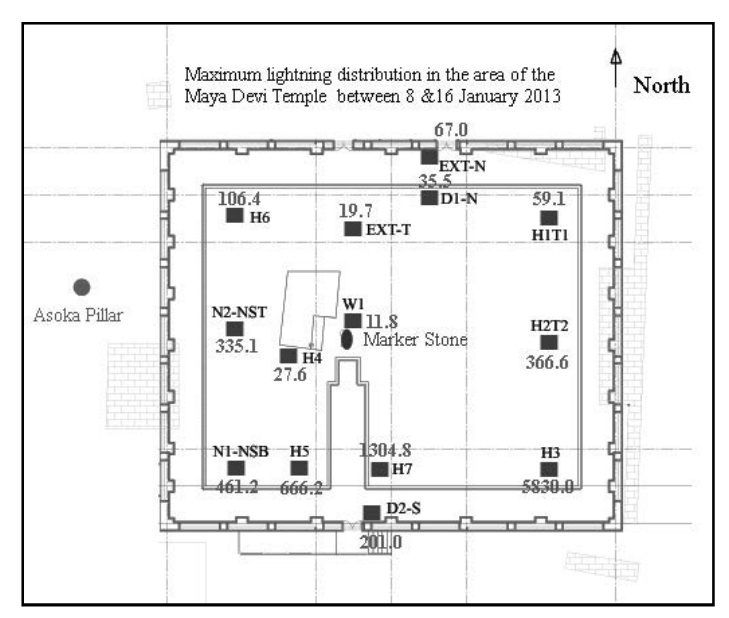


Figure 101. Maximum lightning in the monitoring time

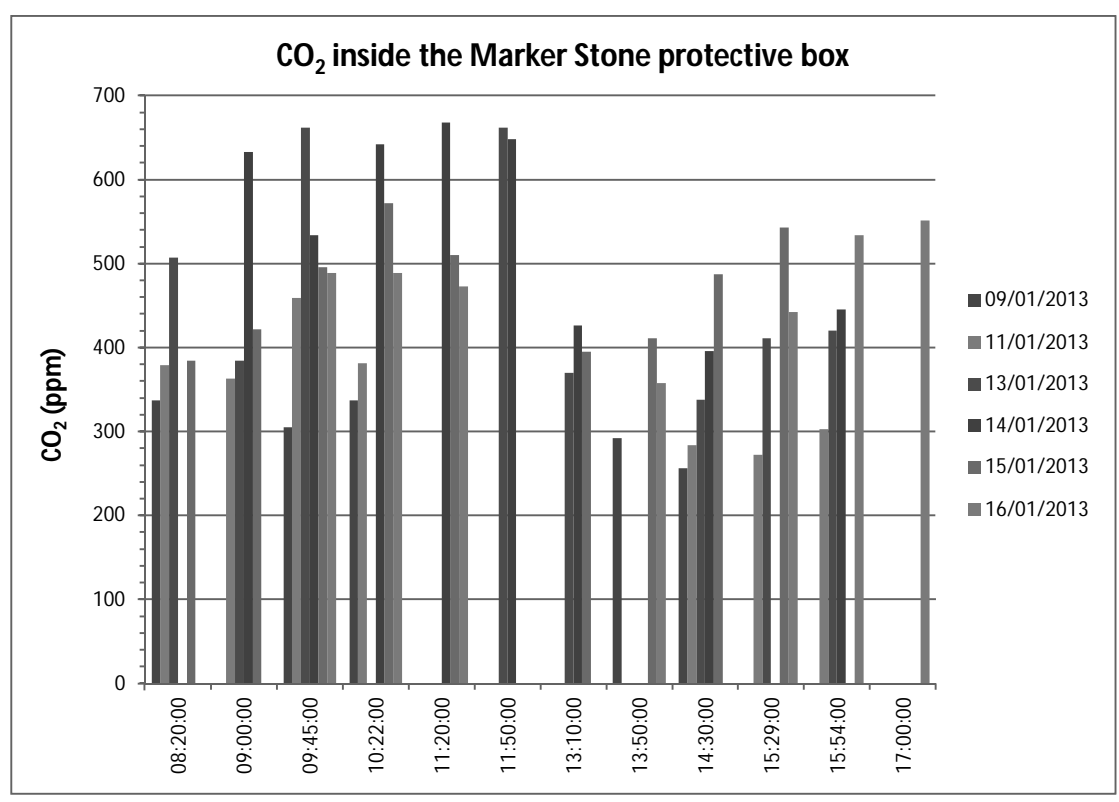


Figure 102. Representation of the CO2 concentration daily fluctuations

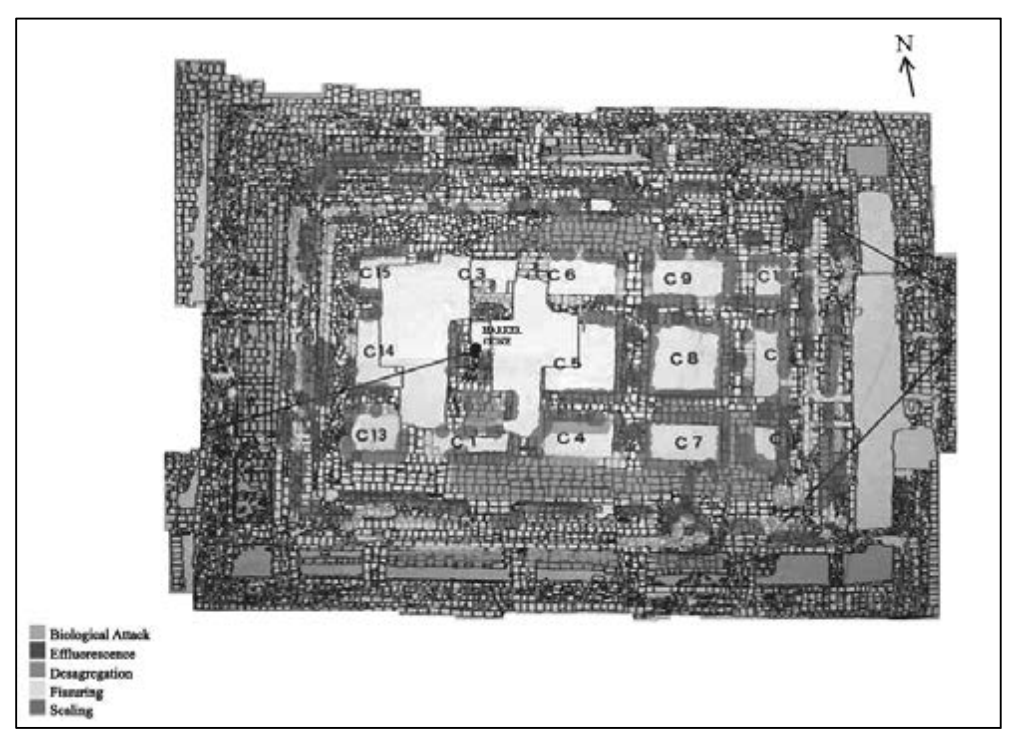


Figure 103. Distribution of the degradation patterns

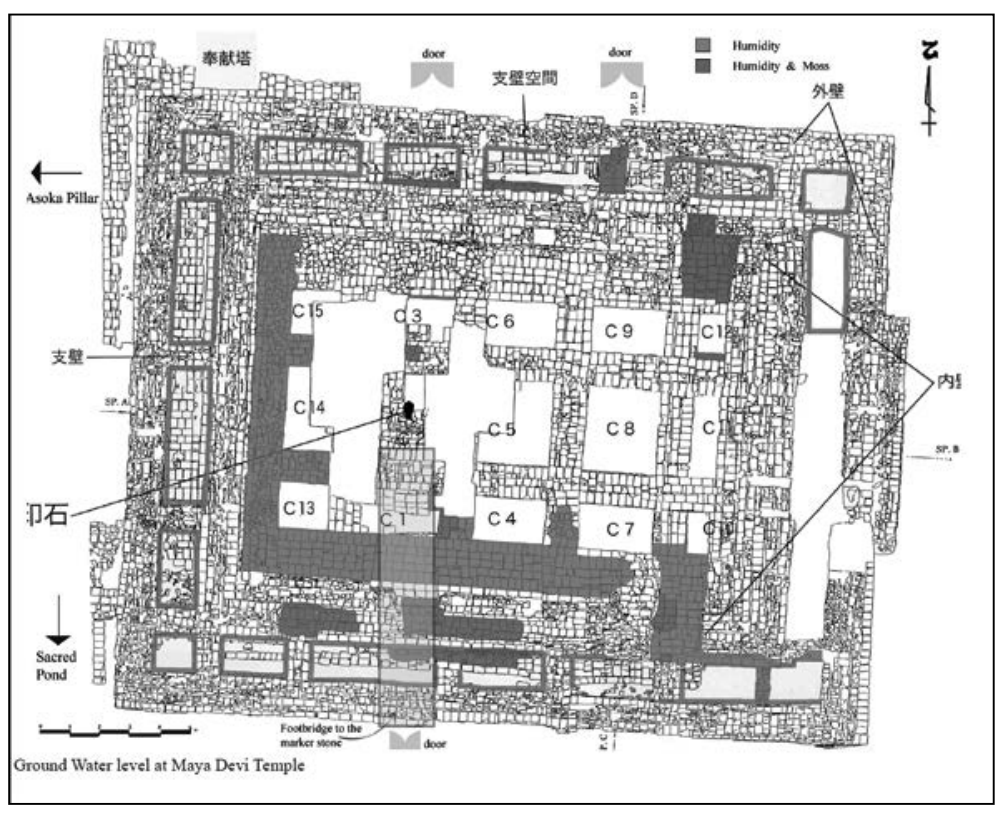


Figure 104. Water and mosses distribution (from Atzori 2006)



Figure 105. Strain gauge location on Asokan Pillar on February 15th, 2012

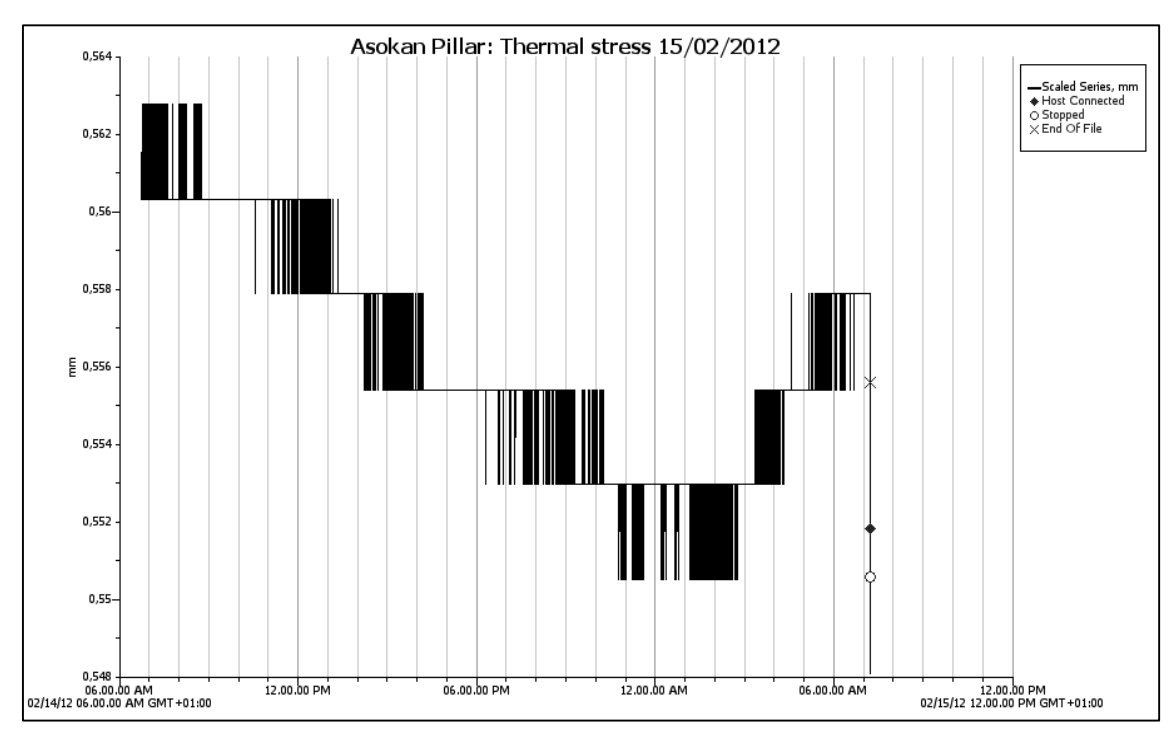


Figure 106. Thermal stress in Asokan Pillar on February 15th, 2012

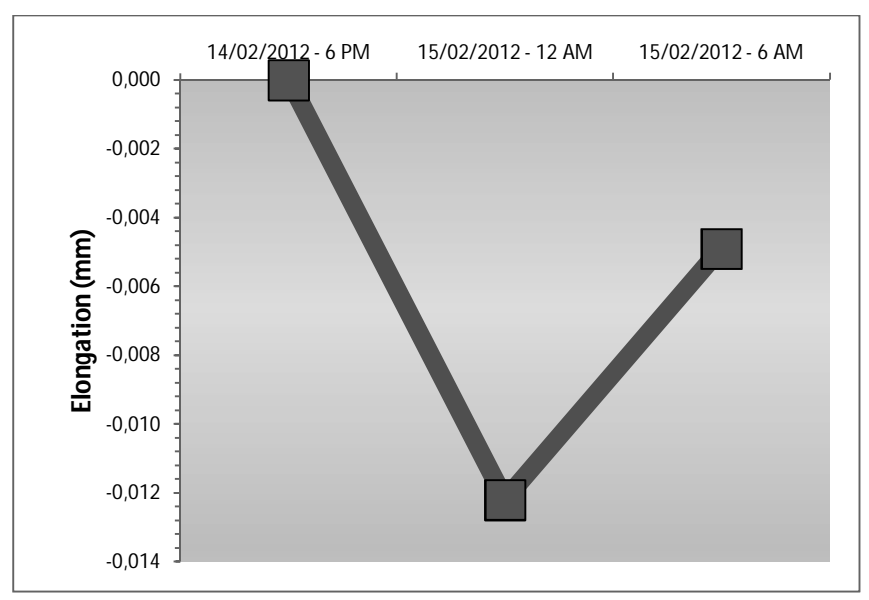


Figure 107. Elongation of the crack recorded on February 15th, 2012

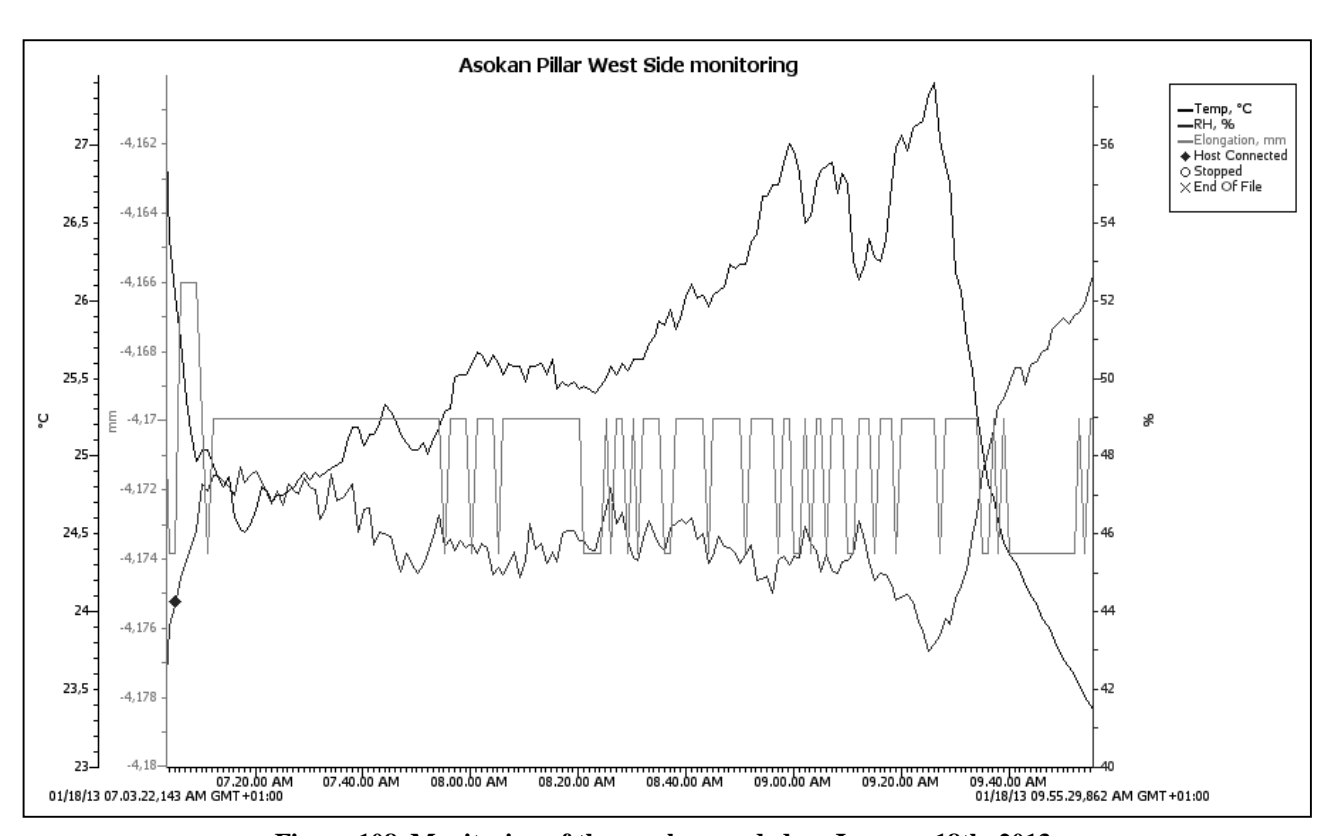


Figure 108. Monitoring of the crack recorded on January 18th, 2013

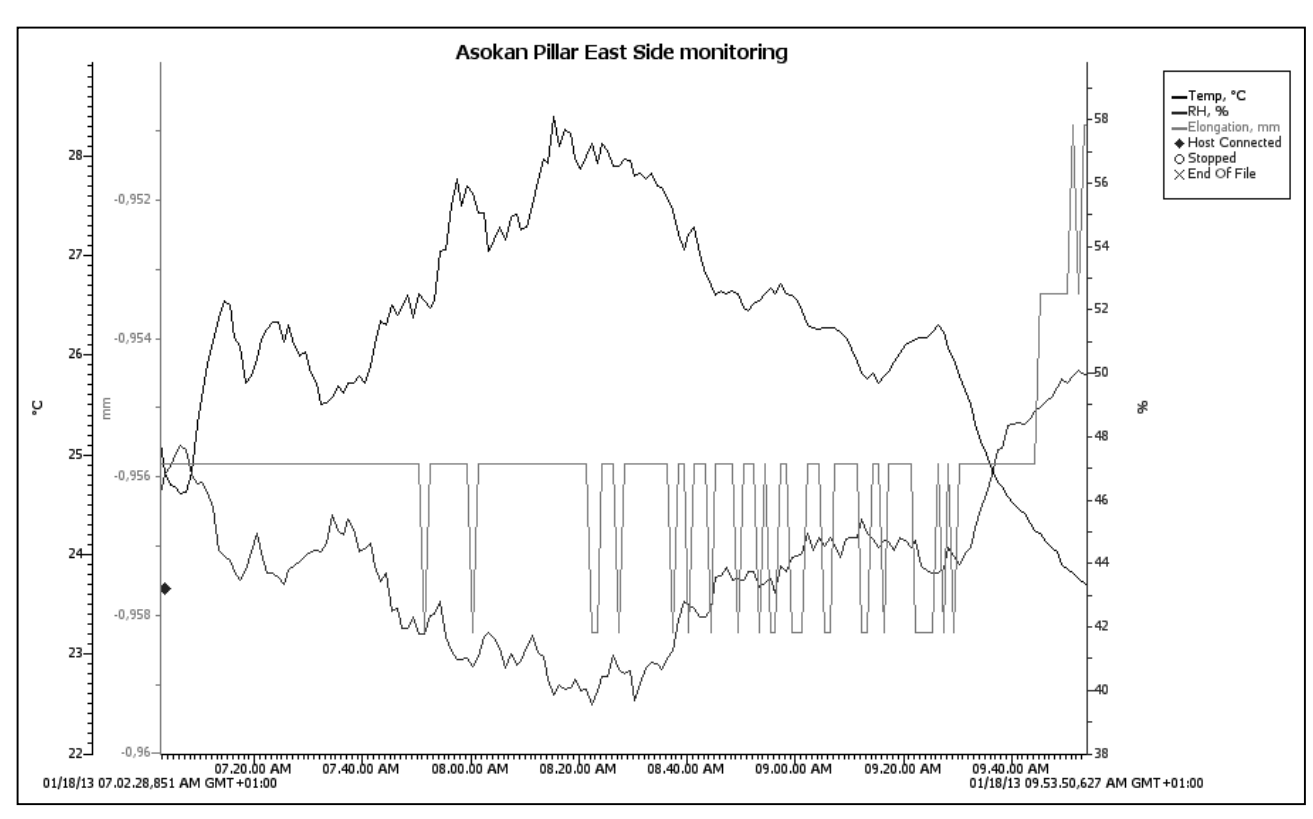


Figure 109. Monitoring of the crack recorded on January 18th, 2013

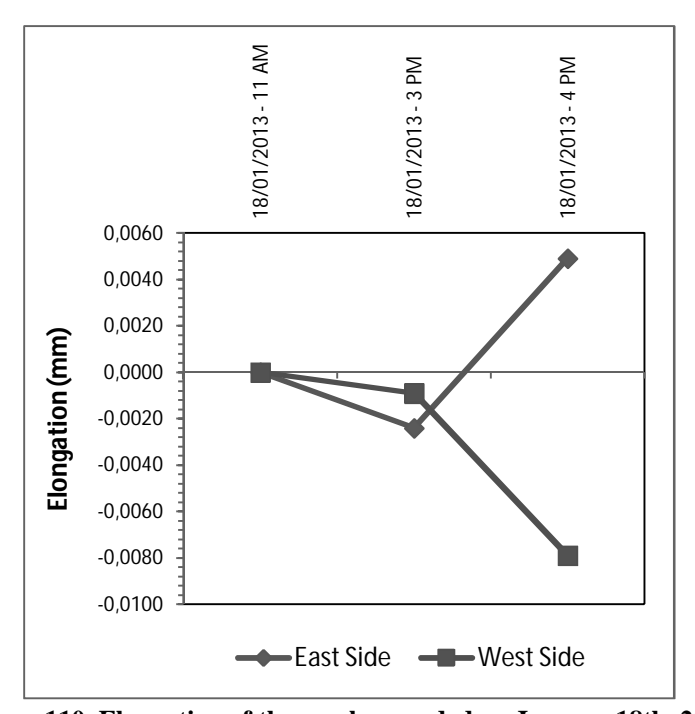


Figure 110. Elongation of the crack recorded on January 18th, 2013

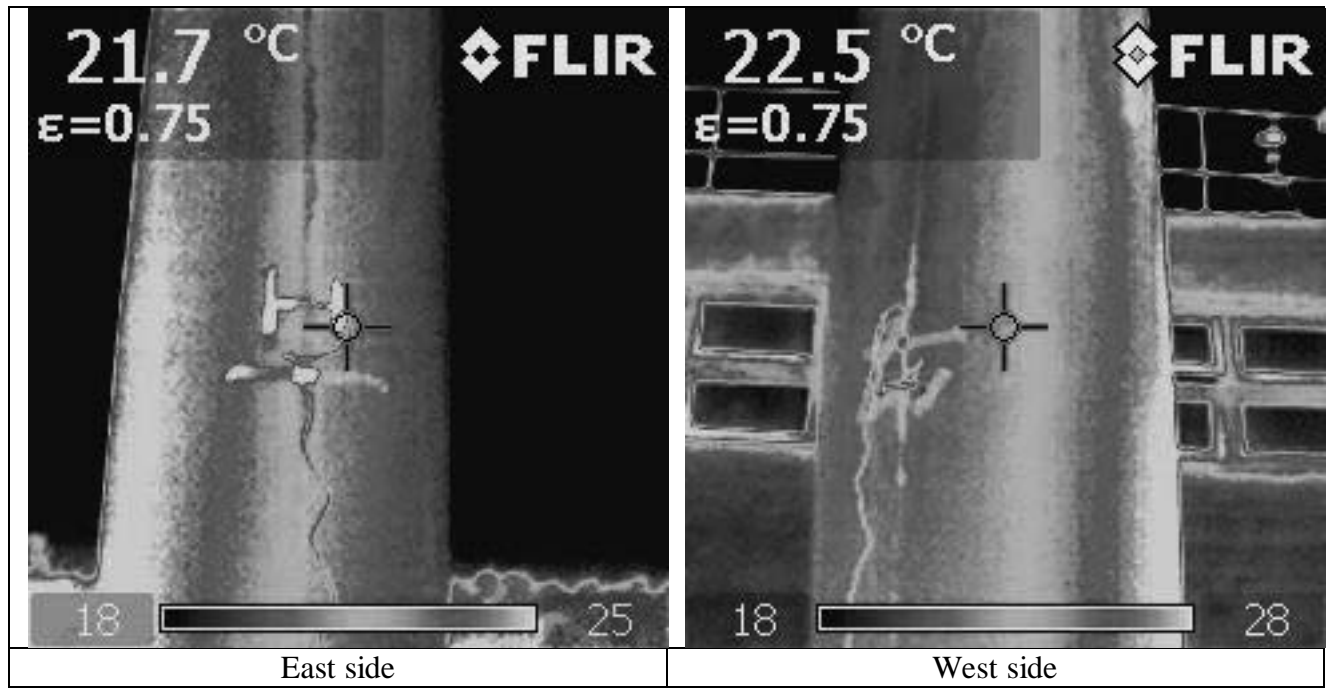


Figure 111. Comparison of the temperature distribution on the Pillar on January 18th, 2013

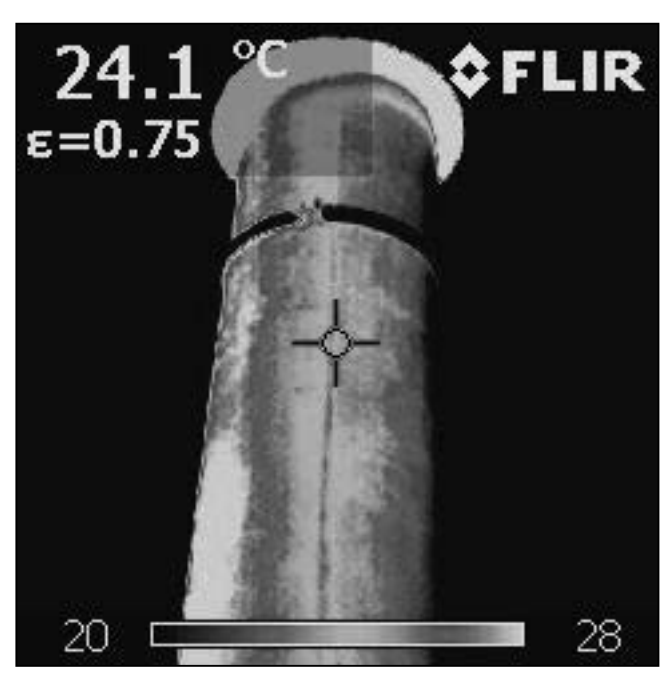


Figure 112. Effects of the warming of the Pillar



Figure 113. Scaffolding around the Asokan Pillar during the restoration work



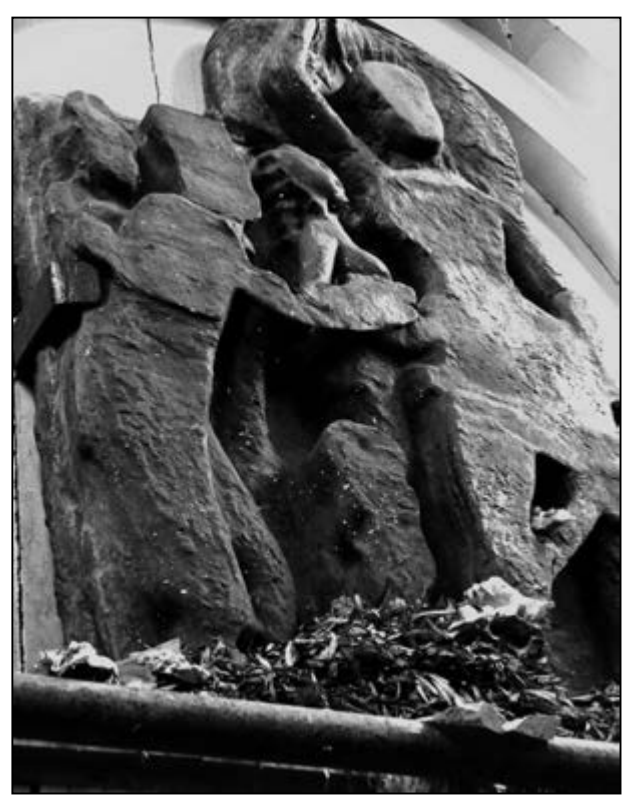
Figure 114. The scaffolding built on the Nativity Sculpture.



Figure 115. The hard resin caused scaling and stone powdering



Figure 116. Cleaning reveals the original color of the stone.



 ${\bf Figure~117.~Nativity~Sculpture~as~appears~after~the~Maya~Festival}$



Figure 118. The Nativity Sculpture after restoration

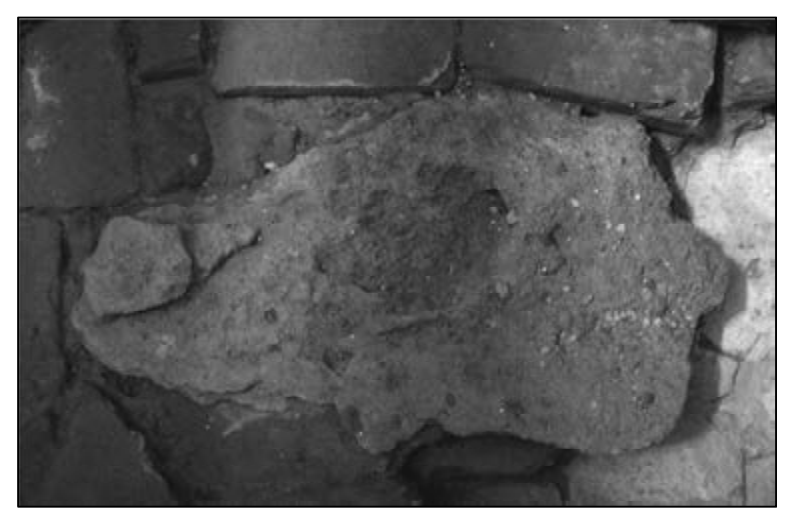


Figure 119. The Marker Stone before cleaning.

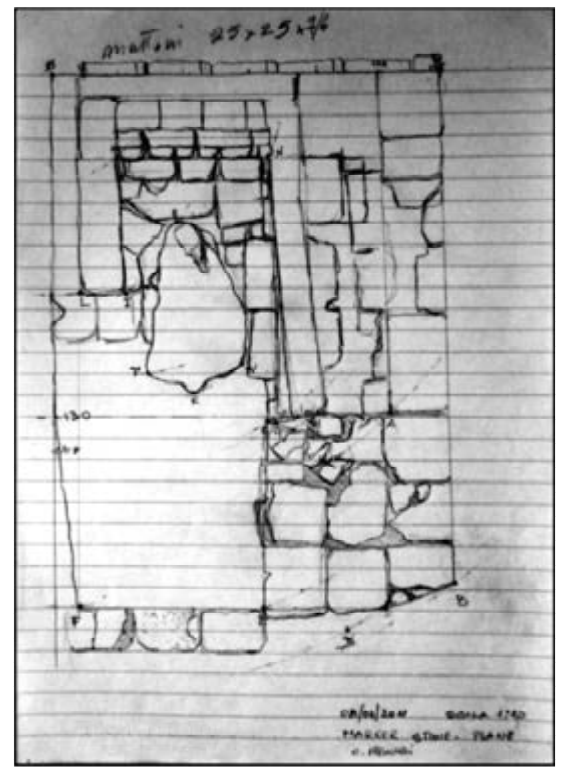


Figure 120. Sketch of the location of Marker Stone



Figure 121. The Marker Stone as appeared after the Maya Festival.



Figure 122. Marker Stone: left) during, and, right) at the end of the final restoration

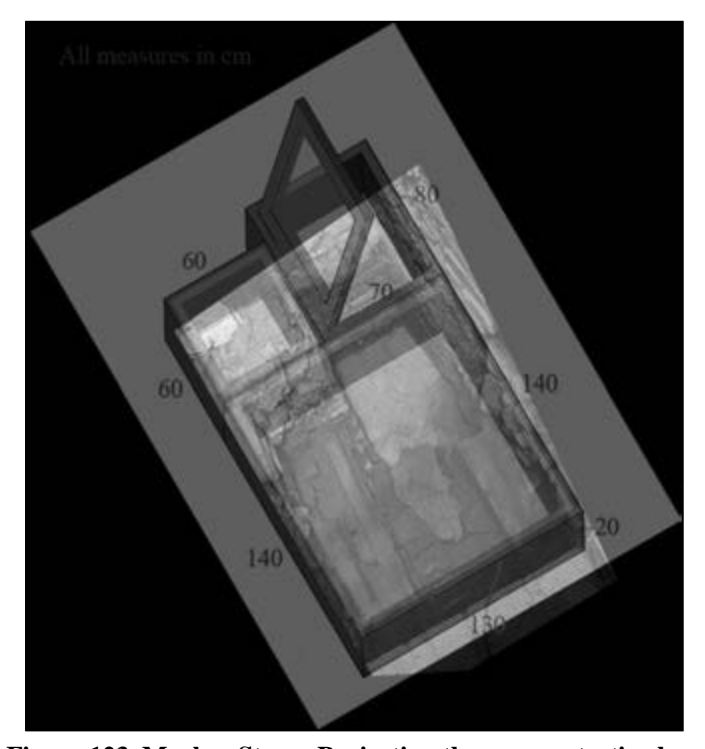


Figure 123. Marker Stone: Projecting the new protective box



Figure 124. The box completed



Figure 125. All spots light violet because of the unsuitable electric power

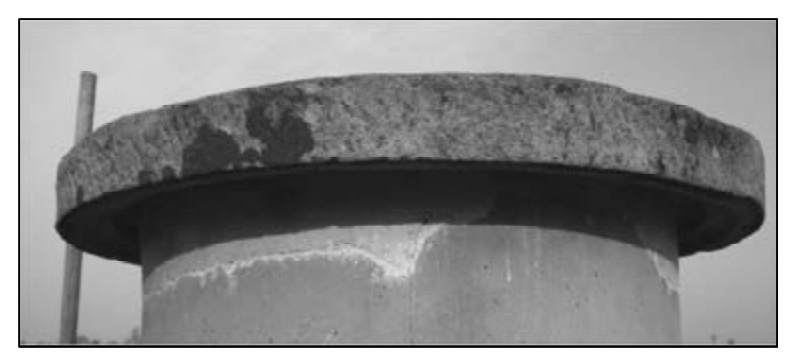


Figure 126. Before cleaning.



Figure 127. During cleaning.

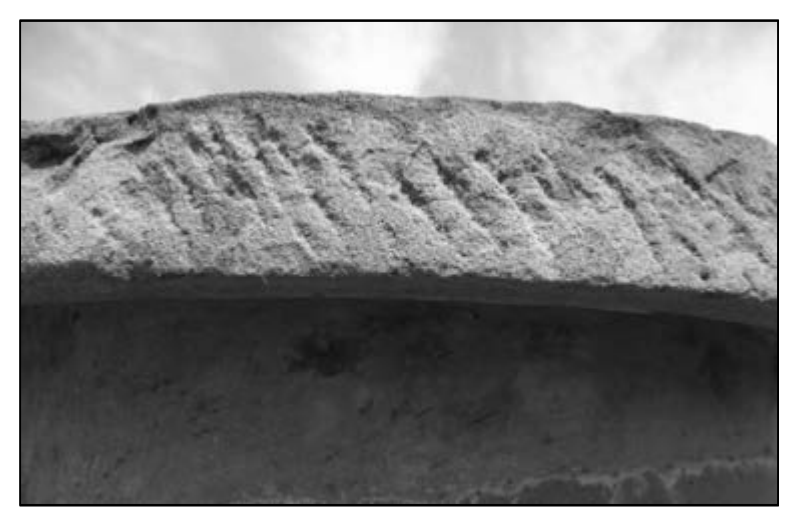


Figure 128. The cap of the pillar as appears after the cleaning.



Figure 129. A layer of resin covers the plaster between cap and pillar. $\,$



Figure 130. Mechanical removal of the cement mortar



Figure 131. Traditional hydraulic mortar



Figure 132. Finishing mortar.



Figure 133. The corroded area on West side after the treatment with ESTEL 1000.

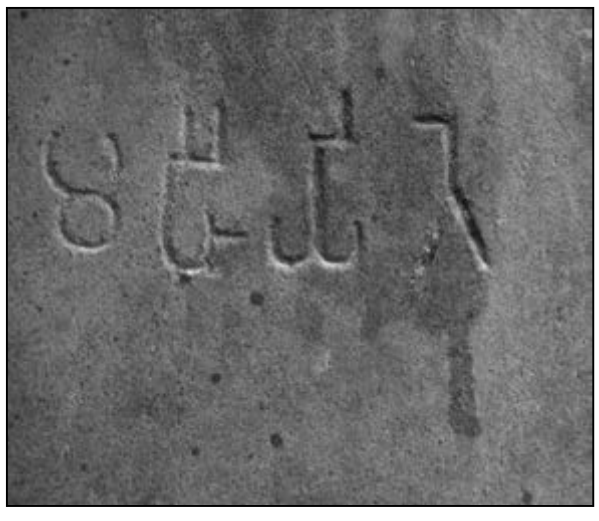


Figure 134. The letters before cleaning show several damages due to the offerings.

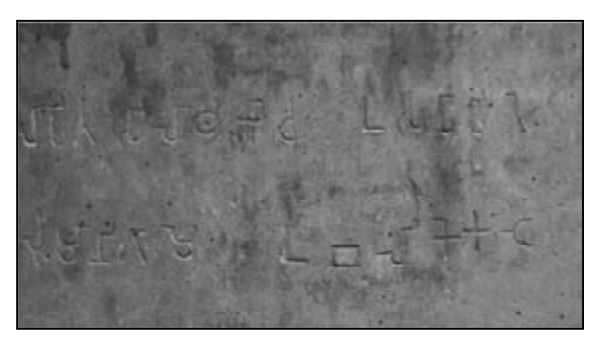


Figure 135. The inscription before cleaning.



Figure 136. The inscription after cleaning.



Figure 137. Corrosion products affect the stone under the belt.



Figure 138. Applying the silicon rubber protects the stone from the iron corrosion products.



Figure 139. Finishing the belt with the varnish.



Figure 140. The capital before restoration



Figure 141. The two elements of the capital are connected with cement concrete



Figure 142. Performing the cleaning with HP/AL mixture.



Figure 143. The new basement supporting the capital.



Figure 144. The seat at the base of the capital.



Figure 145. Placement of the first fragment.



Figure 146. Connecting the second fragment



Figure 147. Filling the fissure with mortar.



Figure 148. After the application of the protective.



Figure 149. Applying soap solution as separating agent



Figure 150. Applying the silicon rubber on the first thin replica layer.



Figure 151. Separating the mold from the Pillar.



Figure 152. Verifying the quality of the replica.

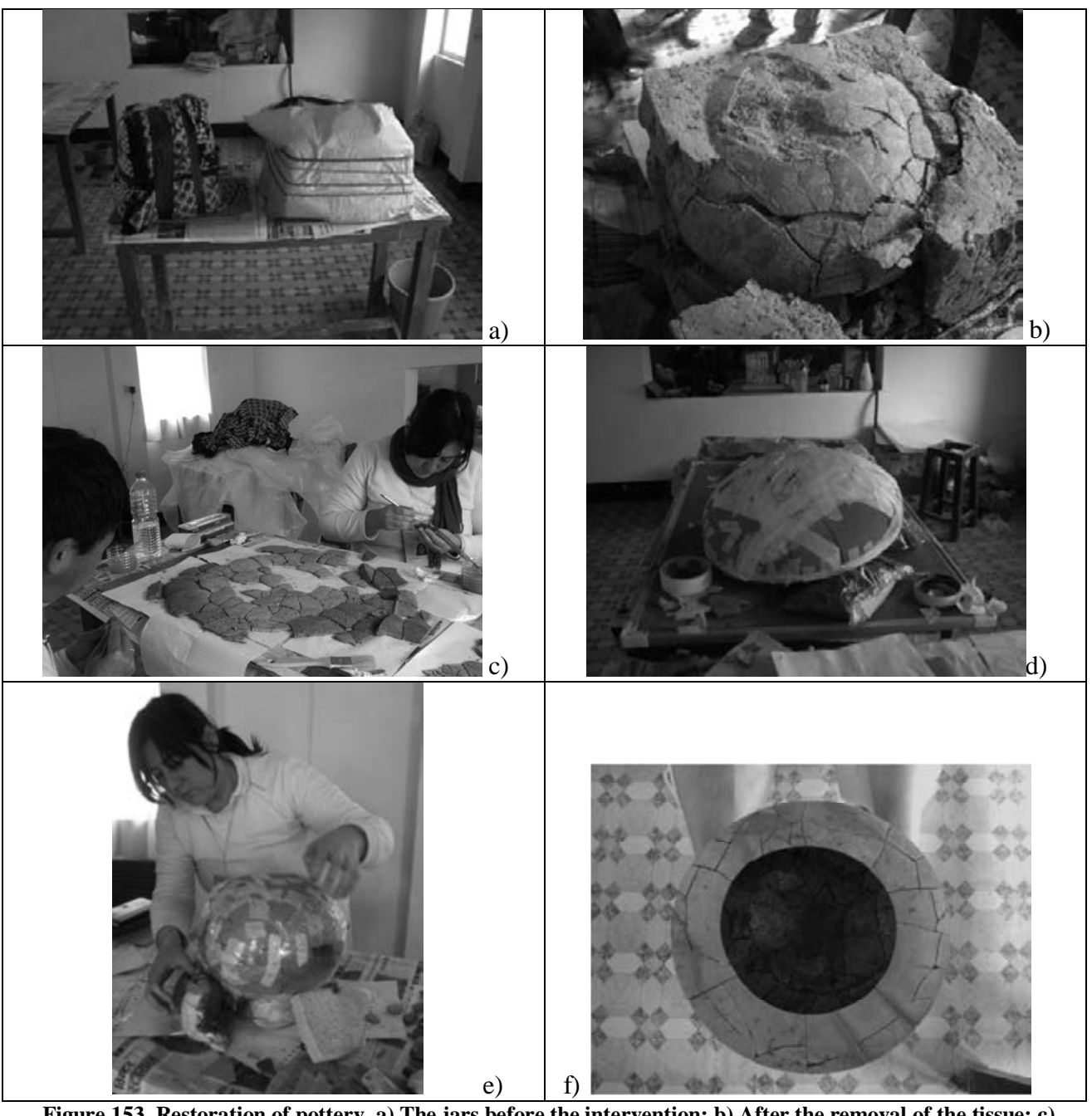


Figure 153. Restoration of pottery. a) The jars before the intervention; b) After the removal of the tissue; c)

During the cleaning; d, e) Preparing the gluing of the fragments; e) After the restoration.



Figure 154. The wall before the restoration

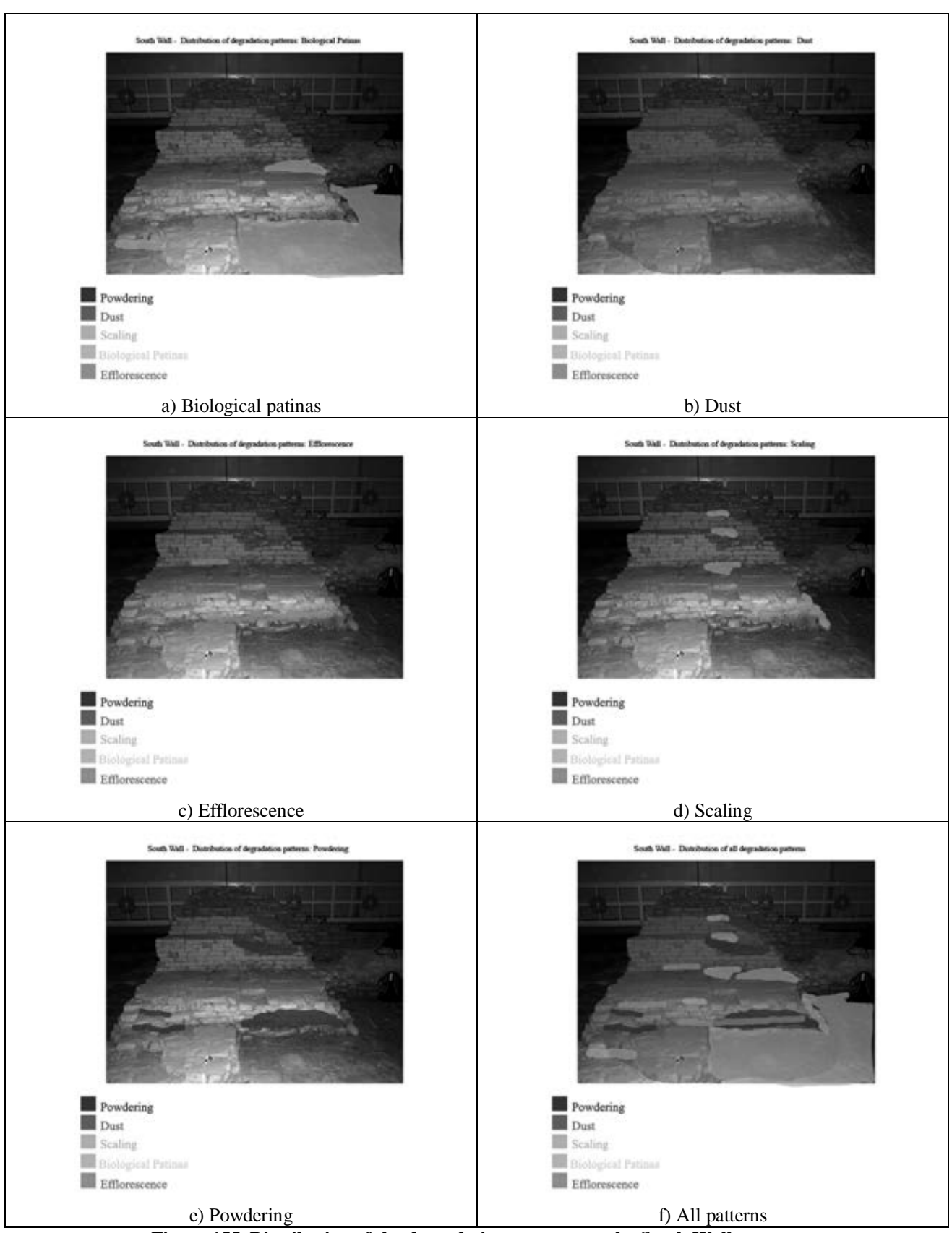


Figure 155. Distribution of the degradation patterns on the South Wall masonry



Figure 156. Degradation of the bricks in Trench C7



Figure~157.~Mechanical~cleaning~of~the~south~Wall



Figure 158. Chemical cleaning of the walls of Trench C7

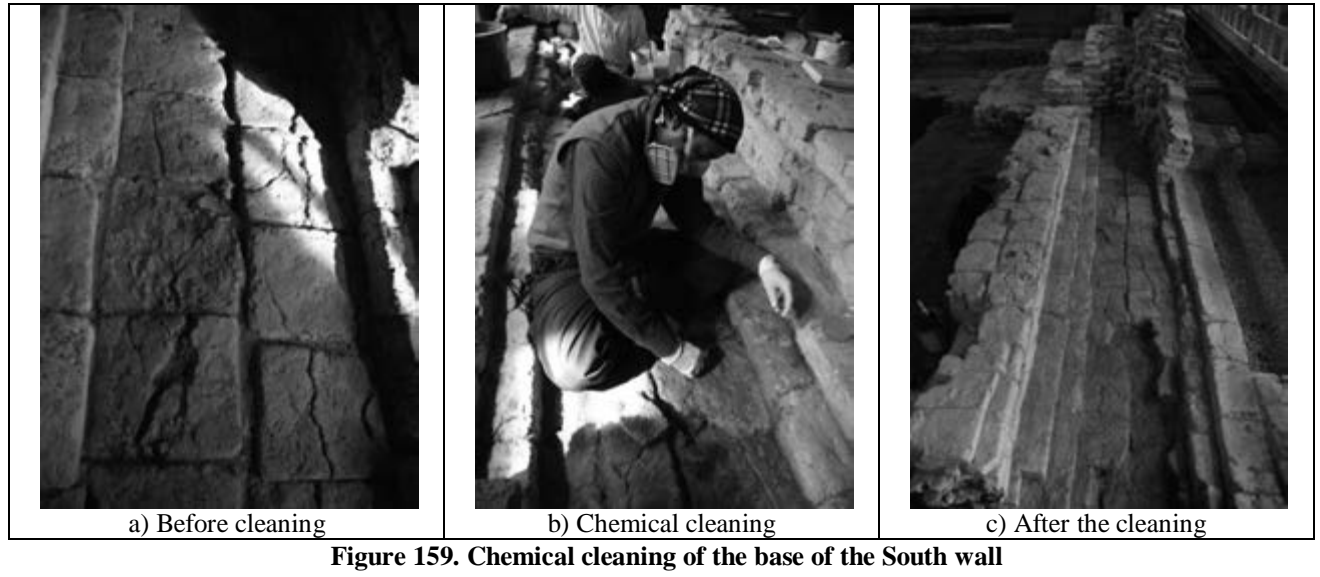




Figure 160. The South wall after the cleaning



Figure 161. Plastering fissures and cracks



Figure 162. Gluing of broken brick with lime plaster



Figure 163. Spraying the final waterproofing/strengthening mixture



Figure 164. The South wall at the end of the restoration



